



**T.C.  
İSTANBUL UNIVERSITY  
INSTITUTE OF GRADUATE STUDIES IN  
SCIENCE AND ENGINEERING**



**M.Sc. THESIS**

**PREDICTION of PRESSURE COEFFICIENT on TUNNEL DAM HIGH  
GATES WITH THE AID of HYDRAULIC MODEL and THE PASW  
STATISTICAL PROGRAM**

**Sheeraz MAJEED AMEEN AMEEN**

**Department of Civil and Infrastructure Engineering**

**Civil and Infrastructure Engineering Programme**

**M. Sc. Student Transferred from Fatih University which Got Shut Down**

**SUPERVISOR**

**Assoc. Prof.Dr. Taha MOHAMMED AHMED TAHER**

**CO-SUPERVISOR**


**Assoc. Prof.Dr. Thamir AHMAD**

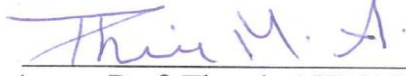
**June, 2016**

**İSTANBUL**

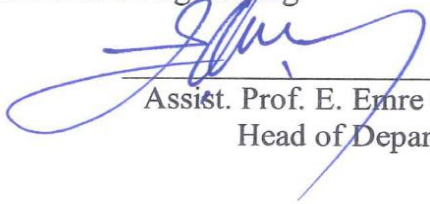
## APPROVAL PAGE

This is to certify that I have read this thesis written by Sheeraz AMEEN and that in my opinion it is fully adequate, in scope and quality, as a thesis for the degree of Master of Science in Civil structure and Infrastructure engineering.

  
Assoc. Prof. Taha TAHER  
Thesis Supervisor

  
Assoc. Prof. Thamir AHMAD  
Thesis Co. Supervisor

I certify that this thesis satisfies all the requirements as a thesis for the degree of Master of Science in civil structure and Infrastructure Engineering.



  
Assist. Prof. E. Emre ÇEÇEN  
Head of Department

Examining Committee Members


Assoc. Prof. Taha TAHER

Assist. Prof. Ziyad ABUNADA

Assist. Prof. Hatice Nur ARAS MEHAN

It is approved that this thesis has been written in compliance with the formatting rules laid down by the Graduate School of Sciences and Engineering.

  
Prof. Dr. Nurullah ARSLAN  
Director

July 2016

# **PREDICTION of PRESSURE COEFFICIENT on TUNNEL DAM HIGH GATES WITH THE AID of HYDRAULIC MODEL and THE PASW STATISTICAL PROGRAM**

Sheeraz MAJEED AMEEN AMEEN

M.S. Thesis - Civil and Infrastructure engineering  
July 2016

Thesis Supervisor: ASSOC. Prof. Taha MOHAMMED AHMET TAHER  
Thesis Co. Supervisor: ASSOC. Prof. Thamir AHMAD

## **ABSTRACT**

Hydrostatics And Hydrodynamics Forces Are Generated And Applied On The Vertical Lift Tunnel Gates Due To A Wide Range Of Operating Conditions. These Forces Are Varying With Different Gate Openings Ratios, Discharges And Gate Geometries. In This Work, Investigation Of The Said Forces Is Made Paying Particular Attention On The Effects Of Varying Discharges, Gate Lip Angles And Longitudinal Slopes On Values Of Downpull Coefficients And Related Outputs. Total Of Seven Angles, Three Discharges And Four Slopes Were Investigated. Hydraulic Model Was Constructed In This Work For The Sake Of Measuring All Parameters Required For Estimating The Top, Bottom And Downpull Pressure Coefficients Which Are All Examined Against The Effects Of Gate Geometries, Flow Rate And Slopes. The Results Show That The Top Pressure Coefficient Is Effectively Affected By Change Of Discharge, Gate Lip Angles, And Slopes Of Tunnel And Less Effect Are Observed With Change Of Gate Openings Ratios. The Maximum Values Are Obtained For At ( $\theta=35^\circ$ ) Angle, (0.5 %) Slope And (0.04 M<sup>3</sup>/Sec) Discharge. The Results Show That The Bottom Pressure Coefficient Is Related To The Said Variables, However, Its Behaviour And Values Not Necessary Regular With Variance Of Studied Variables. The Downpull Force Coefficient Results Show Significant Relationships With The Studied Variables, However, Negative Values Are Obtained At A Certain Gate Lip Shapes And Openings. The Values Are Seen More Significantly Related To The Discharge Level And For Some Extent To The Slopes Of Tunnel. An Attempt By Using The Nonlinear Regression Of Statistical Package Of Social Sciences (SPSS) Was Made To Set Equations Relating Bottom Pressure Coefficient With Gate Openings For Several Angles Of Gate Lips. The Obtained Equations Are Shown In Good Agreement With The Selected Cases Of Experimental Results.

**Keywords:** Lift Gates, Bottom Pressure Coefficient, Top Pressure Coefficient, Down Pull Pressure Coefficient.

# Hidrolik Model ve PASW İstatistiksel Yazılımı ile Tünel Baraj Kapakları Üzerindeki Basınç Katsayılarının Tahmini

Sheeraz MAJEED AMEEN AMEEN

Yüksek Lisans Tezi – İnşaat Yapı ve Altyapı Mühendisliği  
Temmuz 2016

Tez Danışmanı: Doç. Dr. Taha MOHAMMED AHMED TAHER  
Tez Eş-Danışmanı: Doç. Dr. Thamir AHMAD

## ÖZ

Geniş ölçekte çeşitli çalışma koşulları altında hidrostatik ve hidrodinamik kuvvetler üretilip dikey baraj kapakları üzerine etkilmiştir. Bu kuvvetler, kapak açıklığı oranları, debi ve kapak geometrisine göre değişmektedir. Bu çalışmada, değişen debi, kapak uç açısı ve aşağı eğim katsayıları ve ilgili çıktılarının etkileri göz önüne alınarak sözkonusu kuvvetler incelenmiştir. Yapılan incelemelerde, toplamda yedi farklı açı, üç farklı debi miktarı ve dört farklı eğimde kullanılmıştır. Kapak geometrisi, debi ve eğimin etkilerine karşı incelenen üst, alt ve aşağı çekim basınç katsayılarının tahmin edilebilmesi için gereken parametreleri belirleme amacıyla bir hidrolik model oluşturulmuştur. İncelemelerde kullanılan açılar;  $\theta=25^\circ$ ,  $\theta=27^\circ$ ,  $\theta=30^\circ$ ,  $\theta=35^\circ$ ,  $\theta=37^\circ$ ,  $\theta=40^\circ$ , ve  $\theta=42^\circ$  dir. Kullanılan debi miktarları 0.028 m<sup>3</sup>/sec ila 0.04 m<sup>3</sup>/sec arasında değişmektedir. Dikkate alınan dikey eğimler (0, 0.25%, 0.5% , ve 0.75%) dir. Çalışmadaki değişkenlerin belirlenmesi için 84 deneysel analiz yapılmıştır. Sonuçlara göre üst basınç katsayısı değişen debi miktarı, kapak uç açısı ve tünel eğiminden oldukça etkilenmektedir fakat değişen kapak açıklıkları oranında bu etki çok daha azdır. En yüksek değerlere, ( $\theta=35^\circ$ ) açı, (0.5 %) eğim ve (0.04 m<sup>3</sup>/sec) debide ulaşılmıştır. sonuçlar alt basınç katsayısı çalışılan değişkenlerin varyans ile onun davranış ve değerler, gerekli düzenli değil, ancak, söz konusu değişkenlere bağlı olduğunu göstermektedir. downpull kuvveti katsayısı sonuçları Ancak, negatif değerler belirli bir kapı dudak şekilleri ve açıklıklar elde edilir çalışılan değişkenler, anlamlı ilişkiler göstermektedir. değerler görülen daha belirgin tahliye düzeyine ve tünelin yamaçları ölçüde için ilişkilidir. sosyal bilimler istatistiksel paketi (SPSS) doğrusal. olmayan regresyon kullanılarak bir girişim hayranlarıyla elde edilen denklemler deney sonuçlarının seçilmiş olgularda ile iyi bir anlaşma gösterilen kapı dudakların çeşitli açılardan için kapı açıklıkları ile alt basınç katsayısı ile ilgili denklemler ayarlamak için yapıldı .

**Anahtar Kelimeler:** Kapak, alt basınç katsayısı, üst basınç katsayısı, aşağı çekim basınç katsayısı.



To my parents

## ACKNOWLEDGEMENT

By the name of God, I am very thankful for Allah for blessing me energy, health, ability to complete this research work. This research project would not have been possible without the financial support of my respective brother (**Dr. Derbaz Majid Amin**), this work is dedicated to him. I would like to designate the entire fruitful outcome of this work to my **Father** who has been waiting for so long to see the result of his daughter work, to my **Mother**, who hasn't stopped praying for this work to be done I would have never been the person I am without the patience and love that she dedicated to me. I cannot put my thankfulness and appreciation to my husband **Dr. Azhin .T.Sabir** who has stood by me through all my travails, my absences, my fits of pique and impatience. He gave me support and help, discussed ideas and prevented several wrong turns. Along with him, I want to acknowledge my two sons, **Allen** and **Alvand**, they have waiting for so long to see their Mom at home and finishing her work, Good boys, both, and great sources of love and relief from scholarly endeavor. Many thanks are due to all my **sisters and brothers** they always remained me strong when I felt weak, they gave me energy and love all the time.

I wish to express my gratitude to my supervisor **Assoc. Prof Dr.Taha Mohammed Ahmed Taher** without his viable advice, guidance, this thesis would have never been come to light. My greatest thanks go to my supervisors **Assoc. Prof. Dr.Thamir Ahmed** he continuously support me during the development of this thesis and giving me ideas he always encouraged and motivated me to continue even in difficult times. Last but not least, many thanks are due to all my friends, fellow students in (**Istanbul**) for the fruitful collaboration work, and their important discussions , and all members of staff at the civil engineering department in **Ishik university(Erbil)** for all support they gave me to work in their laboratory .

## TABLE OF CONTENTS

ABSTRACT.....	vi
ÖZ.....	ivi
DEDICATION.....	v
ACKNOWLEDGEMENT.....	vi
TABLE OF CONTENTS.....	vii
LIST OF TABLES.....	ix
LIST OF FIGURES.....	x
LIST OF SYMBOLS AND ABBREVIATIONS.....	xiii
CHAPTER 1 INTRODUCTION.....	.1
1.1 Objectives.....	2
1.2 Limitations.....	2
CHAPTER 2 LITERATURE REVIEW.....	4
CHAPTER 3 EXPERIMENTAL WORK.....	16
3.1 Experimental Set –Up:.....	17
3.2 Procedure Of Measurements.....	20
CHAPTER 4 RESULTS AND DISCUSSION.....	25
4.1 Flow Analysis.....	25
4.2 Downpull Coefficients:.....	26
4.2.1 Top pressure Coefficient (Kt):.....	26
4.2.2 Bottom Pressure Coefficient (Kb):.....	37
4.2.2.1 Effects of Flow Rates and Longitudinal Slope on (Kb):.....	38
4.2.2.2 Effects of Gate lip Geometry on (Kb):.....	46
4.2.2.3 Distribution of (Kb) on Bottom Gate Surface:.....	52
4.2.3 Downpull Pressure Coefficient (Kd):.....	58
4.3 Statistical Package Of Social Sciences (Spss) Analysis:.....	63

4.4	Upstream Pressure Coefficient ( $K_f$ ):.....	69
CHAPTER 5 SUMMARY, CONCLUSION AND RECOMMENDATIONS.....		73
5.1	Summary: .....	73
5.2	Conclusion: .....	74
5.3	Recommendation: .....	75
REFERENCES .....		76



## LIST OF TABLES

### TABLE

4.1 Mean values of submerged flow rates and corresponding Reynolds Number. ....	26
4.2 Results of SPSS for [ (Qmed. S=0.75% ) ( $\theta=35^\circ$ , $\theta=37^\circ$ and $\theta=40^\circ$ )].....	64
4.3 Results of SPSS for[ (QL. S=0 ) ( $\theta=35^\circ$ , $\theta=37^\circ$ , $\theta=40^\circ$ and $\theta=42^\circ$ )].....	65
4-4 Results of SPSS for[ (QL. S=0 ) ( $\theta=35^\circ$ , $\theta=37^\circ$ , $\theta=40^\circ$ and $\theta=42^\circ$ )] .....	66
4.5 Results of SPSS for [ (QL. S=0.25% ) ( $\theta=37^\circ$ , and $\theta=42^\circ$ )].....	67

## LIST OF FIGURES

### FIGURE

2.1 Diagram of tunnel gate under flow condition .....	9
2.2 Diagram of tunnel gate under semi-flow condition .....	10
2.3 Diagram of tunnel gate under fully-submerged flow condition .....	11
3.1 Tunnel Sketch with explanation of parameters. ....	17
3.2 Main components of hydraulic model. ....	18
3.3 Main Details of gate model.....	18
3.4 Gate shaft lip detail .....	19
3.5 Flow chart of runs for each angle. ....	21
3.6 Hydraulic model .....	23
3.7 Data sheet.....	23
4.1 Variation of $K_t$ with opening ratio for slope zero in different gate shape lips, and different discharges.....	29
4.2 Variation of $K_t$ with opening ratio for slope % 0.25 in different gate shape lips, and different discharges.....	30
4.3 Variation of $K_t$ with opening ratio for slope %0.5 in different gate shape lips,and different discharges.....	31
4.4 Variation of $K_t$ with opening ratio for slope zero in different gate shape lips, and different discharges.....	32
4.5 Variation of top pressure coefficients with gate openings of shape lip $27^\circ$ for different Slopes. ....	34
4.6 Variation of top pressure coefficients with gate openings of shape lip $37^\circ$ for different slopes.....	35
4.7 Variation of top pressure coefficients with gate openings of shape lip $42^\circ$ for different slopes.....	36
4.8 Location of the piezometer holes on the bottom lip surface while $X_0$ and $B$ are constants ( $X_0=7\text{cm}, B=20\text{ cm}$ ) .....	38

4.9 Variation of bottom pressure coefficient with gate openings for gate shape lips(25,27,30) when the slope is zero. ....	39
4.10 Variation of bottom pressure coefficient with gate openings for gate shape lips(35,37,40,42) when the slope is zero. ....	40
4.11 Variation of bottom pressure coefficient with gate openings for gate shape lips (25,27,30)when the slope is (S= 0.25%)......	41
4.12 Variation of bottom pressure coefficient with gate openings for gate shape lips (35, 37, 40, 42) when the slope is (S= 0.25%)......	42
4.13 Variation of bottom pressure coefficient with gate openings for gate shape lips(25,27,30) when the slope is (S= 0.5%)......	43
4.14 Variation of bottom pressure coefficient with gate openings for gate shape lips (35,37,40,42) when the slope is (S= 0.5%)......	44
4.15 Variation of bottom pressure coefficient with gate openings for different gate shape lips when the slope is (S= 0.75%). ....	45
4.16 Variation of bottom pressure coefficient with gate openings for different discharge ( $\theta=25^\circ$ ) . ....	46
4.17 Variation of bottom pressure coefficient with gate openings for different discharge ( $\theta=27^\circ$ ). ....	47
4-18: Variation of bottom pressure coefficient with gate openings for different discharge ( $\theta=30^\circ$ ). ....	48
4.19 Variation of bottom pressure coefficient with gate openings for different discharge ( $\theta=35^\circ$ ). ....	49
4-20 Variation of bottom pressure coefficient with gate openings for different discharge ( $\theta=37^\circ$ ). ....	50
4.21 Variation of bottom pressure coefficient with gate openings for different discharge ( $\theta=40^\circ$ ). ....	51
4.22 Variation of bottom pressure coefficient with gate openings for different discharge ( $\theta=42^\circ$ ) . ....	52
4.23: Variation of (Kb) with ( $\theta=30^\circ$ ) ,(Y/Yo=20%), (QL.) and (S=0) . ....	53
4.24: Variation of (Kb) with ( $\theta=30^\circ$ ) , (Y/Yo=30%), (QL.) and (S=0) . ....	54
4.25: Variation of (Kb) with ( $\theta=30^\circ$ ) , (Y/Yo=20%), (QL.) and (S=0.25 %) . ....	54
4.26: Variation of (Kb) with ( $\theta=30^\circ$ ) , (Y/Yo=30%), (QL.) and (S=0.25 %) . ....	55
4.27: Variation of (Kb) with ( $\theta=30^\circ$ ), (Y/Yo=20%), (QL.) and (S=0.5 %) . ....	55

4.28: Variation of (Kb) with ( $\theta=30^\circ$ ), ( $Y/Y_0=30\%$ ), (QL.) and ( $S=0.5\%$ ) .....	56
4.29: Variation of (Kb) with ( $\theta=30^\circ$ ), ( $Y/Y_0=20\%$ ), (QL.) and ( $S=0.75\%$ ).....	57
4-30: Variation of (Kb) with ( $\theta=30^\circ$ ), ( $Y/Y_0=30\%$ ), (QL.) and ( $S=0.75\%$ ) . .....	57
4.31 Downpull coefficient pressures with gate openings for different shape lips in different discharges when ( $S=0$ ).....	59
4.32 Downpull coefficient pressures with gate openings for different shape lips in different discharges when ( $S=0.25\%$ ).....	60
4.33 Downpull coefficient pressures with gate openings for different shape lips in different discharges when ( $S=0.5\%$ ).....	61
4.34 Downpull coefficient pressures with gate openings for different shape lips in different discharges when ( $S=0.75\%$ ).....	62
4.35 Measured and Predicted (Kb) values.....	65
4.36 Measured and Predicted (Kb) values.....	66
4.37 Measured and Predicted (Kb) values.....	67
4.38 Measured and Predicted (Kb) values.....	69
4.39 Scheme of taps on upstream face of gate.....	69
4.40 Variation of pressure coefficient (Kf) along the gate upstream face, for $X=0.25B$ , and the discharge is low.....	70
4.41 Variation of pressure coefficient (Kf) along the gate upstream face, for $X=0.5B$ , and the discharge is low.....	71
4.42 Variation of pressure coefficient (Kf) along the gate upstream face, for $X=0.25B$ , and the discharge is maximum .....	71
4.43 Variation of pressure coefficient (Kf) along the gate upstream face, for $X=0.5B$ , and the discharge is maximum .....	72

## LIST OF SYMBOLS AND ABBREVIATIONS

### SYMBOL/ABBREVIATION

A	Appropriate cross sectional area of the tunnel, $m^2$
B	Tunnel width, m
$b_1, b_2$	U/S & D/S gap widths between the gate & the gate shaft, m
$C_c$	Coefficient of contraction for the jet flow below the gate.
$C_d, C$	Discharge coefficients.
$C_2$	Discharge coefficients for the rate of flow released over the gate.
d	Gate thickness, m
dz	tail water downstream of the gate.
Fr	Froude number, dimensionless
$F_b$	Upward force . N
$F_d$	Downpull force, N
g	Gravity acceleration , $m^2/sec$
$H_i$	Pressure head at a point on the gate bottom, m
$H_t$	Pressure head on the top surface of the gate, m
$H_e$	Overall entrance loss that occurs between reservoir & gate section, m
$H_{ce}$	Loss in the total head along the tunnel ceiling due to the corner eddy Between the tunnel ceiling & the upstream face of the gate, m
$H_f$	Total head U/S of the gate, m
$H_2$	Pressure head U/S of the gate, m
$H_1$	Pressure head D/S of the gate, m
$K_b$	Bottom pressure coefficient, dimensionless
$K_d$	Downpull coefficient, dimensionless
$K_t$	Top pressure coefficient, dimensionless
P	Perimeter of tunnel section, m
Q	Total rate of flow, $m^3/sec$

$Q_1$	Rate of flow released under the gate, $m^3/sec$
$Q_2$	Rate of flow released over the gate, $m^3/sec$
$Re$	Reynolds number, dimensionless
$V$	Average velocity, $m/sec$
$V_j$	Velocity in the contracted jet issuing from under beneath the gate, $m/sec$
$X_o$	Horizontal distance along gate bottom surface, $m$
$X$	The horizontally distance from the leading edge of gate lip toward trailin edge , $m$
$Y$	Height of gate opening, $m$
$Y_o$	Tunnel height, $m$
$Y_s$	Piezometric head in contracted jet, $m$
$Z$	Height of the gate, $m$
$Z_o$	Vertical distance along upstream face of the gate, $m$
$\nu$	Kinematic viscosity , $m^2/sec$ ,
$\theta$	Angle between horizontal and sloping bottom of the gate, weighting Coefficient, degree
$\rho$	Density of water , $kg/m^3$
$\gamma$	Specific weight of water, $N/m^3$

# CHAPTER 1

## INTRODUCTION

Vertical lift gate is almost installed within the dam tunnel to satisfy the requirements of power generation and demand of water downstream the dam. The major function of such gate is to control the pressurized flow established by wide range of high heads which are occupied the dam reservoir. Many hydrostatic and hydrodynamic forces are applied to the vertical lift gate due to the effects of high heads. The downpull is the more effective force that exerted by flow on the gate. This force is generated as a difference result of two opposite forces. The first one is obtained from the impact of high pressure induced by water jet issuing below the gate bottom surface which denoted as uplift force. The second force is resulting from the influence of flow passing over the gate top surface; this force is termed as downward force.

The prediction of these forces depend upon the measurements of many dominated parameters ,such as ,the upstream head ,downstream head ,jet velocity and piezometer heads distribution along and across the bottom gate surface. A random physical hydraulic model was used to study the effects of the behaviour of water flow pattern below the gate, the generation of pressure for different gate lip geometries, flow rate, gate openings and longitudinal slope of tunnel model on downpull force coefficients.

The measured values were analyzed and relation between the downpull force coefficients were drawn with different gate opening ratios for many values of gate lip angles, flow rates and longitudinal slopes .Furthermore, the results were analyzed by using Statistical package of social sciences (SPSS) , and the behaviour of bottom pressure coefficients have been assessed by using the representation of a three dimensional surfer software for further clarification and validation. Many conclusion

are listed and recommendations are suggested. The studying of downpull forces is so important due to its vital role on the designing and operation of vertical lift gates and it needs always to cover all cases and conditions. The main target of current study is to cover the influences of different parameters on the variation of pressure coefficients and hence on the hydrodynamic forces to meet the requirements of optimum design by integrating the results of present study with those attained by another researchers.

## **1.1 OBJECTIVES**

The objectives of the present study can be listed as follows:

1. To evaluate the effects of gate geometries, flow rate conditions and longitudinal slopes on the top, bottom and consequently, downpull pressure coefficients for seven selected gate lip angles.
2. To identify the proper shape, slope and flow rate for best value of downpull.
3. To study the behaviour of bottom pressure coefficient along and across the bottom gate surface and indicate the portions of separation and reattachments and their effects on vibration and hence on stability of gate.
4. Prepare a wide range of data for any convenient Mathematical model studies.
5. To specify, which element or parameter should be focused to dominate the results of downpull coefficients.
6. To analyze the results by using the Statistical package of social sciences (SPSS) software and compare the outputs with measured results.

## **1.2 LIMITATIONS**

The following are limitations of present study:

1. The dimensions of simulated tunnel are (4 m long, 0.2 m wide, 0.3 m height) which are randomly selected and not relative with any prototype scale.
2. The measurements are carried out for only the case of submerged flow conditions.

3. The upstream and downstream clearances of gate shaft (b1 & b2) are considered constant.
4. The results obtained for the following conditions (The angles are  $\theta=25^\circ$  ,  $\theta=27^\circ$  ,  $\theta=30^\circ$  ,  $\theta=35^\circ$  ,  $\theta=37^\circ$  ,  $\theta=40^\circ$  , and  $\theta=42^\circ$  .The discharges are ranged from 0.028 m<sup>3</sup>/sec up to 0.04 m<sup>3</sup>/sec .The considered longitudinal slopes are (0, 0.25%, 0.5% , and 0.75%)) .
5. The equations those have been deduced by using (SPSS) software are restricted with the cases that have been selected.



## CHAPTER 2

### LITERATURE REVIEW

The dam tunnel lift vertical gates are exposed to many hydrodynamics forces exerted by pressurized water flow on different direction. The tunnel flow stream lines almost takes two paths ,and accordingly the two major forces will created .The uplift pressure force is produced by water jet flow issuing beneath the gate and caused a big effects on its bottom surface and consequently on the mechanical system of gate operation .The other force it may established vertically downward along the gate top surface due to the effects of water flow passing from upstream to downstream gate shaft clearances .The net force obtained from the difference of these two forces is named as downpull force which indicates a very important reference for safe and economical design of gate. The hydrodynamic forces are influenced by many main parameters which were studied by many researchers through mathematical and experimental approaches. The flow conditions, gate lip geometrics have been examined and a lot of results were analyzed and suggestions being recommended.

The dimensionless relationship of hydrodynamic force was proposed by **Cox et al (1960)** .which reflect the impact of aeration, geometry of gate bottom, clearances of gate shaft on the stability of the gate. Such criterion was founded to analytical approach which has been adopted in many subsequent researches. The air tunnel tests were conducted by **Naudascher et al (1964)** to evaluate the influences of flow conditions and geometry limits on downpull force applied to high head leaf gates. It is found that the following one dimensional for

based upon the bottom and top pressure coefficients can be utilized for evaluating the downpull force.

$$F_d = (K_t - K_b) \cdot B \cdot d \cdot \rho \quad (2.1)$$

Where:

$F_d$  = downpull force,

$B$  = gate width,

$d$  = gate thickness,

$\rho$  = water mass density, and

$V_j$  = velocity of the contracted jet issuing from underneath the gate.

$$K_t = (H_t - H_1) \cdot 2g / V_j^2 \quad (2.2)$$

$$K_b = (1 / B \cdot d) \iint [(H_i - H_1) / (\frac{V_j^2}{2g})] dB dx \quad (2.3)$$

Where:

$H_t$  = Piezometric head on gate top surface

$H_1$  = Piezometric head in the contracted section below the gate.

$H_i$  = Piezometric head at a point on the gate bottom

The experimental simulation of the TVAS Melton Hill Dam 3-leaf intake gate is presented by **Elder (1964)** to explore the effects of gate geometries on downpull force. The study includes five suggested shapes and also nine of normal shapes. It is found the uses of many gate shapes lead increase the downpull force values, then after; many problems were generated such as oscillation close failure.

In the few examinations completed by the **Murray, R. I. (1966)**, it was found that downpull force can be represented as function of upstream head.

$$F_d = \gamma \cdot H \cdot A \quad (2.4)$$

Where:

$\gamma$ : specific weight of water,

$H$ : Operating head, m.

The various forces acting on gate during opening and closing were discussed by **Sagar (1977)**. It is concluded that the following form of downpull force on gate can also be used:

$$F_d = F_t - F_b \quad (2.5)$$

$$F_t = \gamma \cdot A_t \cdot \left(H - \frac{V_0^2}{2g}\right) \quad (2.6)$$

$$F_b = \gamma \cdot B \cdot d \left[ H_z - \left( \frac{q^2}{y \cdot (y + d \tan \theta)} \right) \right] \quad (2.7)$$

Where:

$F_t, F_b$  : Forces on the top and base of gate respectively.

$A_t$ : top area of gate exposed to water pressure,

$D$ : thickness of the gate downstream skin plate and seal get together,

$B$ : width of skin plate and seal get together,

$d$  : thickness of downstream skin plate and seal assembly,

$$H_z = \left(H - \frac{V_0^2}{2g}\right).$$

$\frac{V_0^2}{2g}$  : Velocity head upstream the gate,

$q$ : discharge of water per unit width of the gate,

$y$ : height of the gate opening and

$\theta$ : angle amongst flat and inclining base of the gat.

The evaluation of pressures caused by the passage of water through the gate shaft was studied by **Sagar (1979)** for the case of free flow conditions. The method is based on the principle that the entire velocity head of the jet flow issuing through the upstream gap is lost because of sudden expansion within the gate shaft as it moves toward downstream gap. Although the method is restricted with some limitations due to the error that could occur as a result of entrance losses and its comparison with San Luis type gate only revealed good agreement between predicted and actual values.

**Sagar (1977)** was identified a set of geometrical variables that govern the behaviour of hydrodynamic forces exerted by water flow on the vertical lift gates which can be listed by the following functional form:

$$F_d = f(H, r/d, e/d, \theta, d/Y_o, b_1/b_2, d'/d, Y/Y_o) \quad (2.8)$$

Where

H: operating head,

r/d: Gate bottom geometry,

e/d: lip extension ratio,

$\theta$ : Inclination lip angle,

d/Y<sub>o</sub>: Gate thickness ratio,

b<sub>1</sub>/b<sub>2</sub>: Gate shaft clearances ratio and

d'/d : Thickness of the skin plate and top seal assembly.

The limited estimation of downpull forces were found to be obtained from two empirical methods as suggested by **Sagar (1977)**, first one named, the downpull coefficient method which is based on Fort Randall Dam data while the other, pressure distribution method, which is based on estimating the total forces acting on the top and bottom surfaces of the gate. These two methods are restricted to be applicable for just similar gate shapes have been considered.

The impacts of various flow approach conditions on intake gate downpull local pressures were considered by **Thang (1983)**. The determination of turbulence conditions close to the separation zone of the gate was demonstrated by utilization of Laser -Doppler-Anemometry. The study presumed that the variety of downpull and relevant coefficients is affected effectively by the separated flow pattern near bluff bodies to free stream turbulence, and to changes in the mean flow frequency. It is found that the streamlines separation from any kind of obstacles it may installed upstream of the gate bottom was produced inverse impacts on the downpull coefficients for a short distance from upstream when compared to mere free stream turbulence.

**Naudascher (1986)** studied on down pull force that might be fundamentally influenced by flow rate passing through the shaft gate studied about compact coefficient

(Cc) and effective factors on down pull power, and detailed these hydrodynamic components; Kb, Kd, Kt. using one dimensional analysis that obtained from data taken in hydraulic tests.

As shown in (Figure 2.1) discharge passing under the gate called  $Q_1$  determined by:

$$Q_1 = C_c \cdot Y \cdot B \sqrt{(2g (H - H_e - C_c \cdot Y - (P/\gamma)))} \quad (2.9)$$

and  $Q_2$  determined by:

$$Q_2 = C \cdot b_2 \cdot B \sqrt{(2g (H - H_e - H_{ce} - Y_o - (P/\gamma)))} \quad (2.10)$$

Where:

$H_e$ : All out misfortunes happening between the store and the passage of tunnel.

$H_{ce}$ : Head misfortunes because of the event of corner swirl between the roof and the upstream face of entryway.

$C_c$ : Constriction coefficient in the vent contract of the plane stream cries gate and

$C$ : Discharge coefficient.

The value of  $H_{ce}$  it can be determined by:

$$H_{ce} = K \frac{V_o^2}{2g} \quad (2.11)$$

Where

$$K = \frac{0.53}{[1+400 (Q_2/Q_1)^{1.5}]} \quad (2.12)$$

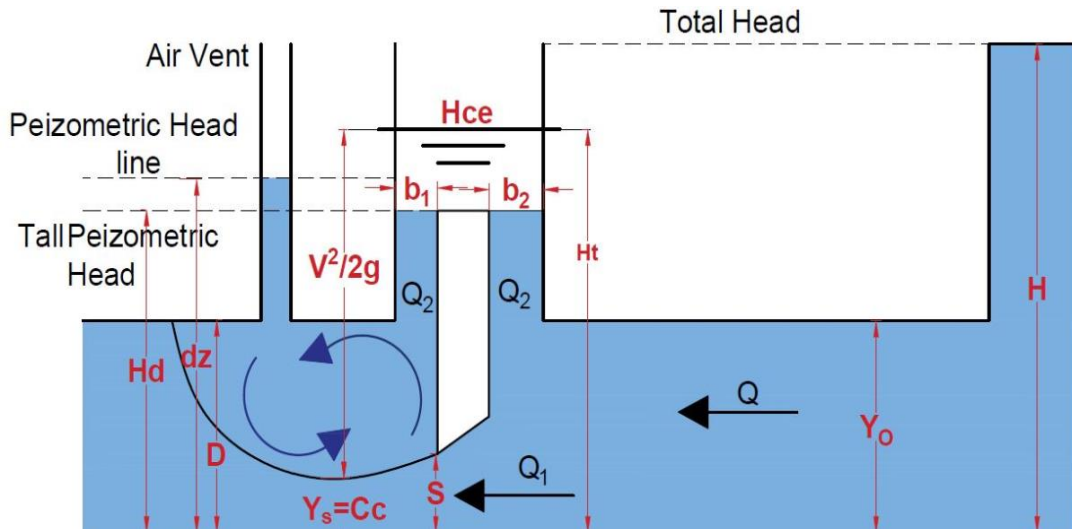


Figure 2.1 Diagram of tunnel gate under flow condition

Semi submerged stream condition (figure 2.2): in which the space downstream the gate is semi-submerged subsequently the flow rate going through the tunnel for this situation can be expressed as:

$$Q = \sqrt{g a_2^2 (-dz + 0.5D + (Q_1^2 / (g a_1 a_2) + B y_s a_s / 2D a_2))} \quad (2.13)$$

And

$$Q_1 = C_c \cdot Y \cdot B \cdot \sqrt{2g (H - H_e - Y_s)} \quad (2.14)$$

$$Q_2 = C \cdot b_2 \cdot B \cdot \sqrt{(2g (H - H_e - H_{ce} - Y_o))} \quad (2.15)$$

Where:

$$a_1 = Y_s \cdot B, \quad a_2 = D \cdot B$$

$Y_s$ : semi-submerged water depth downstream of the gate,

$D$ : downstream tunnel height, and

$dz$ : tail water downstream of the gate.

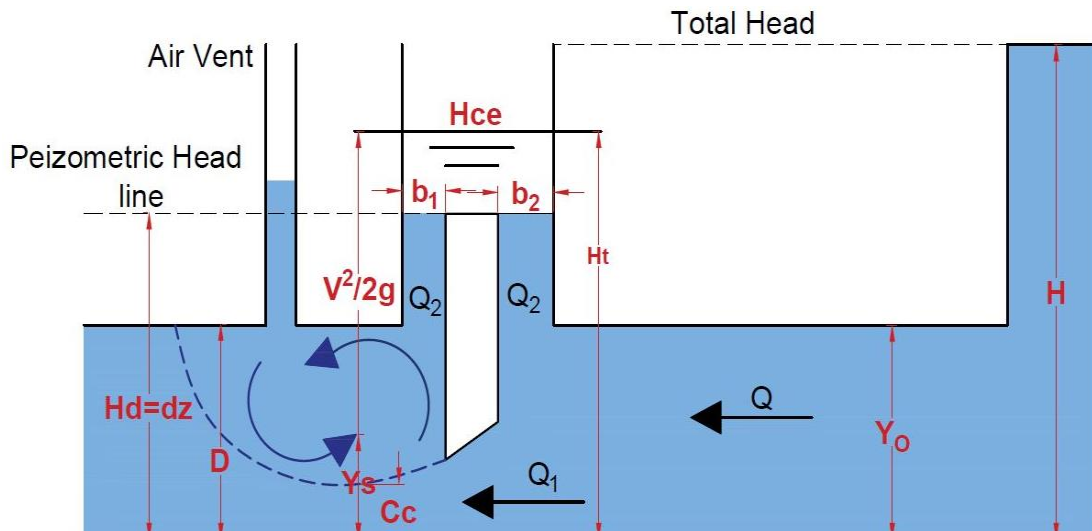


Figure 2.2 Diagram of tunnel gate under semi-flow condition

Fully submerged flow condition, (Figure 2.3): in which the tunnel downstream the gate is under pressurized state and the flow beneath and over the gate can be anticipated separately as takes after:

$$Q_1 = C_c \cdot Y \cdot B \sqrt{2g (H - H_e - Y_s)} \quad (2.16)$$

$$Q_2 = C \cdot b_2 \cdot B \sqrt{2g (H - H_e - H_{ce} - Y_s)} \quad (2.17)$$

Where:

$Y_s$ : Piezometric head in the contracted jet beneath the gate.

The flow over the gate  $Q_2$  can also be written as:

$$Q_2 = C' b_2 B \sqrt{2g (H - H_e - Y_s)} \quad (2.18)$$

Where:

$$C' = C \sqrt{\frac{(H - H_e - H_{ce} - Y_s) - (H - H_e - Y_s)}{(H - H_e - Y_s)}} \quad (2.19)$$

Then the total flow passing through the tunnel is equal to:

$$Q = Q_1 + Q_2 = B (C_c Y + C' b_2) \sqrt{2g (H - H_e - Y_s)} \quad (2.20)$$

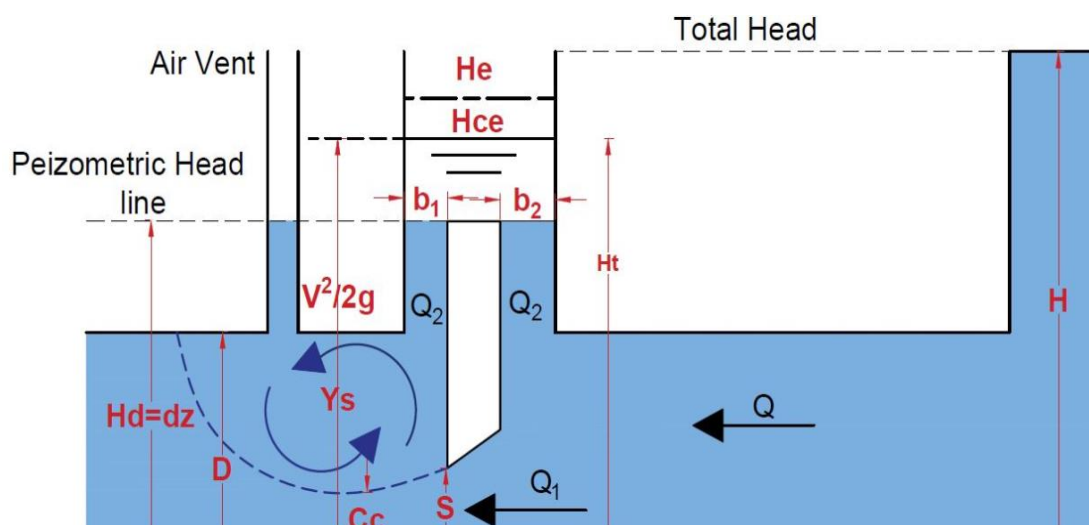


Figure 2.3 Diagram of tunnel gate under fully-submerged flow condition

**Bhargava (1989)** was examined the pressure fluctuations on different geometries of vertical-lift gate. The study consists of the estimations and investigation of numerous hydraulic parameters that impact the values and distributions and pressure heads for various gate openings. The intensity of pressure and its distribution pattern were studied when the gate is enforced to vibrate in the vertical direction at specific frequencies and amplitude. Total intensity of fluctuating pressures on vibrating gates was obtained by integrating the profiles of pressure fluctuations over the gate thickness. The study specifies a pressure of common frequency which is considered as critical condition for gate design.

The unsteady loads applied for different lip geometries and flow conditions of vertical lift gate were studied by **Nguyen (1990)**. The behaviour of the gate was examined under the effects of vibrations which had been created as results of separation and reattachment of flow stream lines beneath the gate bottom surface with specific ranges of dimensionless velocities. Such fluctuation was caused by the combined action of instable shear layer below the gate bottom and the vortices established just upstream the gate edge. The analysis leads to indicate the critical range of gate opening corresponding to potential gate vibrations.

The most common types of high-head gates, including slide gates, fixed-wheel gates, radial gates, and jet-flow gates, and their application were discussed by **Sagar (1995)**. The study includes the hydraulic design considerations to all types of High-head gates those are required to withstand and operate under water heads greater than 25 m were also discussed to confine all related conditions , limits and state the criterion for evaluate the performance of high head gate operation. The downpull force was estimated by the one dimensional finite element model conducted by **Al-Kadi (1997)**. This model based upon the velocity and mean pressure distribution along the bottom gate surface. Two cases were considered, one for invariant eddy viscosity and the other with variable eddy viscosity. The model was verified with the results of analytical prediction and gave a good agreement.

**Ahmed (1999)** was investigate the effect of many gate geometries with various gate width ratios on down pull forces, the study was based on the analysis results of the measurements gained by the experimental runs conducted by using hydraulic lab model. This study concludes that the downpull coefficient is influenced by various parameters such as; gate geometry and gate opening.

A numerical analysis for calculating viscous flows controlled by a vertical lift gate and hydrodynamic forces acting on the gate was developed by **Amorim and Andrade (1999)**. The numerical solution is obtained from the incompressible Navier-Stokes equations and turbulence effects are simulated by a k- $\epsilon$  turbulence model. The results of simulations the numerical model were compared with available experimental data at various opening positions and a good agreement were observed.

The effect of numerous tail water flow condition on down pull was investigated by **Drobir et al (2001)** by proposing the hydraulic model of tunnel type-high head gate. In this model the measurements were carried out for free and submerged flow behind the gate shaft. The experimental results were compared with those attained from the method of calculation Subjected by **Naudascher (1991)**.

**Shamsai and Soleymanzadeh (2006)** investigate the use of two phases of finite volume mixture flow model based on high Reynolds number and standard two equations (k- $\epsilon$ ) turbulence model. Model was confirmed by backward-facing step flow, and the results have been compared with experiments founded by (durst and Schmitt

1985). Air demand ratio had been determined as a function of Froude number at contracted section. Flow pattern matched at two categories of slug and stratified flows, air mean concentration profile had been attained at downstream tunnel. Moreover they investigate comparison of flow pattern at two cases with and without of aeration. Pressure drop behind of the gate and development of vortex flow after the gate section had been discussed. Measurement of flow discharge and determination of contraction coefficient of the gate was defined.

Experimental work on downpull force on gates installed in the intake structures of hydroelectric power plants including lip pressure distribution measurements and direct weighing of downpull are presented by **Aydin et al. (2006)**. The downpull coefficient was defined as a function of the lip angle and gate opening. The function is combined with unsteady flow one-dimensional mathematical model which based on the integral energy and continuity equations. The downpull force was evaluated for both cases of stationary and closing modes. The Predicted mathematical model was compared with the results obtained from the direct weighing method in order to confirm its validity.

**Akoz et al. (2009)** have conducted laboratory experiments to measure the velocities of a 2D open channel flow under a sluice gate and carried out simulations using computational fluid dynamics. A different mesh sizes have been used to investigate the effects of the mesh size and compared k- $\epsilon$  and k- $\omega$  turbulence models for the same model. It is found out that k- $\epsilon$  turbulence model has predicted the velocity field more accurate and faster by means of simulation time than the k- $\omega$  model.

A two-dimensional CFD model is applied by **Almani et al (2010)** to predict a downpull coefficient (KT and KB) which is named as FLUENT program. The finite volume method is employed on a Reynolds averaged Navier-Stokes equations. The turbulence effects are simulated using the standard (k- $\epsilon$ ) model. The simulation model is used for relevant experimental data obtained from hydraulic model tests conducted by (Ahmed 1999) in laboratory for nine gate lip shape with different gate openings for each gate lip geometry. It is found that the minimum positive downpull force can be reached for lip geometry with ( $\theta=35^\circ$ ).

**Dargahi (2010)** investigated the discharge characteristics of a bottom outlet with a moving gate by FLOW-3D software. The study based upon the pressurized and free

surface conditions applied for the scale model of scale model of Aswan Dam in Egypt. The establishment of fully flow was achieved by open the gate slowly so that it stays totally by filled water. The gate fully opening it was lead to produce the free flow condition. The Numerical model was applied for these two conditions and was well presented the water surface profiles, flow patterns and the estimation of discharges.

The distribution of pressure around the bottom of outlet leaf gate and its potential risk of cavitations and destructive vibrations of the gates was studied by **Amir Khosrojerdi (2012)**. The study based upon the three dimensional simulation of numerical method which was used to indicate the change in pressure and downpull forces during the vertical gate movements. It is found the downpull forces influenced by the upward and downward direction of gate movements.

**Naderi and Hadipour (2013)** were examined the distribution of pressure and consequently the related hydrodynamic forces on the valve of channel outlet for many opening ratios by utilizing the numerical method based upon the finite volume principles .The numerical model was verify by the corresponding results of physical as well as previous studies where the comparison gave good agreement .The study reveals that the differences in top and bottom of the valve pressures lead to create downpull force.

**Jelena Markovic – Brankovic and Helmut Drobier (2013)** in this study exhibits new smooth upstream face high head gate form that reduces hydrodynamic forces in conjunction to a total (negative downpull) forces. The investigations distinguished various changes in the configuration, which would decrease downpull and by and by the expense. After various attempts an adequate development change was found in the model. The consequences of the model tests demonstrate that an expansion in vertical openings of the gate leaf reduces the hydrodynamic forces fundamentally.

**Mehmet akiş uysal in 2014** proposed a method to predict the downpull forces on the tunnel gates which is installed in the intake of a hydropower plant. It is focusing on the evaluation of downpull forces for various closure rates and gate lip geometries. The outcomes are contrasted with results which were achieved by using ANSYS FLUENT programming as a tool for calculation. Downpull coefficients which have been got

from computational study demonstrated great concurrence with those obtained from measurements.

**Taha et al (2016)** were used a random hydraulic model to study the effects of twelve gate lips orientation on the behaviour of flow and consequently on the bottom pressure coefficient. The main conclusion indicates that the values of bottom pressure coefficient ( $K_b$ ) are inversely proportional to gate opening ratios ( $Y/Y_0$ ) and range from high values with small gate openings ratios and low values for ( $Y/Y_0 > 30\%$ ). The study finds that the bottom pressure coefficient ( $K_b$ ) and the fluctuations flow pattern below the gate surface are influenced mainly by the gate geometry.

In the current study, the down pull forces on the gates are evaluated for different flow rates, different gate lip geometries and different longitudinal slopes. The PASW Statistical Program is used for analyses and surfer program to represent the results. The measurements carried out by using the hydraulic of tunnel model with seven different lip shapes. The validity of the results is indicated by the comparison with corresponding cases of previous related works.

## CHAPTER 3

### EXPERIMENTAL WORK

As shown in previous studies, the hydraulic downpull force is based primarily on the prediction of downward vertical pressure coefficient termed as ( $K_t$ ) and uplift pressure coefficient ( $K_b$ ). These two important coefficients are influenced significantly by several parameters (see Figure 3.1) which mostly can be identified by the following function, **Ahmed (2016)**:

$$K_d = f \left( \frac{x}{x_0}, \theta, H_i, H_t, H_d, \frac{v_j^2}{2g}, \frac{Y}{Y_0} \right) \quad (3.1)$$

Where

$K_d$ : Downpull force coefficient,

$\frac{x}{x_0}$ : Distance ratio along bottom gate Surface,

$\theta$  : Angle of inclined lip gate,

$\frac{Y}{Y_0}$ : Gate opening ratio,

$H_i$ : Piezometric head on bottom gate surface,

$H_t$ : Piezometric head on top gate surface

$\frac{v_j^2}{2g}$ : Jet velocity head, and

$H_d$ : Downstream Piezometric head.

In order to explore the unbalanced forces applied on the top and bottom gate surface, many experiments carried out in this investigation, involved all required measurements and regarded the mentioned basic parameters and flow conditions. The experiments includes more than (84) runs covering (7) different gate lip geometries.

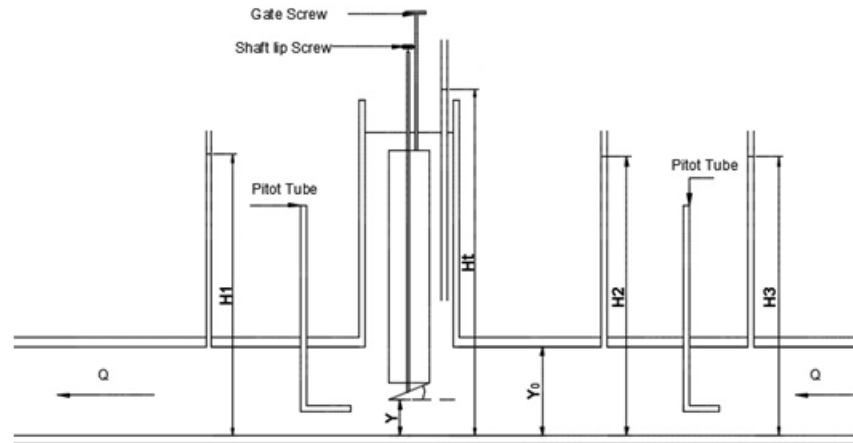


Figure 3.1 Tunnel Sketch with explanation of parameters.

The random hydraulic model which was designed by Ahmed (2016) has been established in Hydraulic Laboratory of Ishik University/Erbil /Iraq to carry out all the tests and measurements needed to cover the required elements of the study. In this chapter the experimental set-up, equipment used and the procedure followed in achieving the measurements are described.

### 3.1 EXPERIMENTAL SET –UP:

The experiments were conducted by using rectangular recirculation flume, 4m long, 0.2 m wide and 0.3m deep. The bed and both sides of channel were made by glass and covered along its upper part by a thick plate representing the tunnel roof. The steel gate shaft (0.3 x 0.15 x 0.6) m was installed mid-way above the flume roof.

The head of tunnel was fed by stilling tank to confine the flow within the acceptable limits due to the turbulence effects .The flow is returned to the storage tank through the control sluice gate which was installed at the end tunnel .The control gate is essential to create a pressurized flow and hence satisfy the flow conditions required for study. AC motor was used to derive a 4 kw pump, thereby providing the discharge which adjusting by a valve. The main components of hydraulic model are shown in (Figure 3.2).

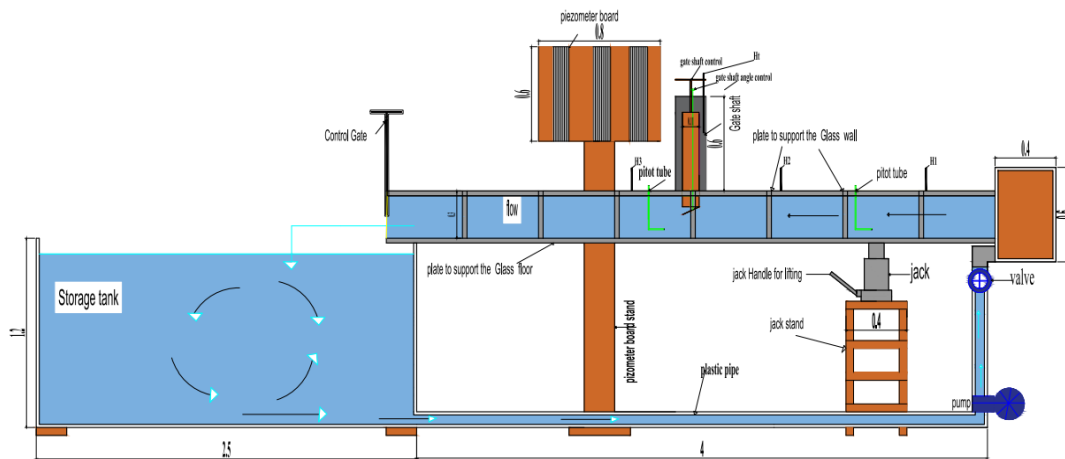


Figure 3.2 Main components of hydraulic model.

The model of gate was made by a thick plate with a thickness ( $d$ ) of 70 mm, 200 mm wide and 50 mm height was supported by steel frame slides in vertical way of the gate shaft, For mechanical function, the gate is provided by two screw shafts had been located on the top cover of gate shaft, one to control the gate openings and the other to adjust the angle of lip gate. (Figure 3.2) shows the main details of gate model.

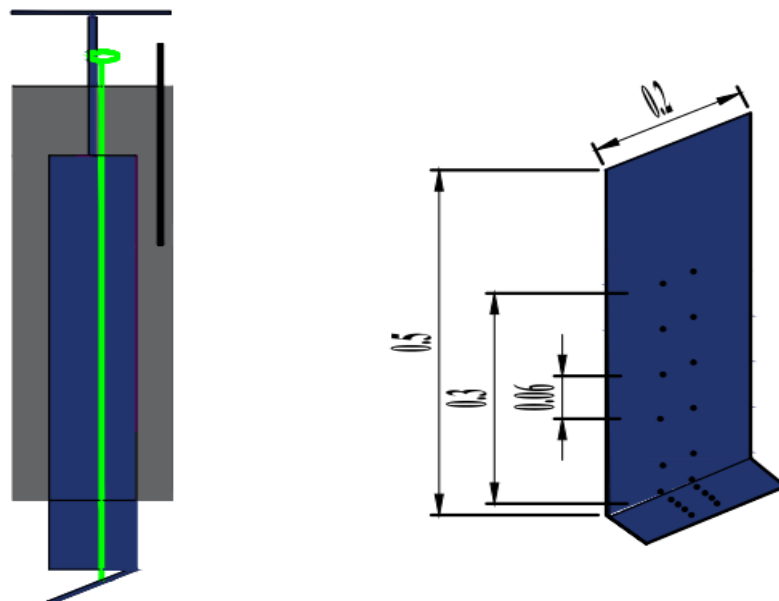


Figure 3.3 Main Details of gate model.

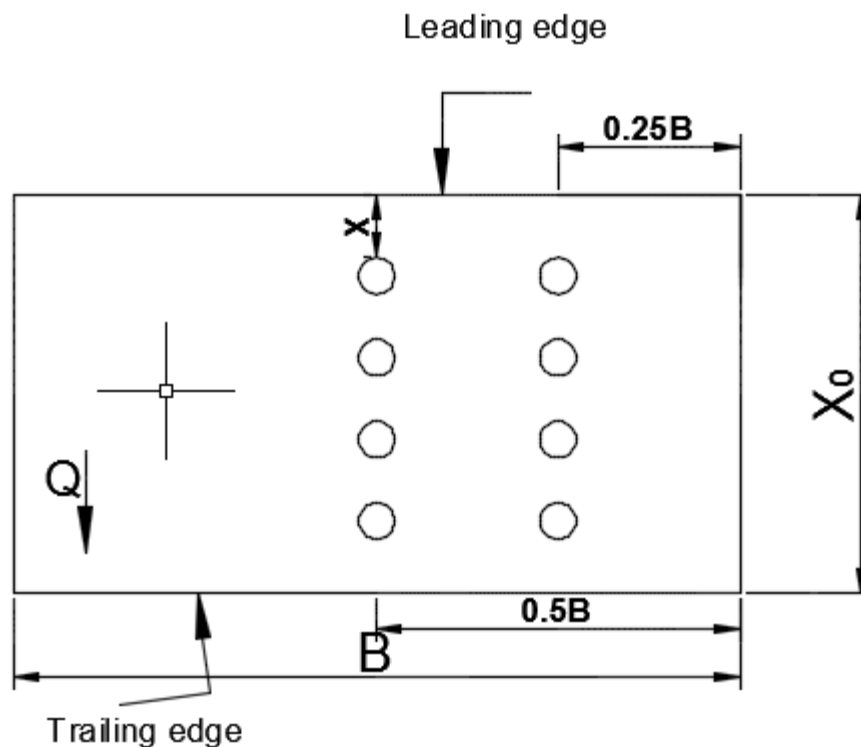


Figure 3.4 Gate shaft lip detail

Twelve taps, 4 mm in diameter, were drilled along two vertical parallel lines of upstream gate face. The first and second six taps were located at distances  $0.25 B$  and  $0.5 B$  respectively from right gate edge with 5 cm interval distance (see Figure 3.4). The small length steel tubes of the same diameter inserted in each tap, and then connected through plastic tubes to a manometer board.

The movable bottom plates of the gate made by steel plate formed different inclined gate lipshapes. Two lines of four taps each were positioned along the gate lip surface in the same direction of flow, first set of taps was fixed at a distance  $0.25 B$  from right gate edge with equal interval distance from each to other, the second set located at  $0.5 B$ . The small length steel tubes were inserted to the taps and then connected to manometers board through plastic tubes.

The estimation of flow rate and the velocity distribution have been carried out by using two pito-tubes. One of them was located at a distance 1 m upstream the gate shaft while the other locates just downstream the gate shaft. Two Piezometers

were installed upstream the gate shaft with consecutive distances (0.25 m and 0.5 m) to represent the operation heads, furthermore, another one it was needed to be 20 cm downstream the gate shaft which is necessary for determine the pressure coefficients. The longitudinal slope of tunnel was adjusted by using a hydraulic jack.

### **3.2 PROCEDURE OF MEASUREMENTS**

The current study includes more than (84) runs .Each run was conducted for specific values of gate lipangle, longitudinal slope and flow rate .Herein , seven gate lipangles were used , each one was examined for three different values of flow rates and four longitudinal slopes. The following flow chart shows a general concept of runs for each angle (see Figure 3.5).

Each run starting by let the constant flow rate enters the stilling tank and move along the tunnel and then return back again to the main tank through the control gate. (Figure 3.1) shows the sections of the tunnel, its apparatus and the main points of measurements.

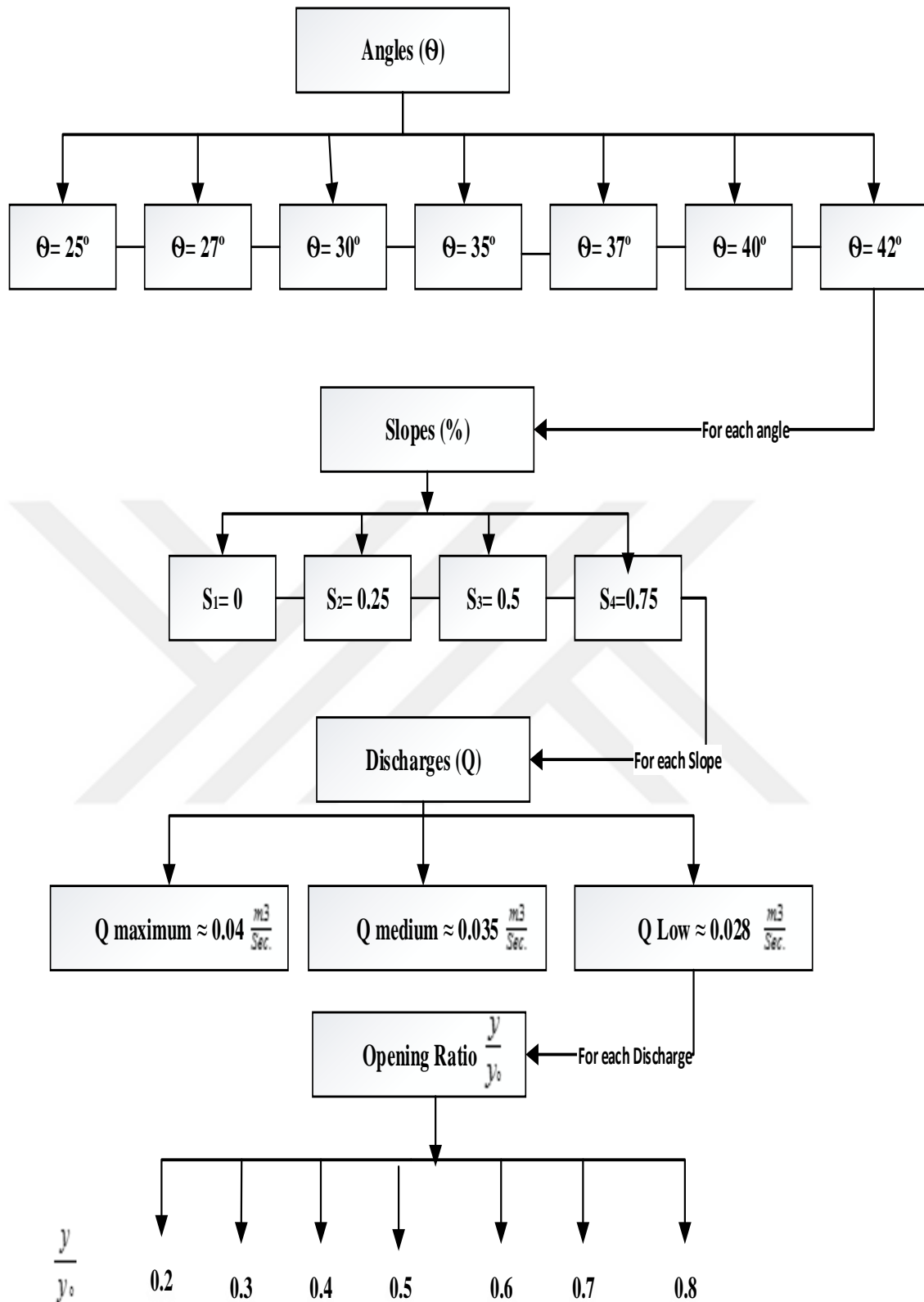


Figure 3.5 Flow chart of runs for each angle.

The following measurements have been achieved for each run with different gate openings ( $Y/Y_0$ ):

1. The two upstream pressure heads ( $H_1$  &  $H_2$ ) and one downstream head ( $H_3$ ) were measured. The determination of ( $H_3$ ) is important to predict the pressure coefficients as mentioned previously.
2. The top pressure head ( $H_t$ ) which reflect the effects of flow rate part passing through the clearances of gate shaft was measured by using a single piezometer installed on the top surface of gate.
3. Eight 4 mm diameter taps with their small steel tubes had been inserted in two parallel lines to measure the distribution of piezometric heads ( $H_i$ ) along and cross the gate lip surface. The fluctuation in pressure head were fixed by takes the average of several readings.
4. The piezometric head on the upstream face of the gate ( $H_f$ ) was measured by means of piezometers openings distributed as mentioned before and connected to the manometer board by plastic tubes, (see Figure 3.5).
5. The measurements of velocity profiles was made in two stations, first located at 1.0 m upstream the gate shaft to measure mainly the total flow rate, and second 0.1m just downstream the gate shaft to measure the jet velocity head beneath the gate. The discharge at each run was estimated by using the integrating area method of the velocity.
6. For each run, the slope of gate lip was adjusted by using the related screw in the top of gate shaft whereas the longitudinal slope was fixed by using hydraulic jack locates below the tunnel bed.

All measurements were conducted in present study have been considered the tunnel bed as datum. The data obtained from each experimental run were listed in data sheets such as shown in (Figure 3.7).



The above procedure was repeated in seven gate openings for each of various seven gate lipshapes considered in present study, thus, as stated before, the experiments carried out through more than 86 experimental runs.



## CHAPTER 4

### RESULTS AND DISCUSSION

The results and analysis of all measurements which had been carried out in present study are presented and discussed in this chapter .The measurements were conducted in the laboratory flume for various inclined gate lip shapes. Each shape was examined for specific longitudinal slope and three different values of flow rate. The experimental work contains more than 84 runs to evaluate top and bottom pressure coefficients in addition to downpull force coefficient.

#### 4.1 FLOW ANALYSIS

The current study includes the measurements of velocity profiles in a point 1 m upstream the gate shaft by using a differential Pito-tube and the following equation was used to determine the discharge (Q) passing through the tunnel for each opening during each run.

$$Q = Y_o \cdot B \sqrt{2g (\Delta h)} \quad (4.1)$$

Where

Q: Main flow rate passing through the tunnel ,m<sup>3</sup>/sec,

B : Gate width, m,

Y<sub>o</sub> :Height of tunnel, m,

Δ h: Pressure head difference of pito-tube readings, m.

In current study ,all considered parameters measurements were carried out for three values of flow rates named as (Q<sub>L</sub> , Q<sub>med</sub> , Q<sub>max</sub> ) .The mean values of these three flow rates had been found by applying Eq. (4-1) and consequently , the corresponding values of Reynolds number were also been found by using Eq.(4.1A).

$$R_e \times 10^5 = \frac{40.A.V}{P.v} = \frac{20.Q}{(B+Y_o).v} \quad (4.1A)$$

The mean values of Turbulent submerged flow rates are listed in following table.

Table 4.1 Mean values of submerged flow rates and corresponding Reynolds Number.

Q	Q <sub>L</sub> . m <sup>3</sup> /sec	Q <sub>med</sub> . m <sup>3</sup> /sec	Q <sub>max</sub> . m <sup>3</sup> /sec
Mean Value	≈0.028	≈0.035	≈0.04
Reynolds No.	0.99 × 10 <sup>5</sup>	1.24 × 10 <sup>5</sup>	1.416 × 10 <sup>5</sup>

## 4.2 DOWNPULL COEFFICIENTS:

The downpull force is defined as the net force produced from the difference between the downward force exerted on the gate top as a result of water pressure in the gate shaft and the upward force on the gate bottom by water jet passing through gate opening. The net force is termed Positive downpull when its direction is downward and negative downpull when it is in the upward direction. The basic hydraulic measurements needed for determining downpull coefficient are described in chapter three. The top pressure coefficient ( $K_t$ ), the bottom pressure coefficient ( $K_b$ ), and downpull coefficient are discussed in the following sections.

### 4.2.1 Top pressure Coefficient ( $K_t$ ):

The top pressure coefficient ( $K_t$ ) considered as a function of several factors related to gate geometry and flow conditions which can be express in the following form[Ahmed 2016]:

$$K_t = f\left(H_t, \frac{v_j^2}{2g}, H_d\right) \quad (4.2)$$

Where

$K_t$ : Top pressure coefficient,

$H_t$ : Piezometric head on top gate surface,

$\frac{V_j^2}{2g}$ : Jet velocity head, and

$H_d$ : Downstream Piezometric head.

The top pressure coefficient ( $K_t$ ) can be found by using the following formula, **Naudascher (1964)**:

$$K_t = 1/Bd \int_0^d \int_0^B (H_t - H_d) / (V_j^2 / 2g) dB. dx \quad (4.3)$$

Where:

$d$  = the gate thickness, and

$V_j$  = the jet velocity beneath the gate.

According to the invariant distribution of top pressure head along top surface of gate the above equation can be reduced to be:

$$K_t = (H_t - H_d) / (V_j^2 / 2g) \quad (4.4)$$

In current study the top pressure coefficient were examined for various angles of inclined lip gate, different values of flow rate and longitudinal slope of simulated tunnel.

Equation (4.4) indicates that the calculation of ( $K_t$ ) is depend upon the measurements of the piezometric head on the top surface of the gate ( $H_t$ ), piezometric head at downstream of the gate ( $H_d$ ), and the average jet velocity beneath the gate ( $V_j$ ). The measurements of ( $H_t$ ) were made by install the scaled glass tube the top surface of the gate. Many readings were taken and the average value was considered and the upstream and downstream gap widths are assumed to be constants.

(Figures 4.1 to 4.4) are showed the relation between the gate opening ratios ( $Y/Y_0$ ) and top pressure coefficients for different flow rates, longitudinal slopes and gate lip angles. It can be seen from these figures that for each gate lip geometry, mostly, a slight change in distribution profile is occur with the increase of gate opening ratios .The general scheme of ( $K_t$ ) profile curves emphasize that only the values have been effectively influenced by gate geometries and consequently an effect it will create on values of downpull force . (Figure 4.1) ,indicates that for ( $S=0$ ) ,the increase in flow rate

has caused increase in (Kt) values for all gate lip angles except ( $\theta=25^\circ, 35^\circ$  and  $42^\circ$ ) which are mostly have lower values .

(Figure 4.2) demonstrates that for (S=0.25%) , the gate lip with ( $\theta=37^\circ$ ) has a peak values and independent effect due the change in flow rates .In general ,some changes have been observed for the (Kt) values not for behaviour of the whole gate lip shapes with the increasing of flow rates.

It can be seen from (Figure 4.3) , that the increase in longitudinal slope and flow rates had not accompanied by a clear changes in values and distributions of (Kt) for all gate lips except for ( $\theta=27^\circ$ ) where the values of (Kt) are dropped as a result to the increase in flow rates.

(Figure 4.4) indicates that for (S=0.75%) and (Q<sub>low</sub>, Q<sub>med.</sub> and Q<sub>max.</sub>) ,the values of (Kt) are seem to be concentrated a round (0.5) for all gate lip shapes except ( $\theta=27^\circ$  and  $35^\circ$ ) where the values are often greater than others.

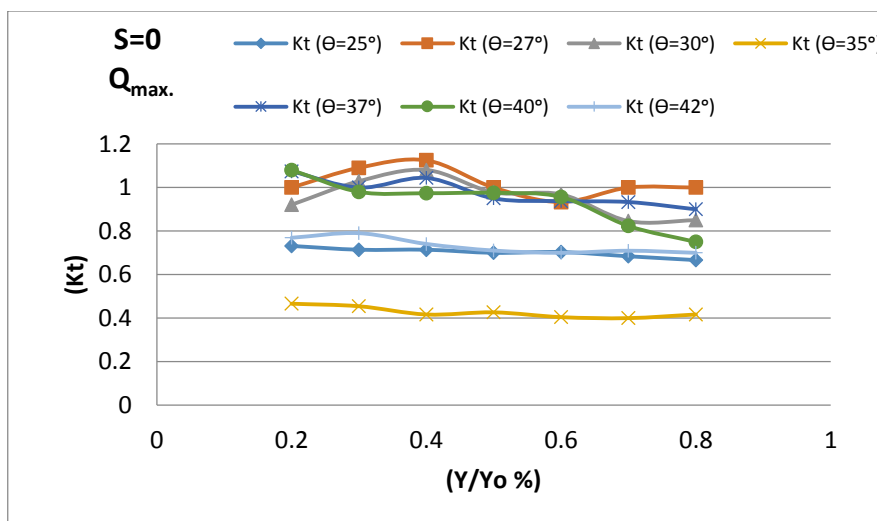
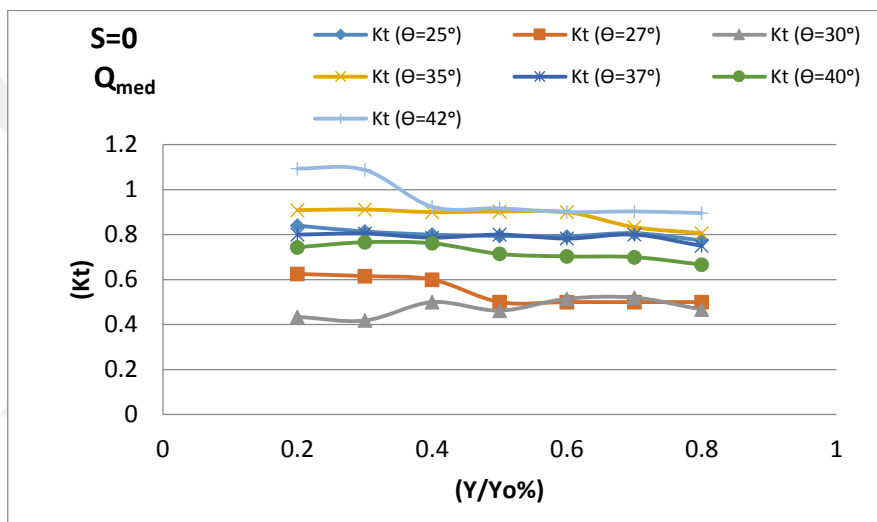
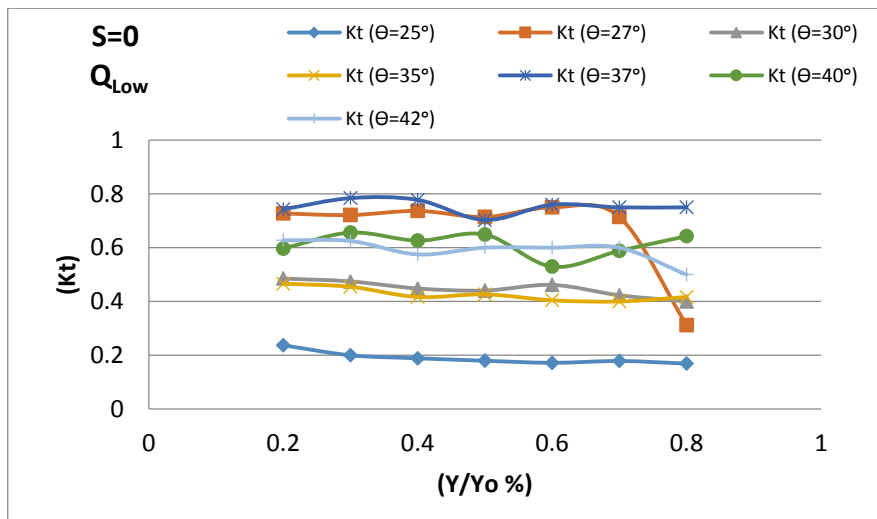
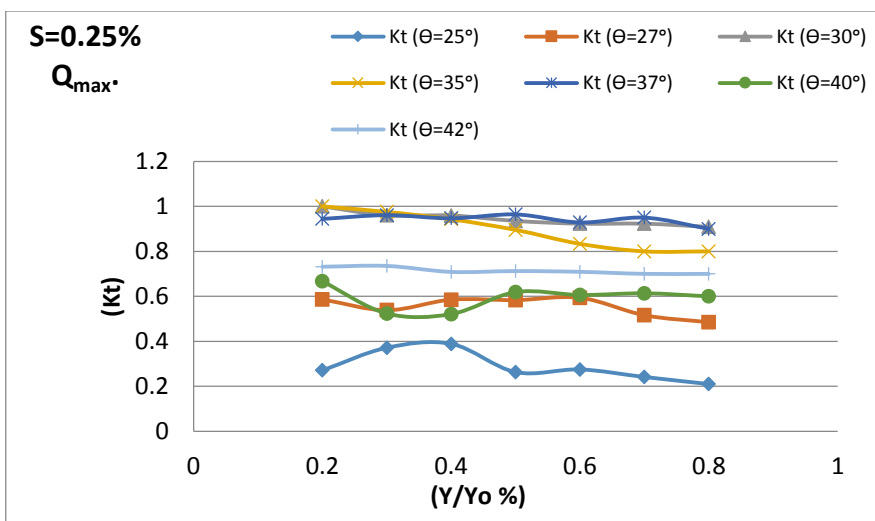
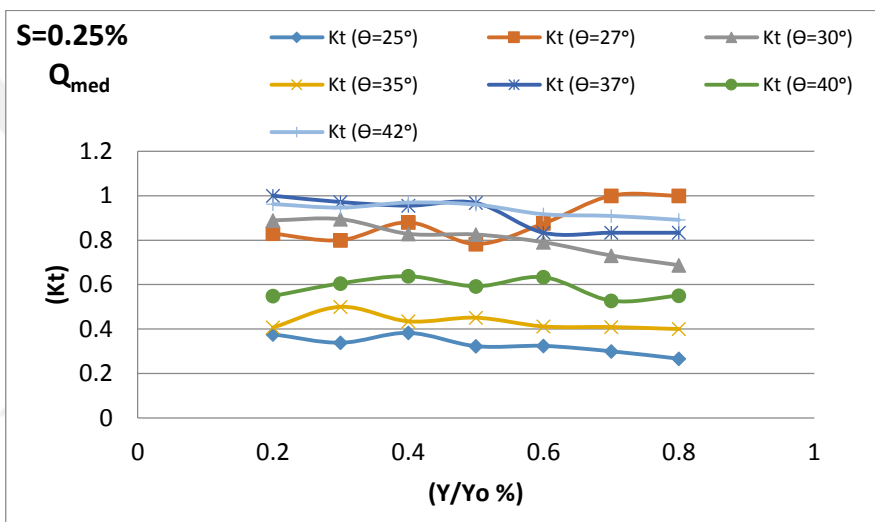
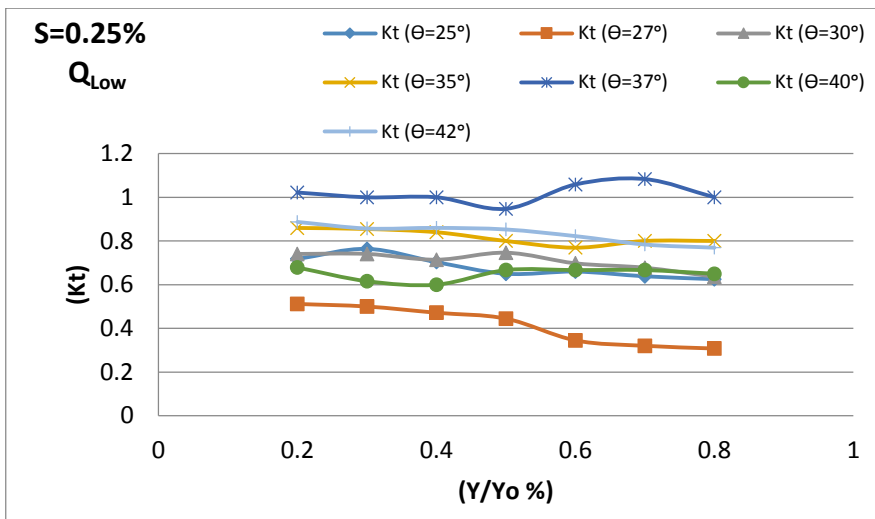


Figure 4.1 Variation of Kt with opening ratio for slope zero in different gate shape lips, and different discharges.



.4-2 Variation of Kt with opening ratio for slope % 0.25 in different gate shape lips, and different discharges.

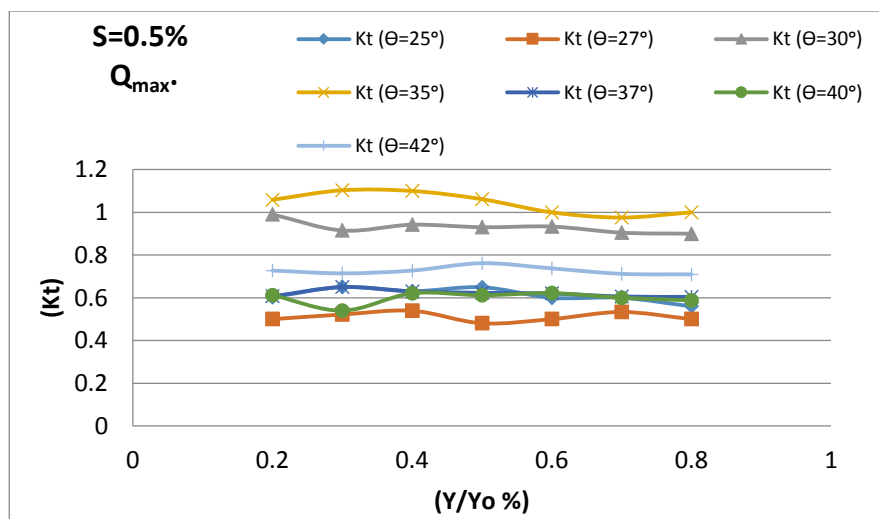
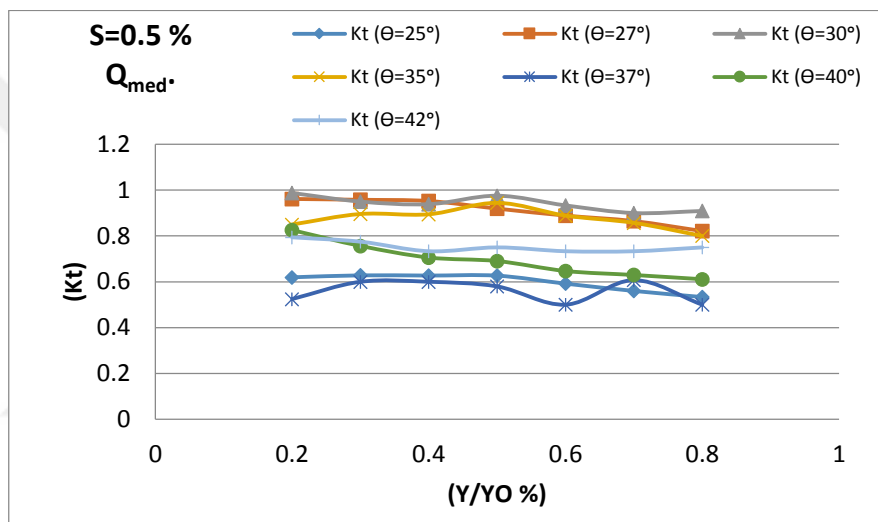
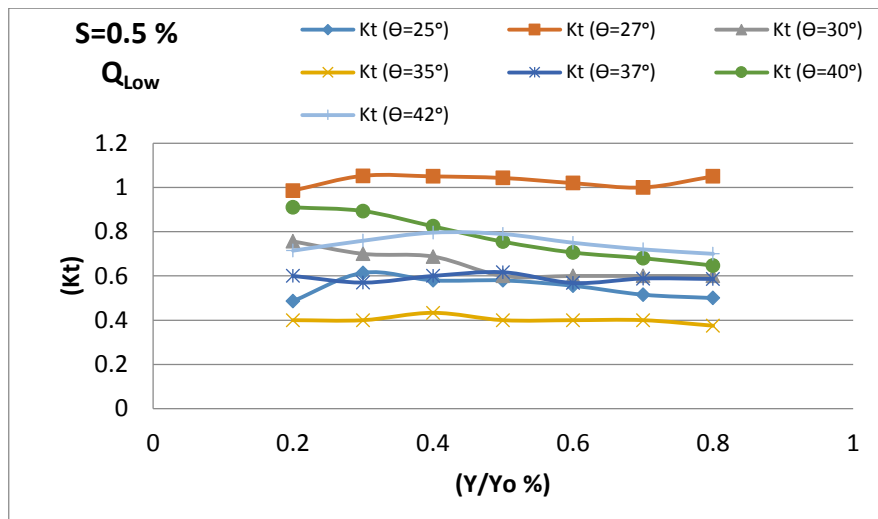


Figure 4.3 Variation of Kt with opening ratio for slope %0.5 in different gate shape lips, and different discharges.

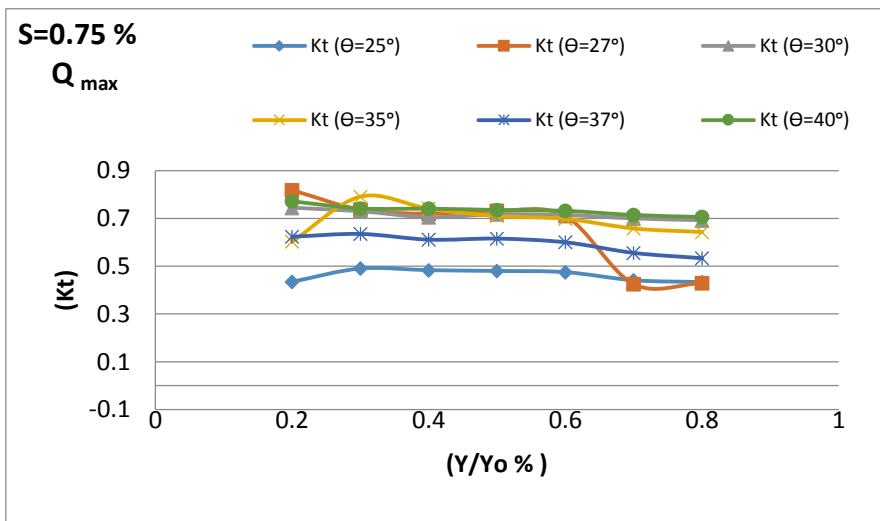
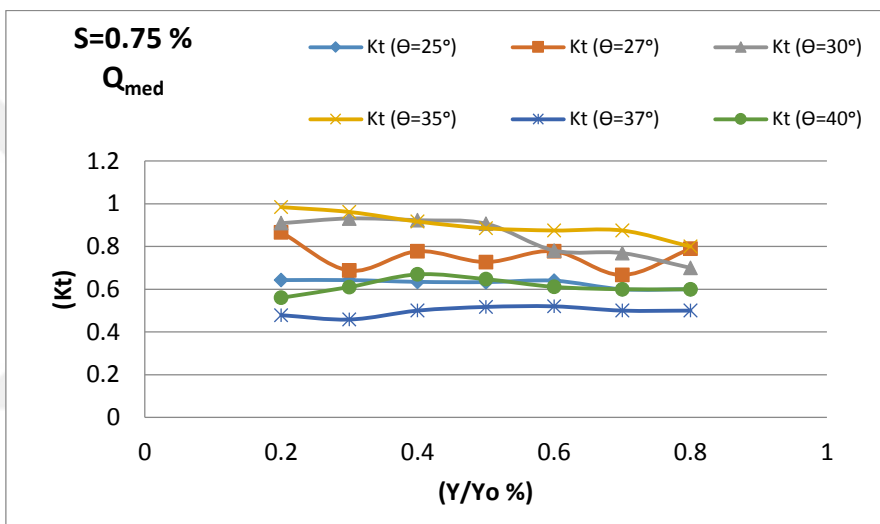
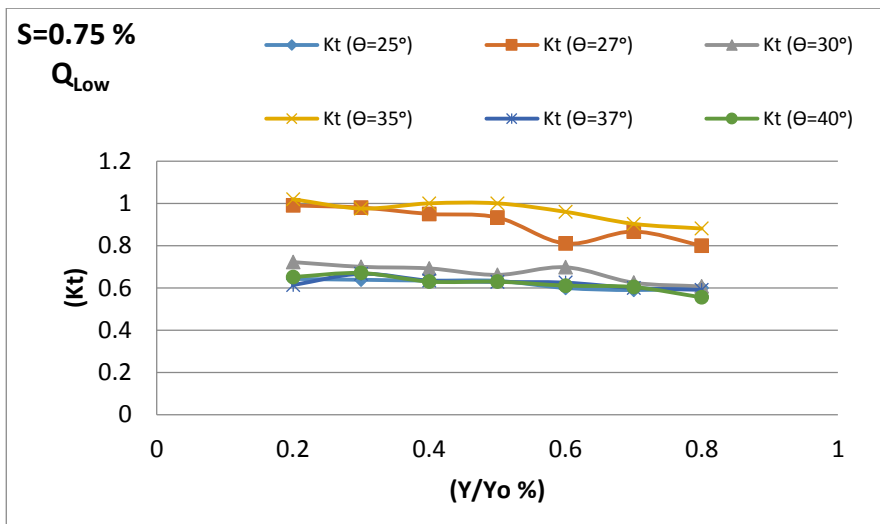


Figure 4.4 Variation of Kt with opening ratio for slope zero in different gate shape lips, and different discharges.

The effects of four considered values of slopes with different geometry shapes of gate lip on (Kt) values have also been studied for specific values of flow rates as shown in Figures from (4.5) to (4.7) .These figures shows that there is no one slope has a definite clearly affects for all cases, and then, each case it may subjected to the influences of its limits. However, the values of slopes (S=0.25%) and to some extent (S=0%) have a greater impact in increasing top pressure coefficient values especially for low and maximum flow rates of angles ( $\theta = 27^\circ$  and  $\theta = 37^\circ$ ) up to ( $Y/Y_0 = 50\%$ ).



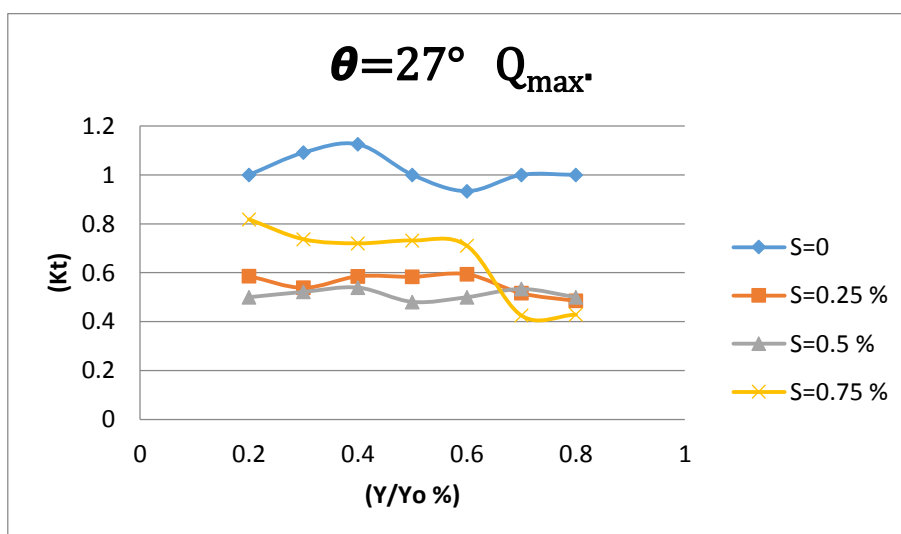
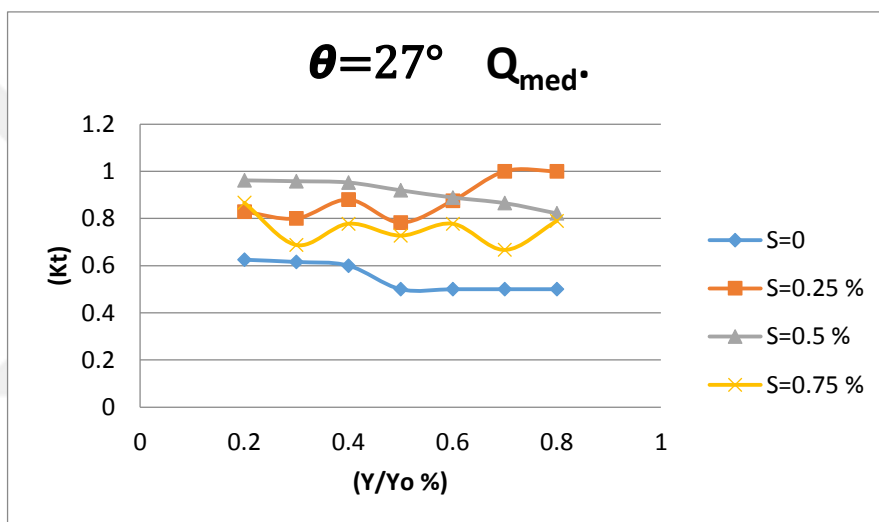
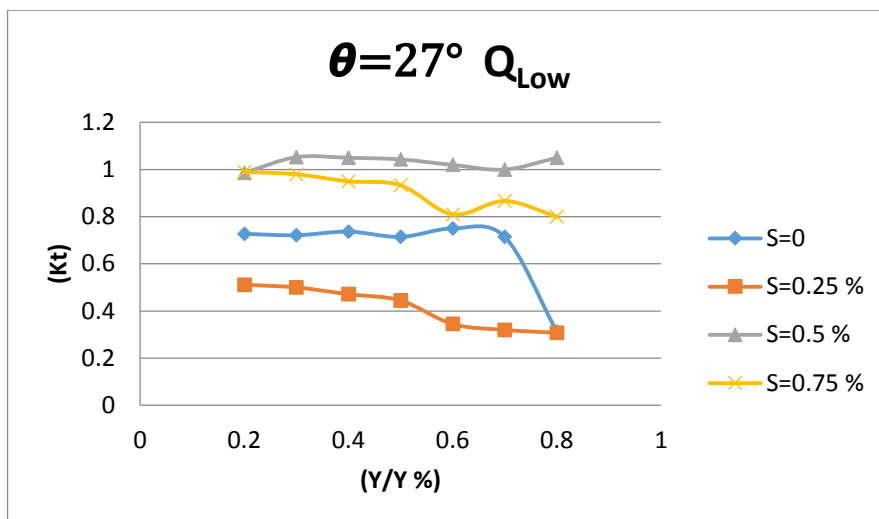


Figure 4.5 Variation of top pressure coefficients with gate openings of shape lip  $27^\circ$  for different Slopes.

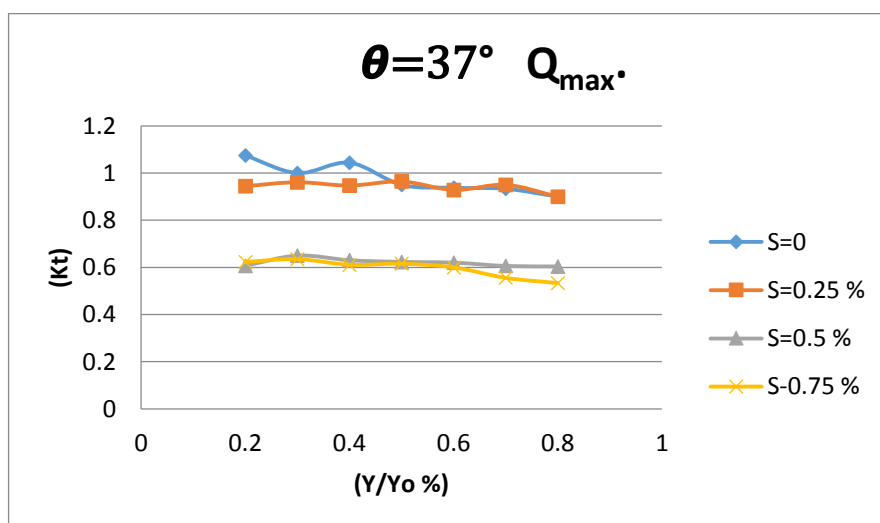
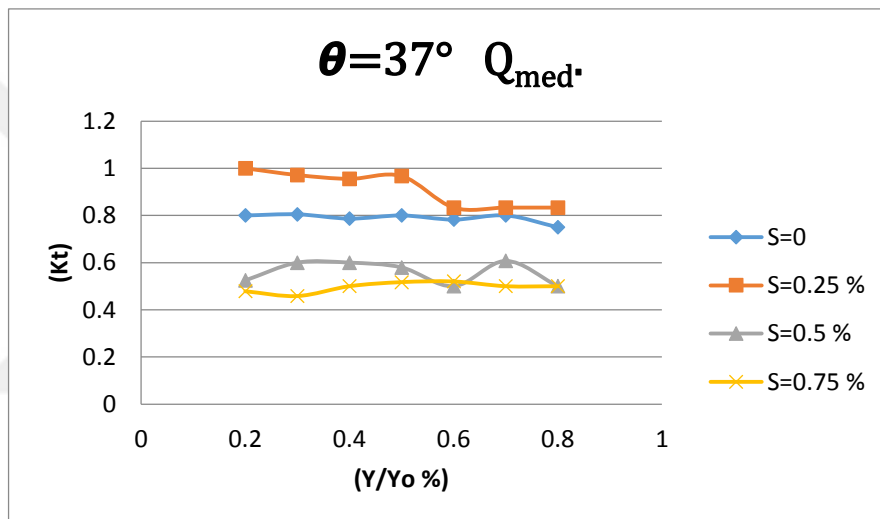
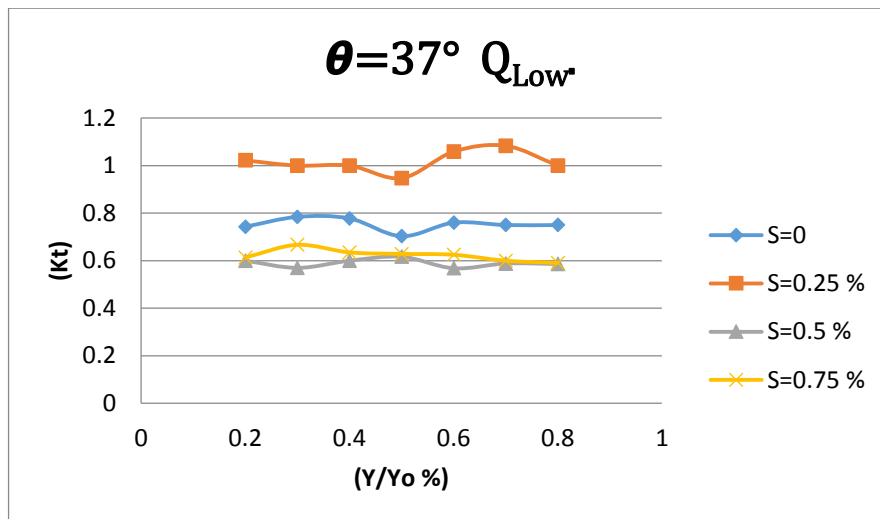


Figure 4.6 Variation of top pressure coefficients with gate openings of shape lip  $37^\circ$  for different slopes.

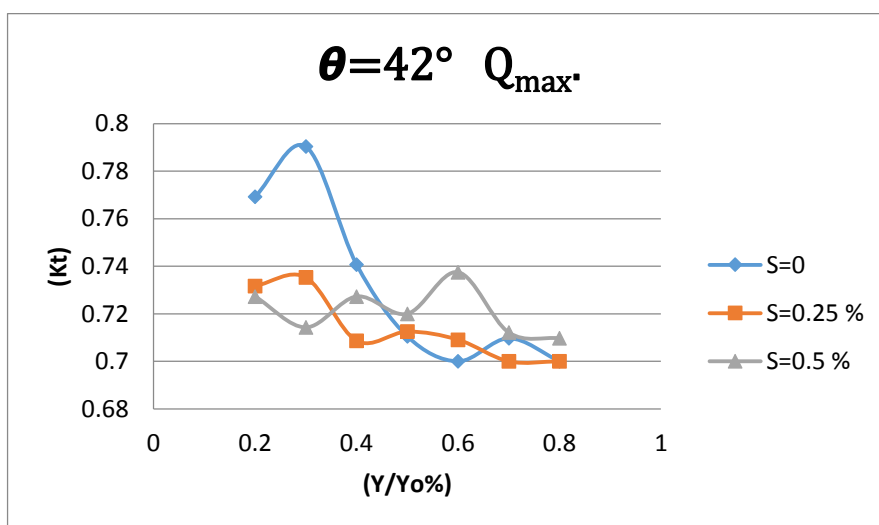
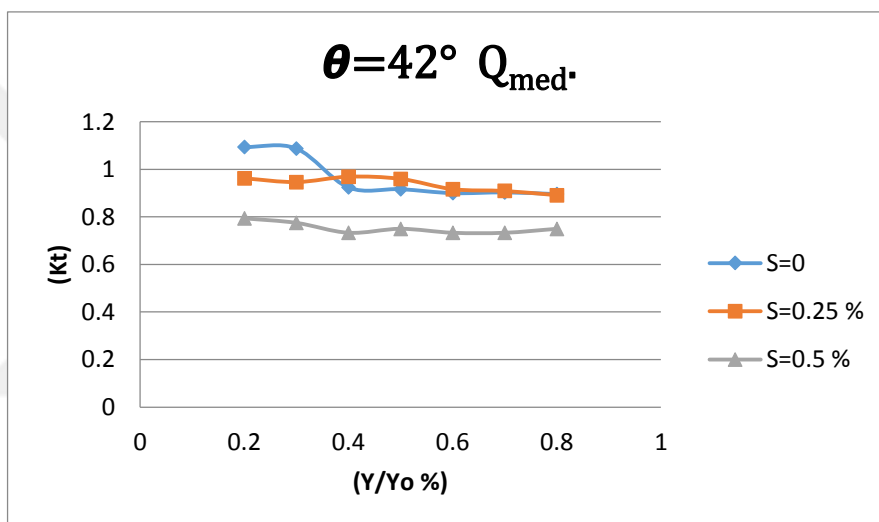
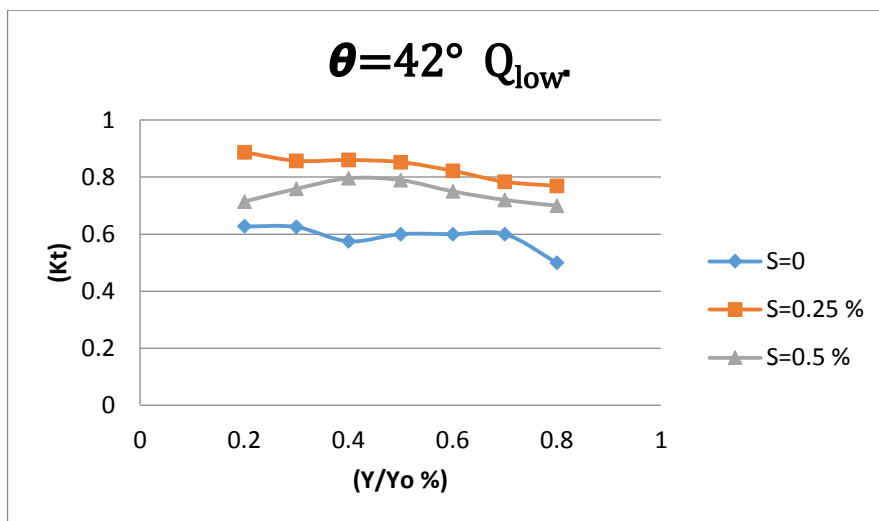


Figure 4.7 Variation of top pressure coefficients with gate openings of shape lip  $42^\circ$  for different slopes.

#### 4.2.2 Bottom Pressure Coefficient ( $K_b$ ):

The pertinent independent variables that affect the bottom pressure coefficient can be representing in the following functional relationship among the significant non dimensional parameters:

$$K_b = f \left( \frac{x}{x_o}, H_i, H_d, \frac{v_j^2}{2g}, \frac{Y}{Y_o} \right) \quad (4.5)$$

Where

$K_b$ : Bottom pressure coefficient,

$\frac{x}{x_o}$ : Distance ratio along bottom gate Surface,

$\frac{Y}{Y_o}$ : Opening ratio,

$H_i$ : Piezometric head on bottom gate surface,

$\frac{v_j^2}{2g}$ : Jet velocity head, and

$H_d$ : Downstream Piezometric head.

The bottom pressure coefficient ( $K_b$ ) is calculated using the expression:

$$K_b = \frac{(H_i - H_d)}{\frac{v_j^2}{2g}} \quad (4.6)$$

Where ( $H_i$ ) is the local piezometric head on the bottom gate surface which is measured eight piezometric holes as shown in (Figure 4.8). The measurements were made with the gate held stationary under free and submerged flow conditions.

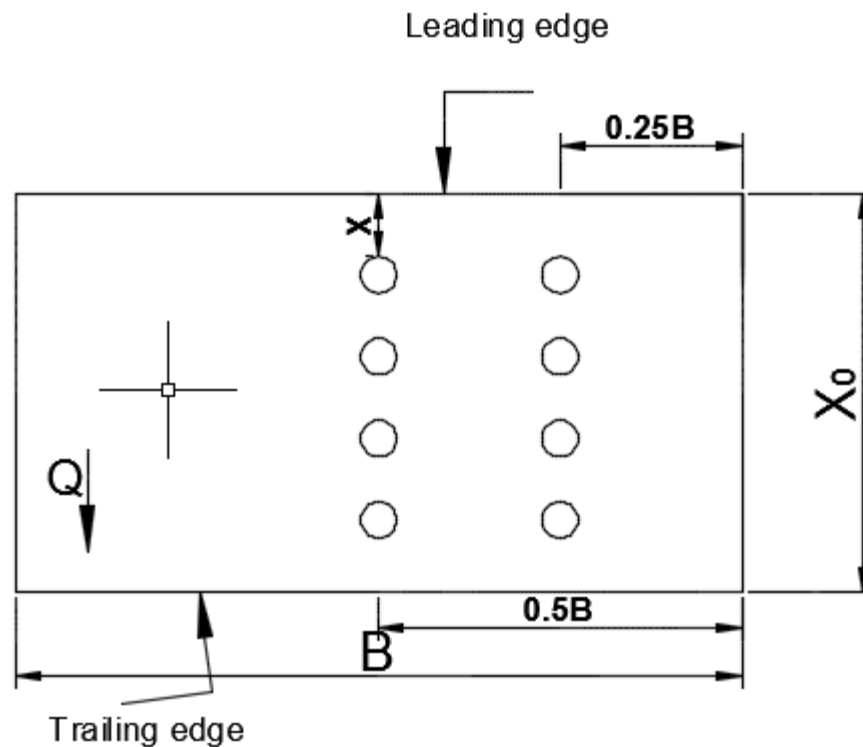


Figure 4.8 Location of the piezometer holes on the bottom lip surface while  $X_0$  and  $B$  are constants ( $X_0=7\text{cm}, B=20\text{ cm}$ ).

#### 4.2.2.1 Effects of Flow Rates and Longitudinal Slope on ( $K_b$ ):

The variation of bottom pressure head coefficients ( $K_b$ ) along the different gate lip shapes, are presented versus various gate openings in (Figures 4.9 to 4.15) for numerous flow rates and slopes. The ( $K_b$ ) values in these figures obtained from average ( $H_i$ ) measurements of eight piezometric holes located along and across bottom gate lip.

It can be seen from (Figure 4.8) that for ( $S=0, QL$ ), the values of ( $K_b$ ) are ranged between low values up to ( $K_b=0.5$ ) and then increased mostly beyond gate openings ( $Y/Y_0=50\%$ ). The increase in flow rate values lead to a slight change in values of ( $K_b$ ) for ( $Q_{med.}$ ) and much more for ( $Q_{max.}$ ) caused also some change in distribution especially for angles ( $\theta = 27^\circ$  and  $\theta = 37^\circ$ ).

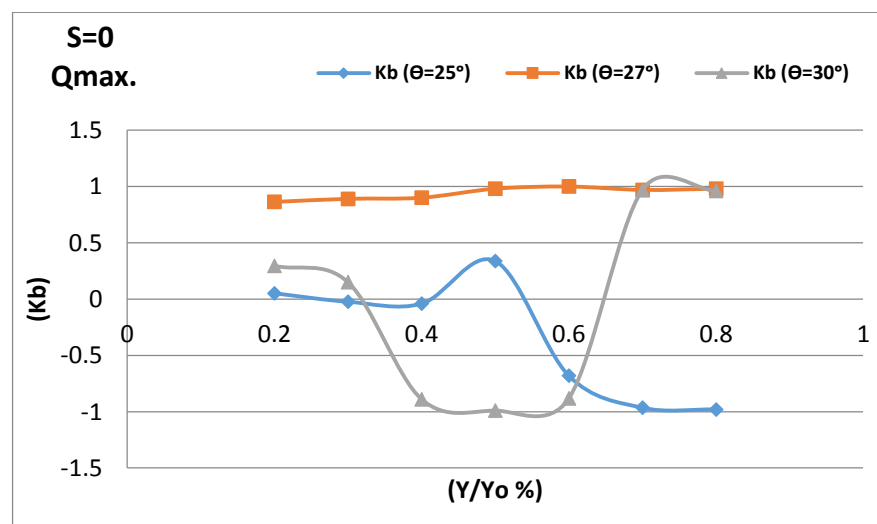
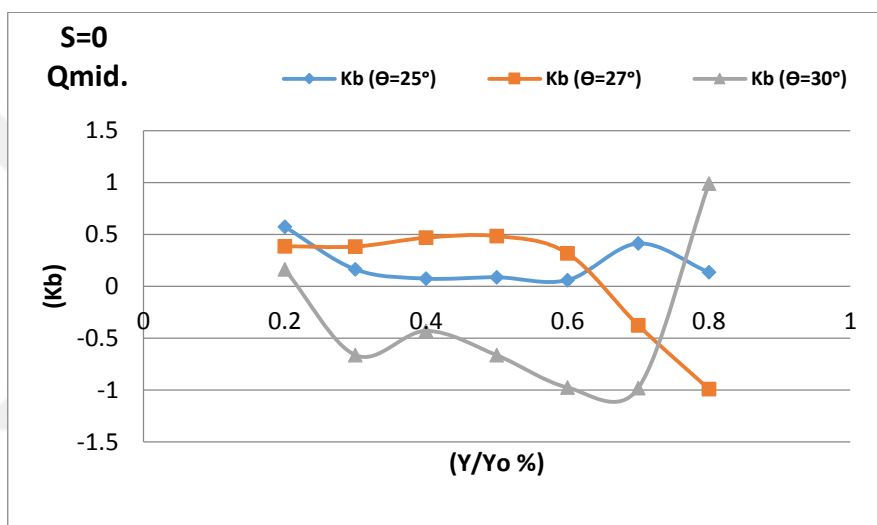
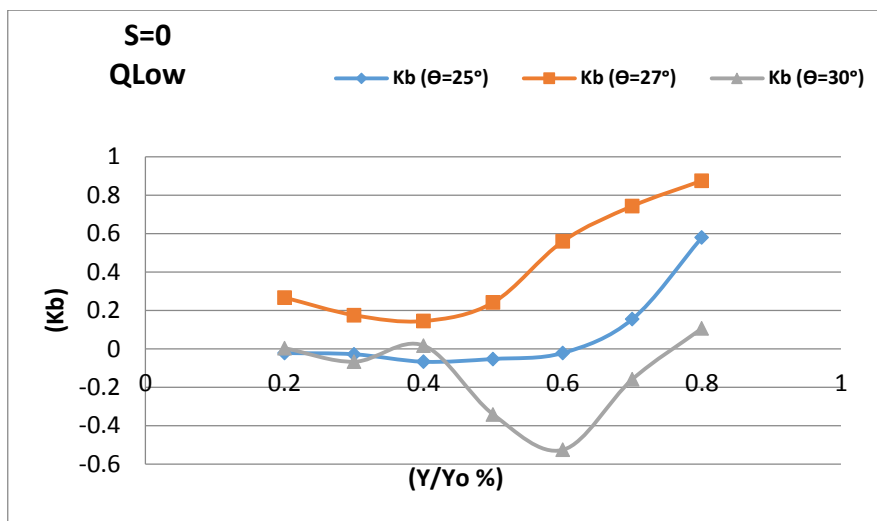


Figure 4.9 Variation of bottom pressure coefficient with gate openings for gate shape lips(25,27,30) when the slope is zero.

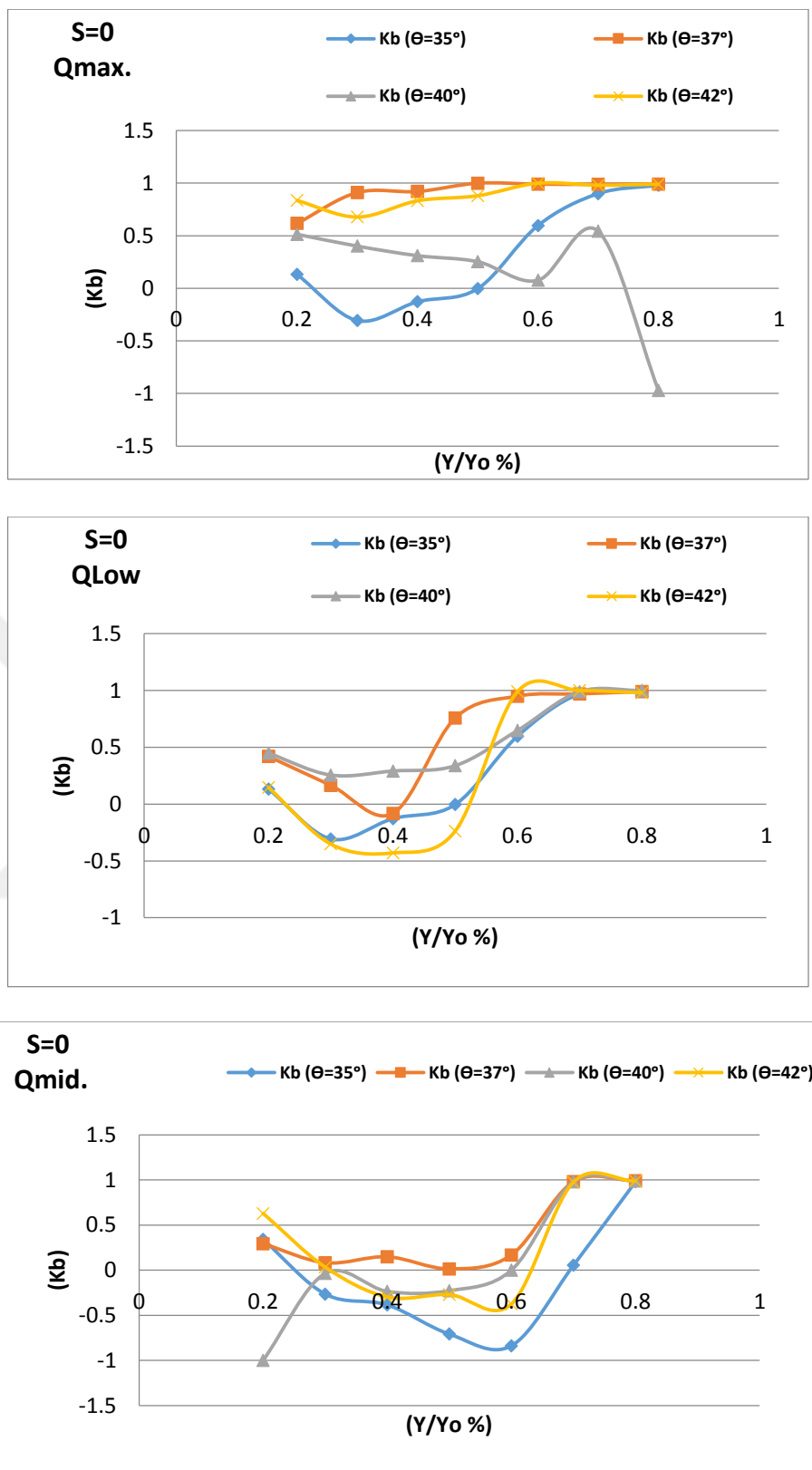


Figure 4.10 Variation of bottom pressure coefficient with gate openings for gate shape lips(35,37,40,42) when the slope is zero.

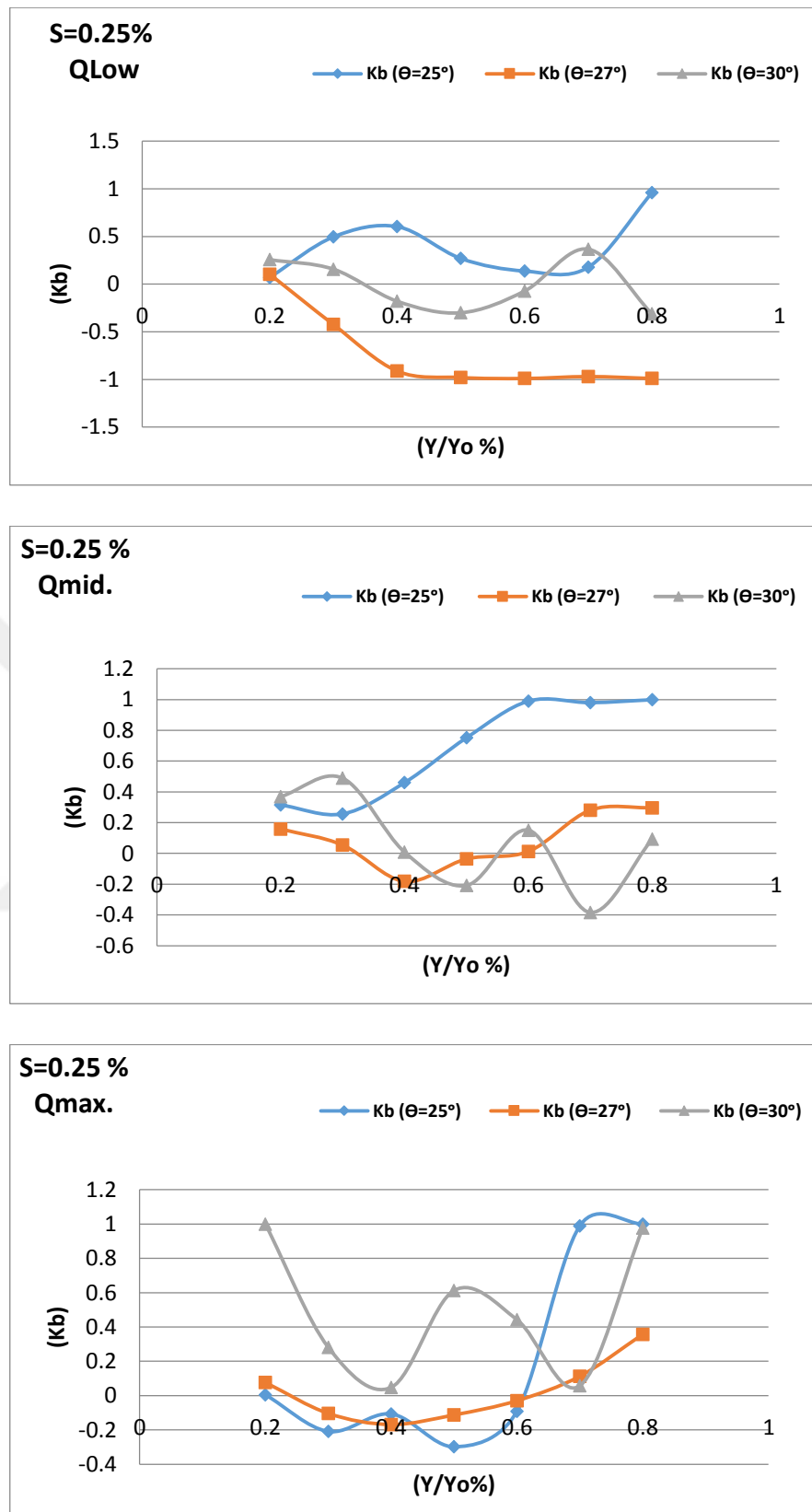


Figure 4.11 Variation of bottom pressure coefficient with gate openings for gate shape lips (25,27,30) when the slope is ( $S= 0.25\%$ ).

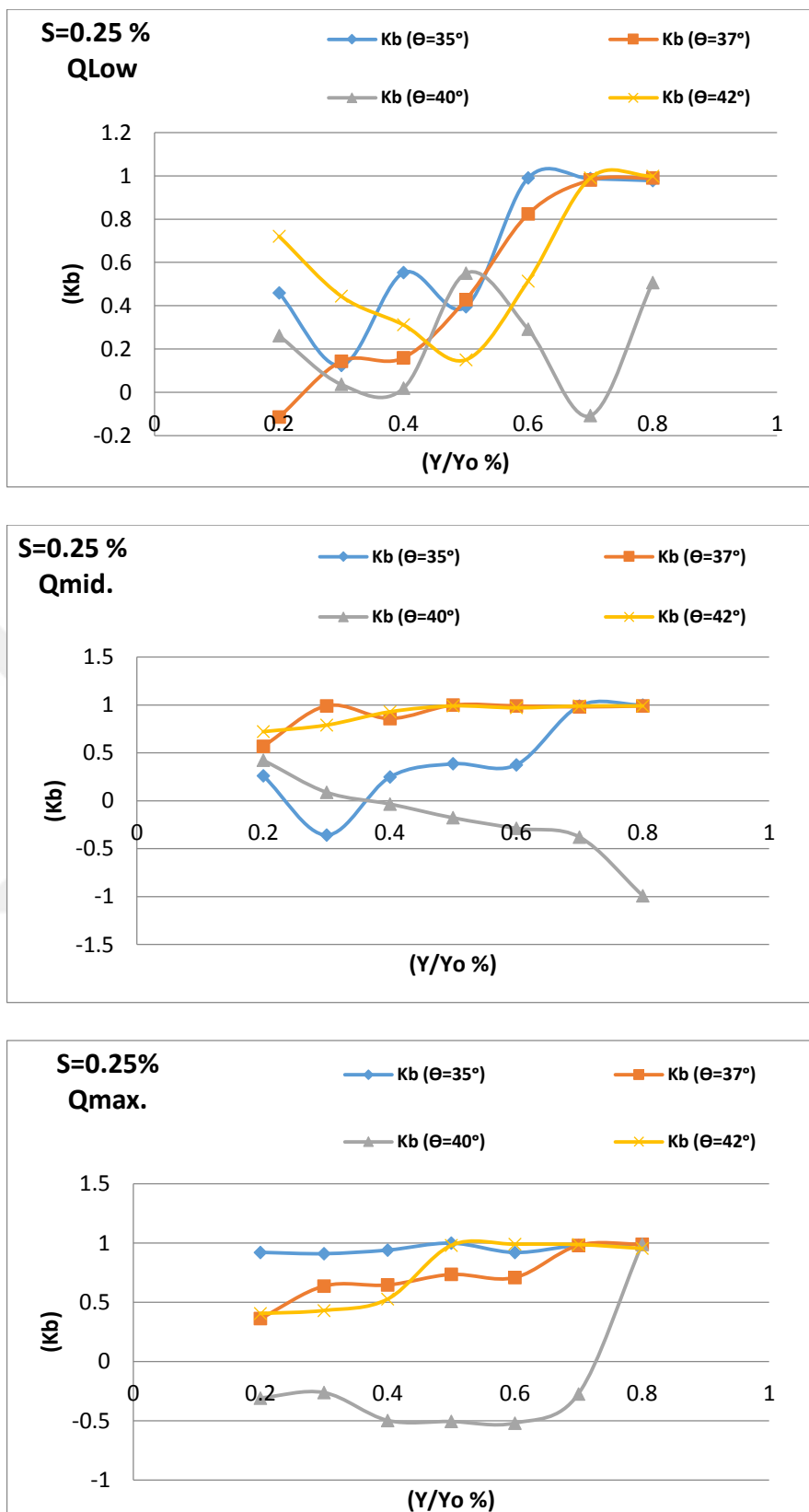


Figure 4.12 Variation of bottom pressure coefficient with gate openings for gate shape lips (35, 37, 40, 42) when the slope is ( $S=0.25\%$ ).

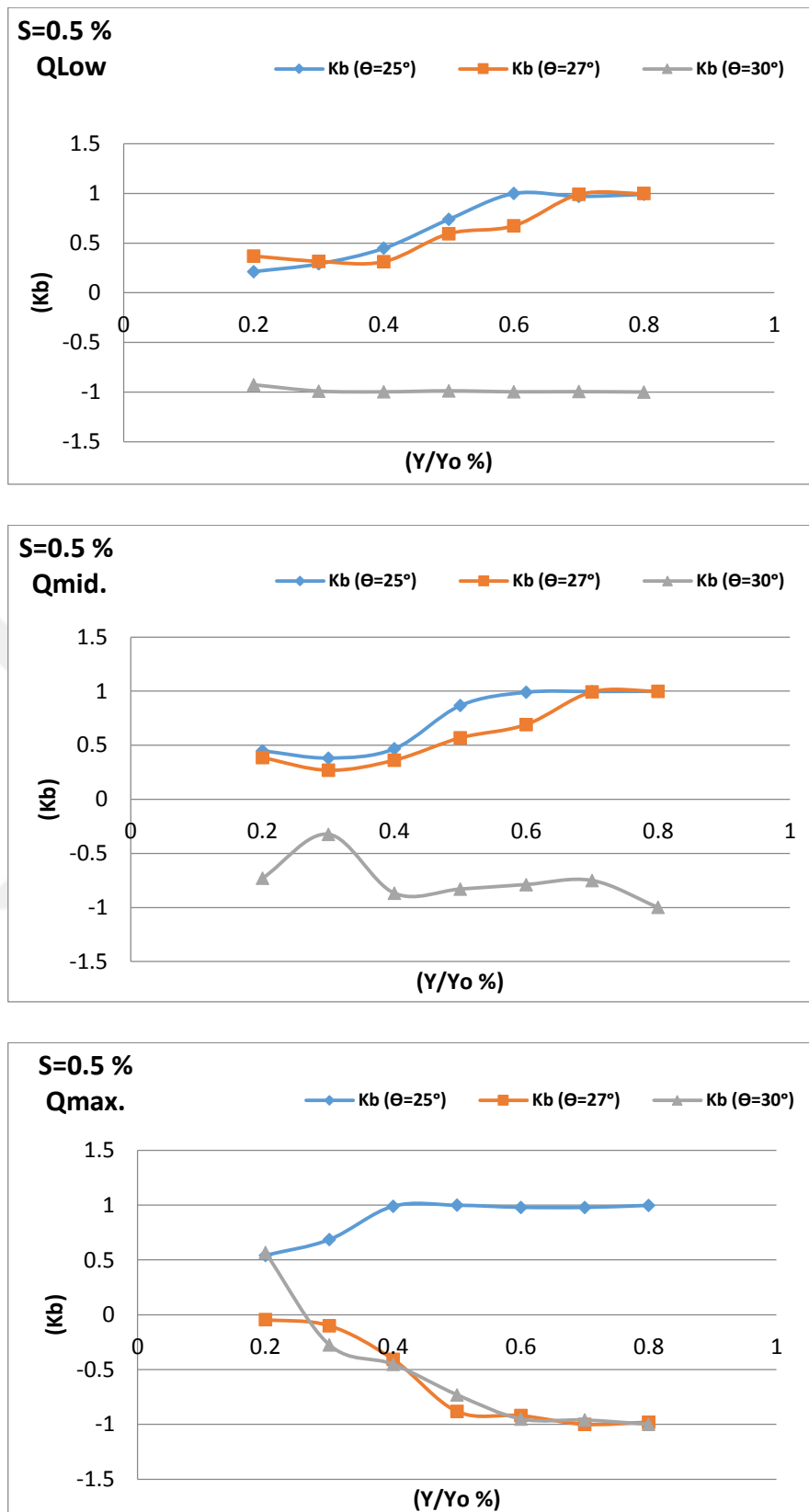


Figure 4.13 Variation of bottom pressure coefficient with gate openings for gate shape lips(25,27,30) when the slope is (S= 0.5%).

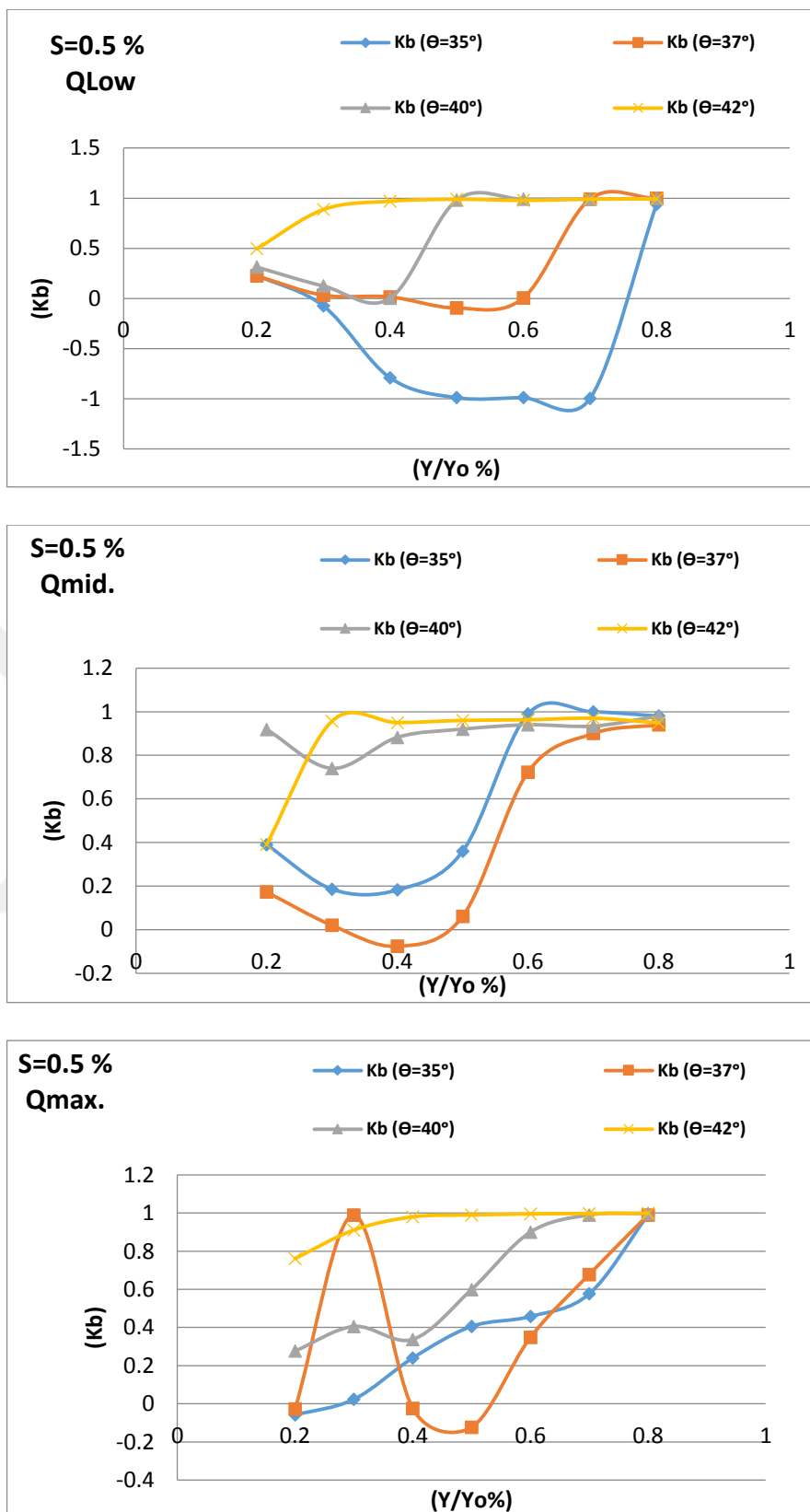


Figure 4.14 Variation of bottom pressure coefficient with gate openings for gate shape lips (35,37,40,42) when the slope is (S= 0.5%).

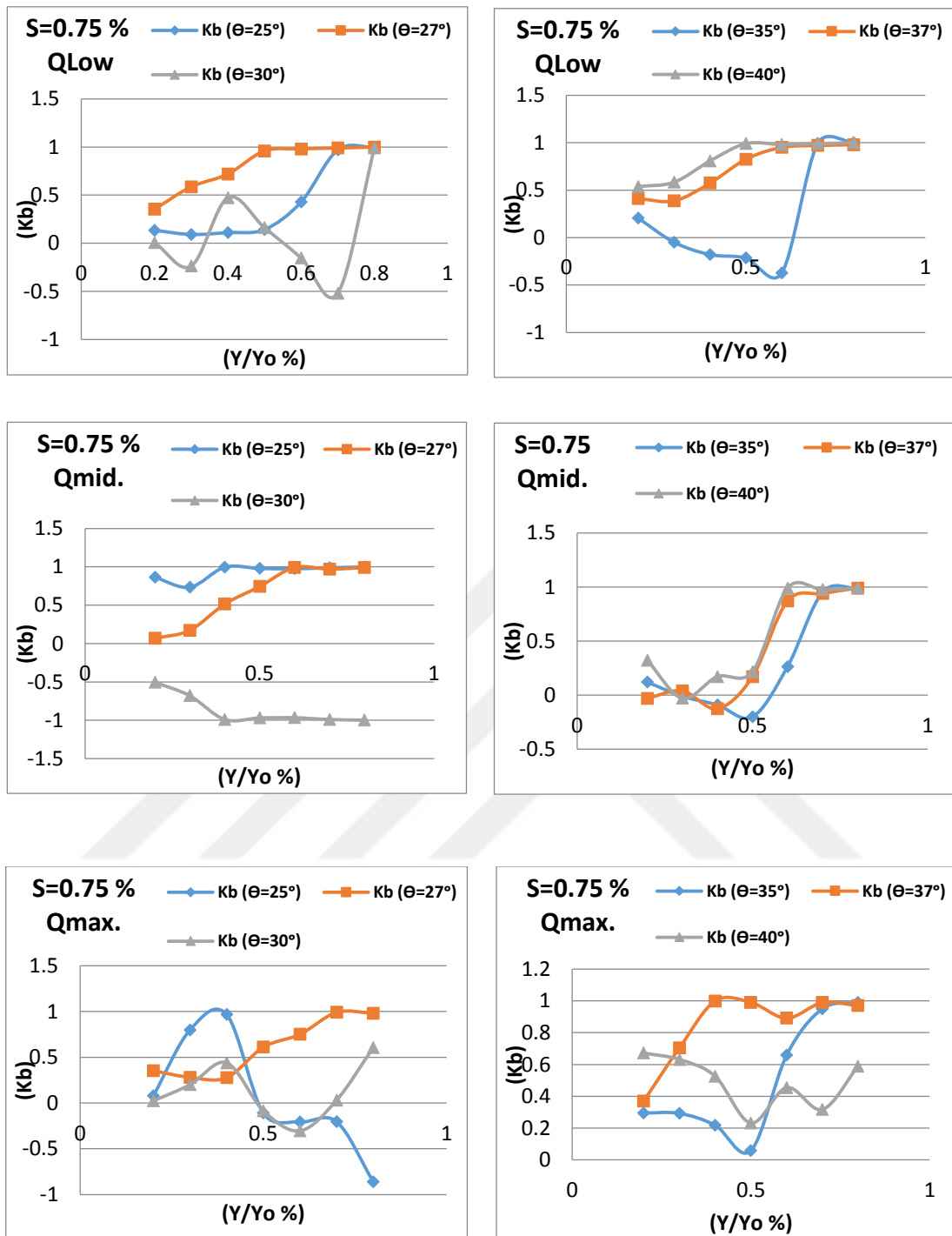


Figure 4.15 Variation of bottom pressure coefficient with gate openings for different gate shape lips when the slope is ( $S=0.75\%$ ).

For slope ( $S=0.75\%$ ), the values of ( $K_b$ ) for gate lip shape with angle ( $\theta = 30^\circ$ ) are continued to decline for low and medium flow rates as shown in figure (4-15), while the other gate lip shape angles were took the same previous trend. The maximum flow rate lead to produce some fluctuations for ( $K_b$ ) of gate lip shapes with angles of ( $\theta = 25^\circ$ ), ( $\theta = 30^\circ$ ) and ( $\theta = 40^\circ$ ).

#### 4.2.2.2 Effects of Gate lip Geometry on ( $K_b$ ):

The effects of flow rates on the values of ( $K_b$ ) for specific gate lip shapes and longitudinal slopes are shown in figures from (4.16) to (4,16). It can be seen from figure (4,16) that for gate lip with ( $\theta = 25^\circ$ ), the increased slope seems to be leading to general increase in values of ( $K_b$ ), moreover, the increasing of flow rate caused disturbance for some extent in pressure coefficients distributions. The figure also indicates that only slope ( $S=0.5\%$ ) has uniform impact on the behaviour of ( $K_b$ ) profile.

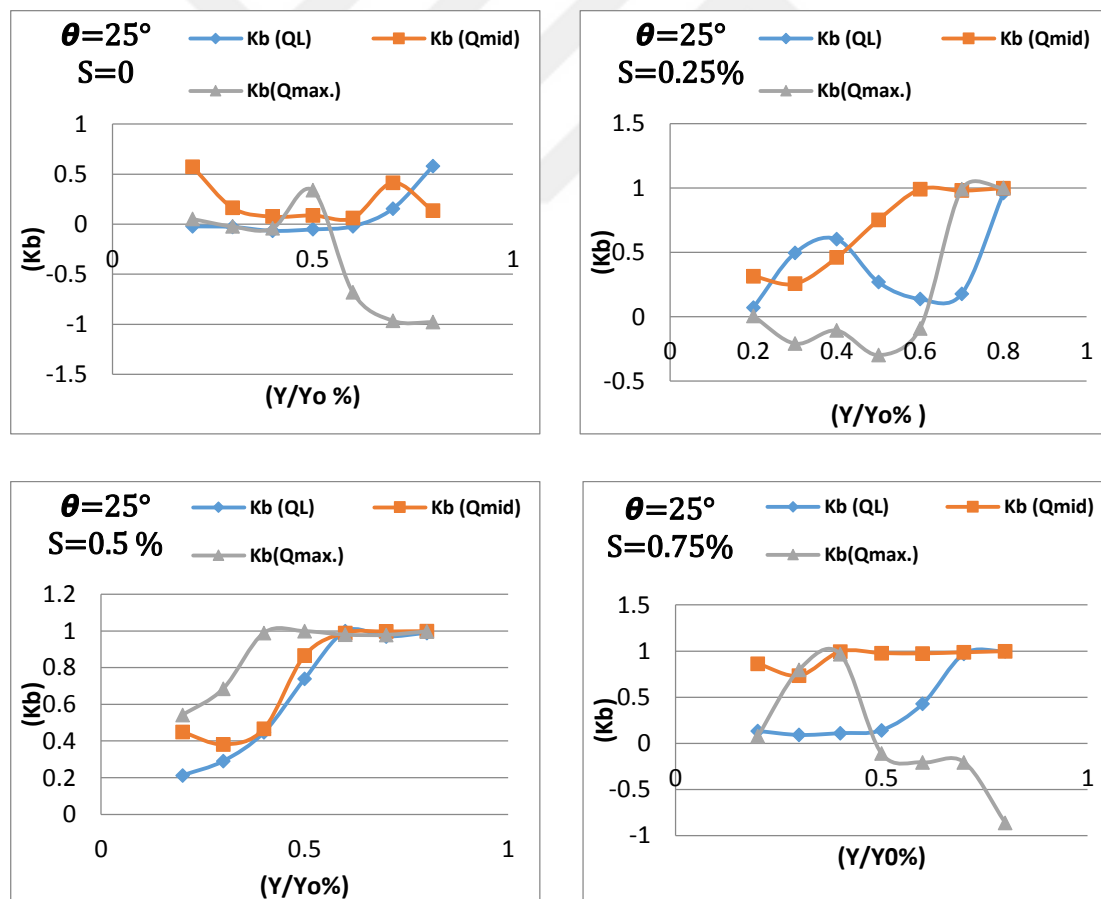


Figure 4.16 Variation of bottom pressure coefficient with gate openings for different discharge ( $\theta=25^\circ$ ).

(Figure 4.17) shows that for gate lip of ( $\theta = 27^\circ$ ), the values of ( $K_b$ ) with all modes of flow rates have been changed uniformly in positive or negative trends as a result of slopes change. The figure obvious that with slope of ( $S=0.75\%$ ), a clear uniform change in values of ( $K_b$ ) were occurred for all values of flow rates.

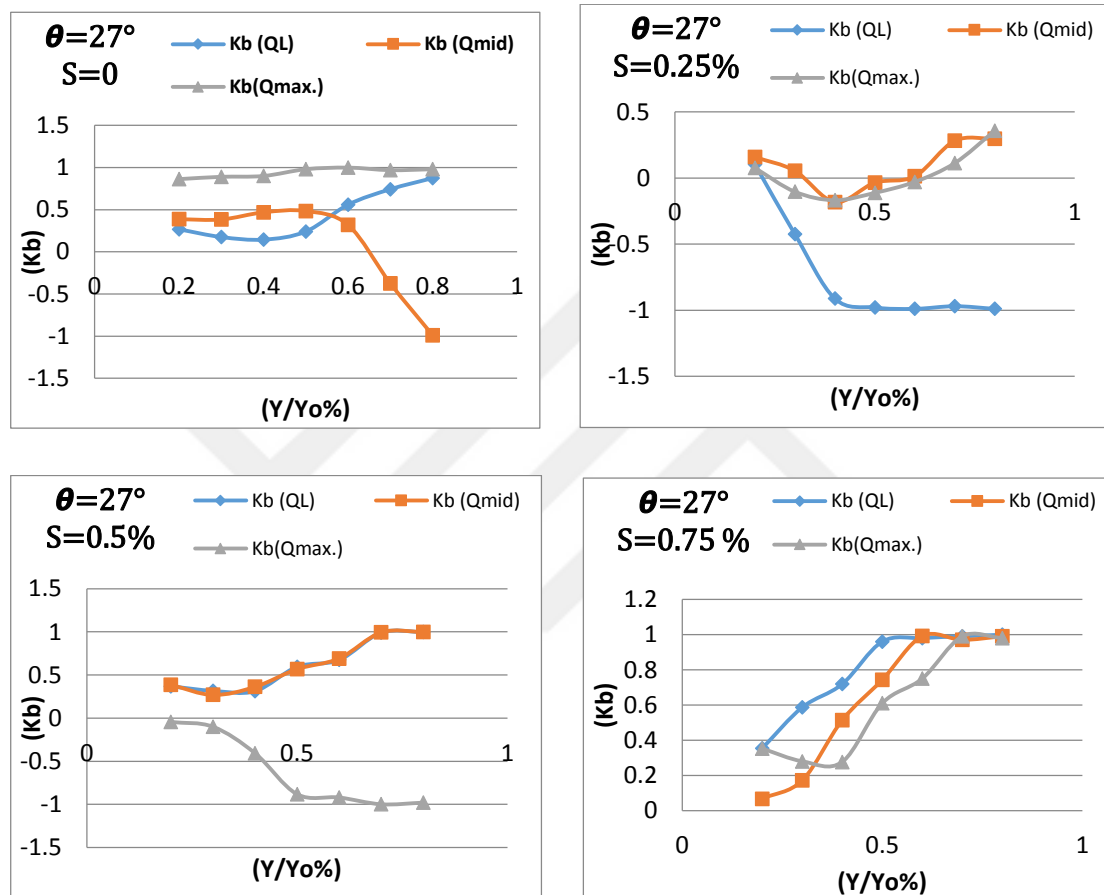


Figure 4.17 Variation of bottom pressure coefficient with gate openings for different discharge ( $\theta=27^\circ$ ).

As noticed before, the ( $K_b$ ) values are effectively influenced for gate lip with angle ( $\theta = 30^\circ$ ). (Figure 4.18) shows a significant fluctuations for most ( $K_b$ ) profiles except for ( $Q_{med.}$ ) and slope ( $S=0.75\%$ ) where the profile is changed gradually from the positive to negative values and no fluctuation is indicated.

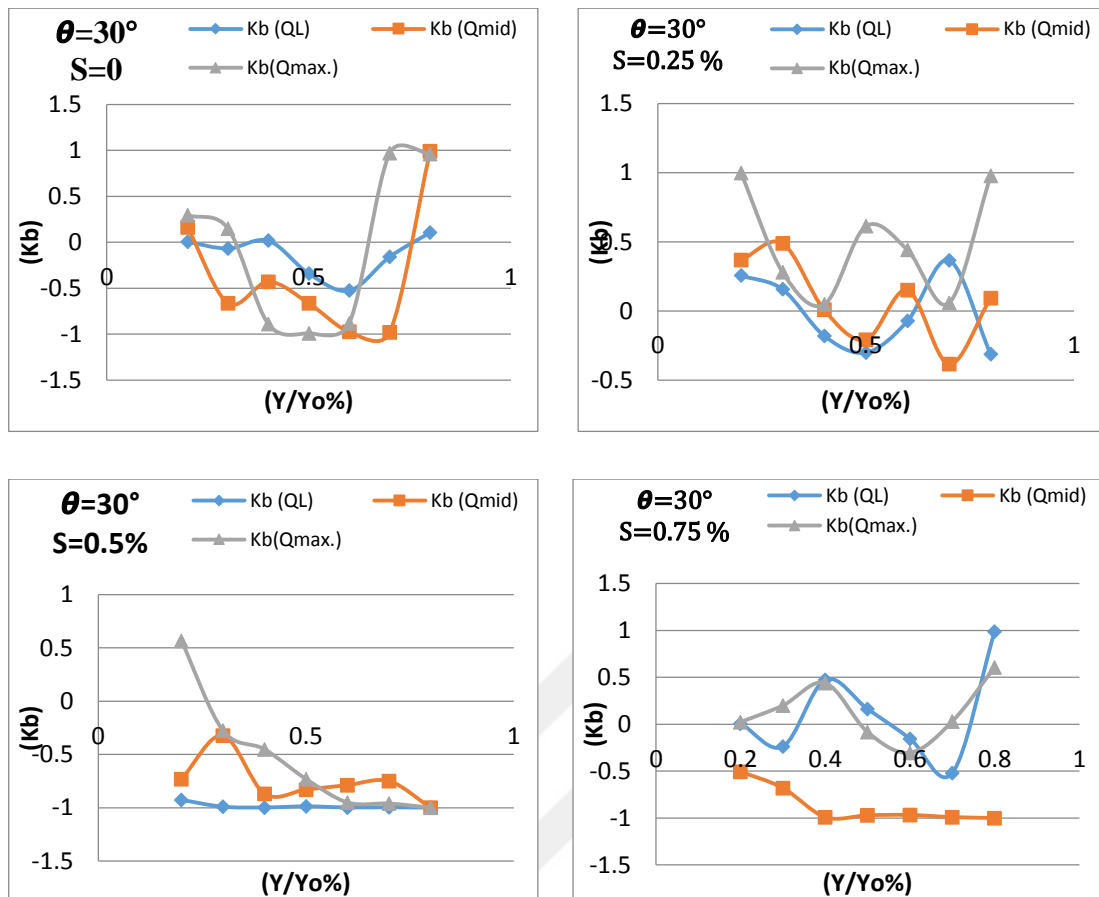


Figure 4-18: Variation of bottom pressure coefficient with gate openings for different discharge ( $\theta = 30^\circ$ ).

(Figure 4.20) indicates the effects of different values of flow rates and slopes on ( $K_b$ ) values for gate lip with angle ( $\theta = 35^\circ$ ). The negative values are observed for ( $Q_{med.}$ ,  $Q_{max.}$ ) with ( $S = 0$ ) ( $Q_{med.}$ ) with ( $S = 0.25\%$ ), ( $Q_{med.}$ ,  $Q_{max.}$ ) with ( $S = 0.5\%$ ) and ( $Q_{low}$ ,  $Q_{med.}$ ) with ( $S = 0.75\%$ ). Mostly, the negative values are located within the range of middle values of gate openings ( $Y/Y_o$ ).

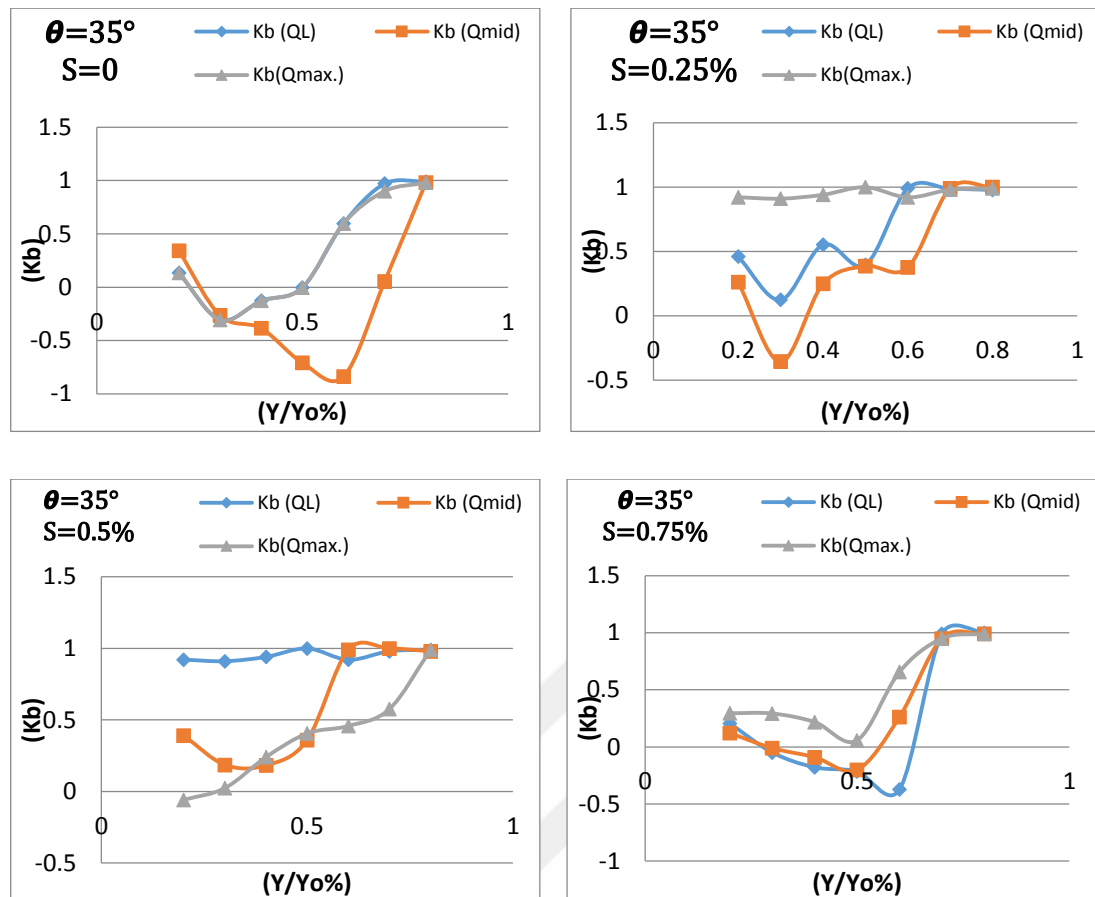


Figure 4.19 Variation of bottom pressure coefficient with gate openings for different discharge ( $\theta = 35^\circ$ ).

In (Figure 4.21), the fluctuation in ( $K_b$ ) profiles were occurred for ( $Q_L$ ) with slope of ( $S=0$ ) and ( $Q_{max.}$ ) with slope ( $S=0.5\%$ ). The general pattern of distribution are revealed that the values of ( $K_b$ ) for ( $Q_{med.}$ ,  $Q_{max.}$ ) with Slopes ( $S=0$ ) and ( $S=0.5\%$ ) respectively have been dropped up to ( $Y/Y_o = 40\%$ ) and then being increased for the remaining values of gate openings. Whereas, the other flow rates and slopes ( $K_b$ ) values have a uniform trend of change.

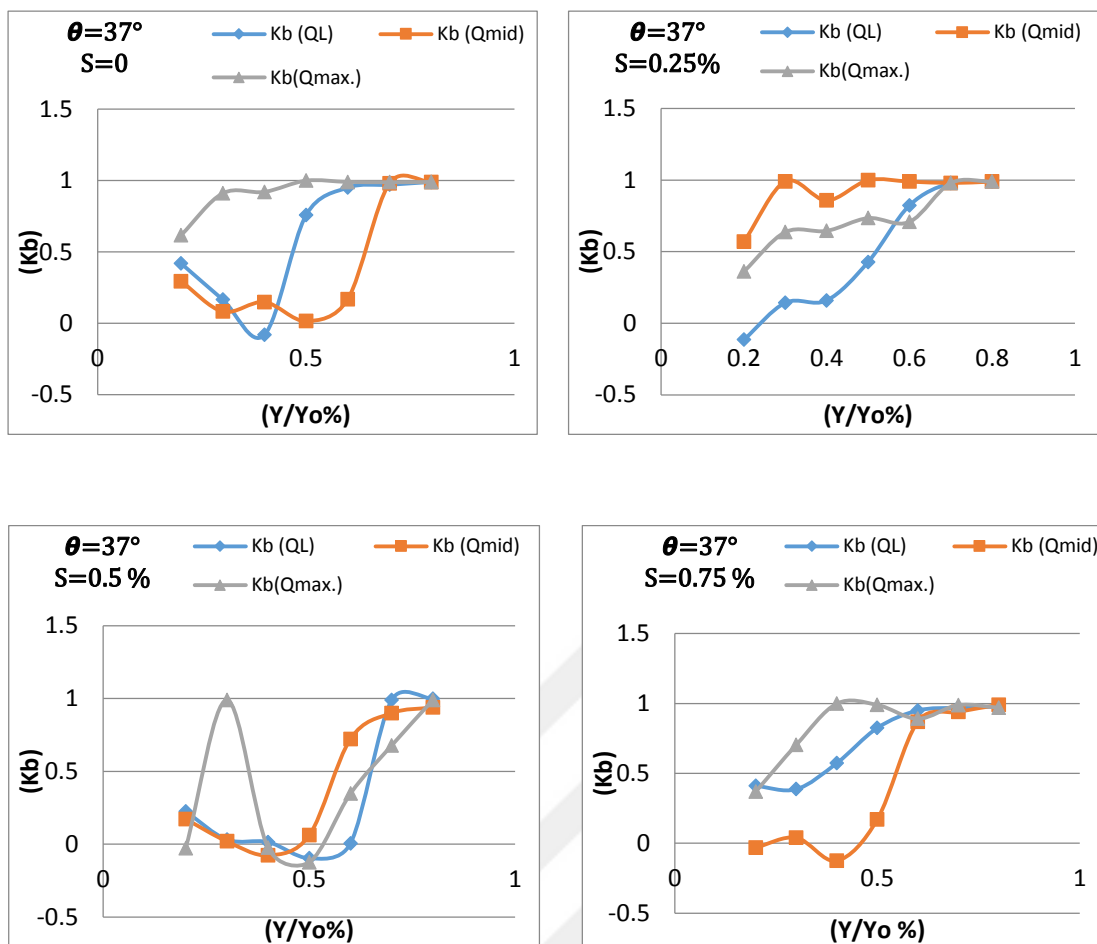


Figure 4-20 Variation of bottom pressure coefficient with gate openings for different discharge ( $\theta = 37^\circ$ ).

(Figure 4.22) indicates that for gate lip with angle ( $\theta = 40^\circ$ ), the values of ( $K_b$ ) are uniformly changed for all flow rates just for slope ( $S=0.5\%$ ). Whereas for other, the profiles mostly are fluctuated with low values of ( $K_b$ ) which have been observed especially for slopes ( $S=0$  and  $S=0.25\%$ ).

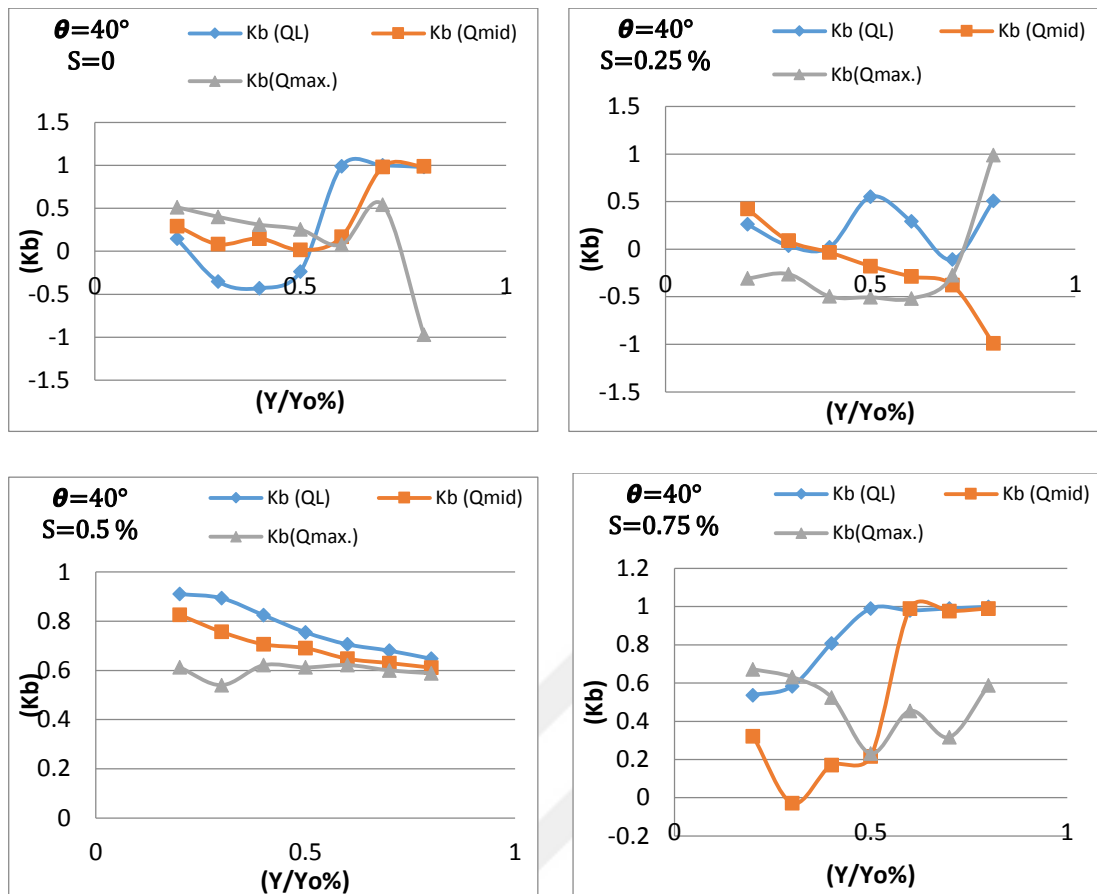


Figure 4.21 Variation of bottom pressure coefficient with gate openings for different discharge ( $\theta=40^\circ$ ).

The ( $K_b$ ) values for ( $Q_{max}$ ,  $S=0$ ) and all values of flow rates with slope ( $S=0.25\%$ ) are seen to be changed with uniform trend while some fluctuations were noticed for the values of ( $K_b$ ) with slope ( $S=0.25\%$ ) as shown in figure (4.23).

The general view of the flow rates and slopes effects on the average values of bottom pressure coefficients does not appear to be subjected to specific form, and there is even a differences in effects on the same gate lip shapes such as noticed in above figures. Moreover, the effects of gate geometry remains the most influential parameters along with the flow conditions and slope of flume. This means, that the response of ( $K_b$ ) values and distribution to the impact of these parameters cannot be expected with a high degree of accuracy, but such results will still give a good and sufficient indices to achieve an appropriate design of gate to meet the challenges of pressures.

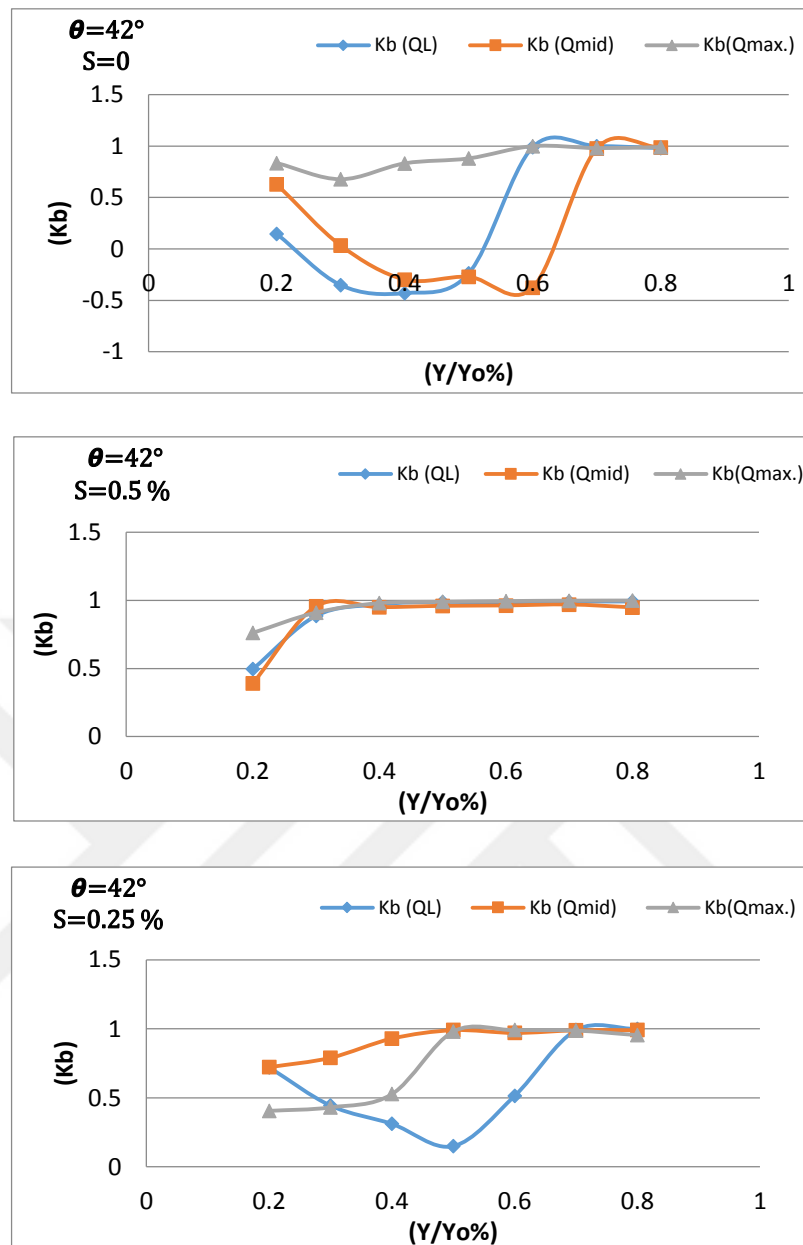


Figure 4.22 Variation of bottom pressure coefficient with gate openings for different discharge ( $\theta=42^\circ$ ).

#### 4.2.2.3 Distribution of $(K_b)$ on Bottom Gate Surface:

One of the major aims of studying the distribution of  $(K_b)$  along and across the bottom gate surface is to confine and analyze the flow pattern beneath the gate and to integrate its behaviour with the fluctuating pressure on the gate bottom. However, such fluctuation in pressure below the gate will produce the phenomenon of separation and reattachment of stream lines along the bottom gate surface. Hence, the position indication of attachment and reattachment of stream lines it may lead to evaluate the

vibration of gate and its importance challenge on the mechanical system of gate operation. The visual observation can be helped in indication the points of attachments and separation, where the region of relative high pressure it may refer to attachment and the low pressure to the separation (1964).

In present study , Two lines of four taps each were inserted in the same direction of flow with distance (0.25 B) and (0.5 B) respectively as shown in (Figure 4.5) .These taps are connected to Piezometric board for reading the pressure heads and then Equation (4.10) was applied to determine the (Kb) values for all these taps .The three dimensional representation is used show the flow pattern below the gate surface and made an attempt to indicate the zones of attachment and separation. Two gate lip shapes with low flow rate and different values of longitudinal slope are considered as it can be seen in figures from (4.17) to (4.25).The (X/Xo) and (B/Bo) are dimensionless positions of taps along and across the bottom gate surface respectively.

(Figure 4.17) shows that for ( $Y/Y_o=20\%$ ) and ( $\theta=30^\circ$  ,  $S=0$  ) ,the values of (Kb) are increased gradually from the leading edge toward the middle point ( $X/X_o=40\%$ ) which represent the impact of peak value and hence indicates the attachment point , then followed by the action of separation for short distance before it rising slightly beyond ( $X/X_o=60\%$ ) toward trailing edge.

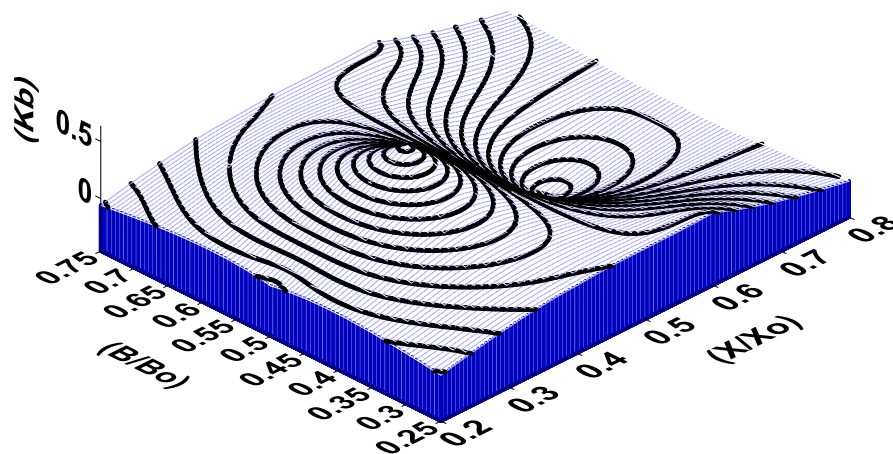


Figure 4.23: Variation of (Kb) with ( $\theta=30^\circ$ ) ,( $Y/Y_o=20\%$ ) , (QL.) and ( $S=0$ ) .

(Figure 4.18) shows that for  $(Y/Y_0=30\%)$  and  $(\theta=30^\circ, S=0)$ , the values of  $(K_b)$  are increased gradually from the leading edge toward the middle point  $(X/X_0=50\%)$  which represent the peak value of some indication for attachment, then followed by rapid decreasing for short distance before it rising slightly beyond  $(X/X_0=60\%)$  and move with steady pattern toward trailing edge.

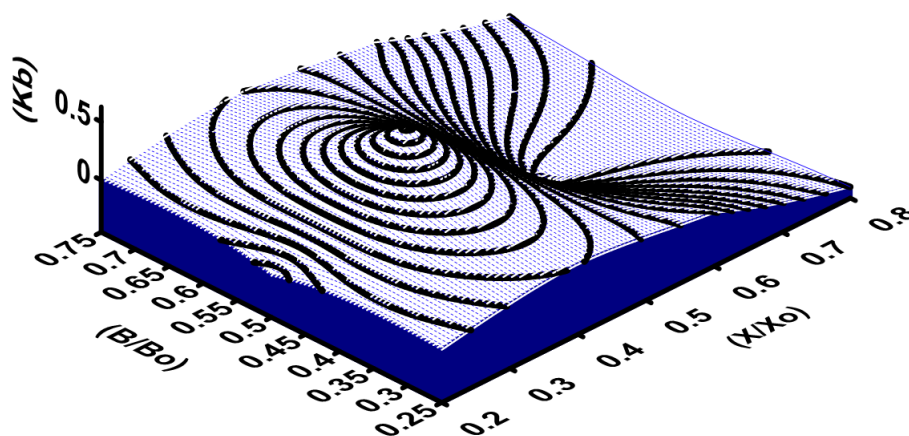


Figure 4.24 Variation of  $(K_b)$  with  $(\theta=30^\circ)$ ,  $(Y/Y_0=30\%)$ ,  $(Q_L)$  and  $(S=0)$ .

(Figure 4.19) shows that for  $(Y/Y_0=20\%)$  and  $(\theta=30^\circ, S=0.25)$ , the values of  $(K_b)$  are again increased gradually from the leading edge toward the peak point of attachment at  $(X/X_0=40\%)$  and then decreasing slightly toward trailing edge.

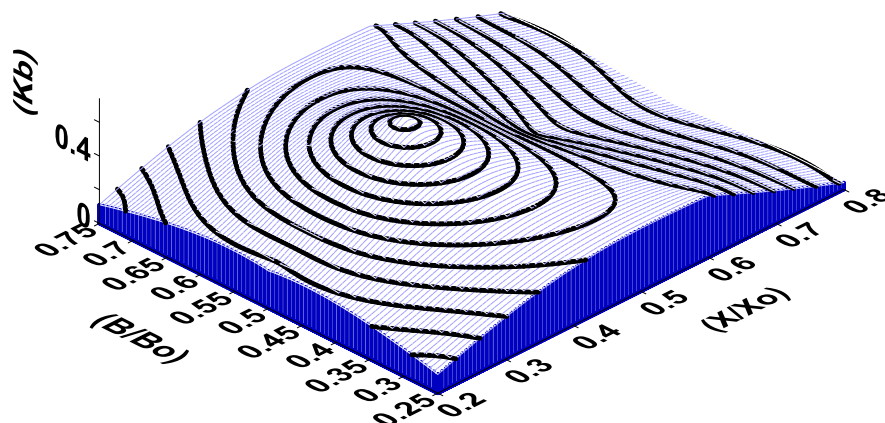


Figure 4.25 Variation of  $(K_b)$  with  $(\theta=30^\circ)$ ,  $(Y/Y_0=20\%)$ ,  $(Q_L)$  and  $(S=0.25\%)$ .

Figure (4.20) indicates that for  $(Y/Y_o=30\%)$  and  $(\theta=30^\circ, S=0.25)$ , the values of  $(K_b)$  are increased gradually from the leading edge toward the zone of attachment indicated by  $(X/X_o=40\%$  to  $X/X_o=60\%)$  and then decreasing slightly toward the both sides of trailing edge.

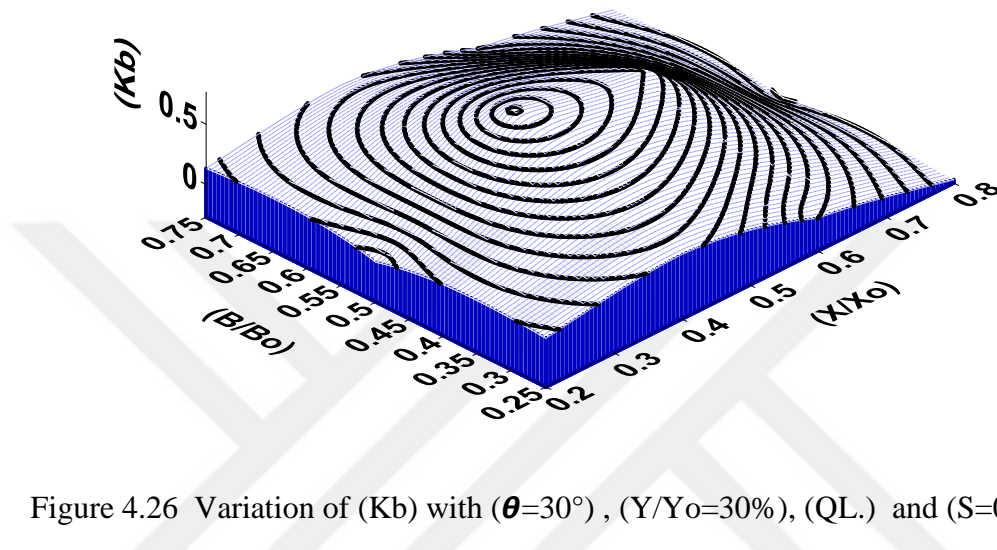


Figure 4.26 Variation of  $(K_b)$  with  $(\theta=30^\circ)$ ,  $(Y/Y_o=30\%)$ ,  $(Q_L)$  and  $(S=0.25\%)$ .

(Figure 4.21) shows that for  $(Y/Y_o=20\%)$  and  $(\theta=30^\circ, S=0.5\%)$ , the values of  $(K_b)$  become negative. The peak values are located at  $(X/X_o=40\%)$  which represent the far point of separation from the bottom gate surface and then the eddies may fill the pocket and lead to some instability in flow pattern.

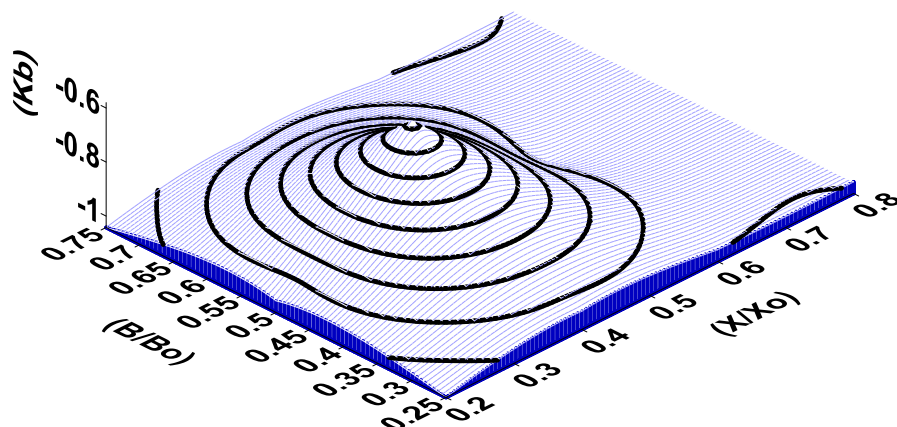


Figure 4.27 Variation of  $(K_b)$  with  $(\theta=30^\circ)$ ,  $(Y/Y_o=20\%)$ ,  $(Q_L)$  and  $(S=0.5\%)$ .

Figure (4.2) shows that for  $(Y/Y_o=30\%)$  and  $(\theta=30^\circ, S=0.5\%)$ , the values of  $(K_b)$  has many peak negative values located at  $(X/X_o=60\%)$  and at both sides of trailing edge. The general view of distribution pattern emphasize that a strong scheme of fluctuation is occurred with a different points far away from the bottom surface of gate.

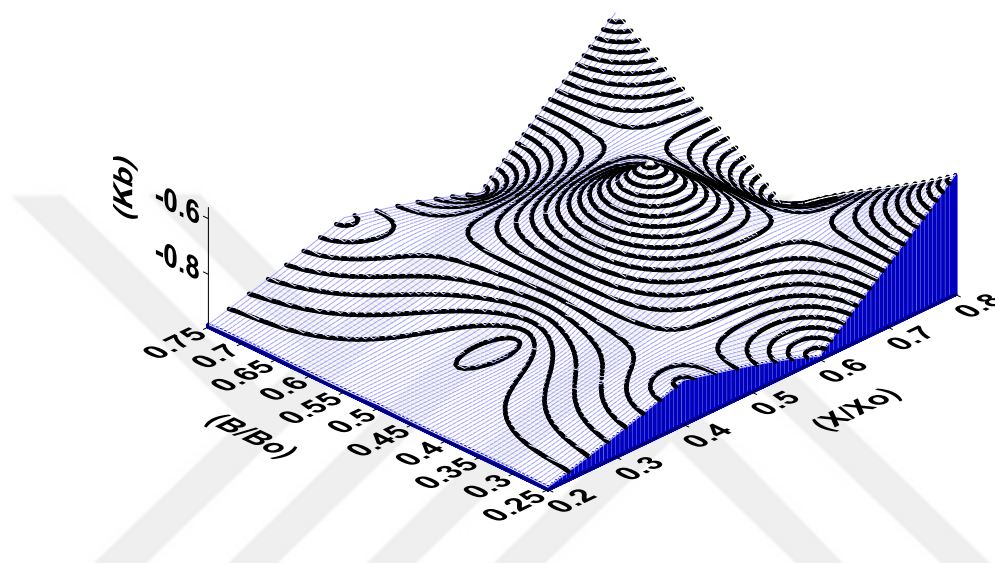


Figure 4.28 Variation of  $(K_b)$  with  $(\theta=30^\circ)$ ,  $(Y/Y_o=30\%)$ ,  $(Q_L)$  and  $(S=0.5\%)$ .

Figure (4.23) shows that for  $(Y/Y_o=20\%)$  and  $(\theta=30^\circ, S=0.75\%)$ , the peak negative value of  $(K_b)$  located at  $(X/X_o=40\%)$  and are changed for all surrounding points.

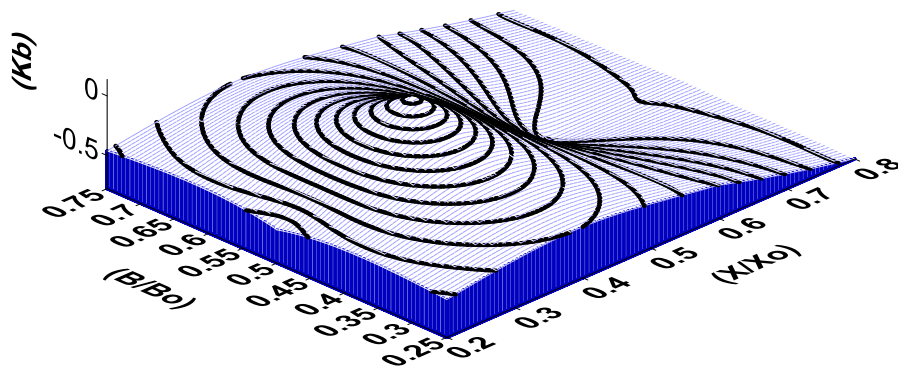


Figure 4.29: Variation of  $(K_b)$  with  $(\theta=30^\circ)$ ,  $(Y/Y_o=20\%)$ , (QL.) and  $(S=0.75\%)$ .

Figure (4.24) indicates that for  $(Y/Y_o=30\%)$  and  $(\theta=30^\circ, S=0.75\%)$ , the peak negative value of  $(K_b)$  are concentrated around  $(X/X_o=40\%)$  and are changed for the region bounded by leading edge and point of  $(X/X_o=60\%)$ .

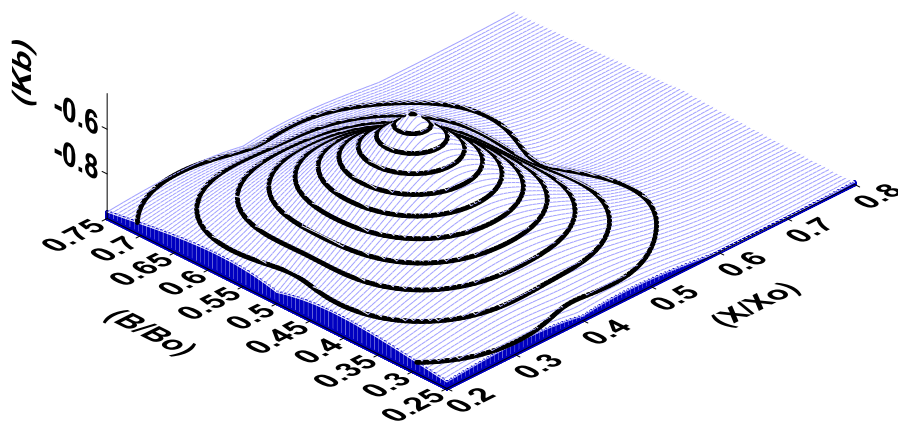


Figure 4.30 Variation of  $(K_b)$  with  $(\theta=30^\circ)$ ,  $(Y/Y_o=30\%)$ , (QL.) and  $(S=0.75\%)$ .

The main conclusion can be specified from the above selected cases, that the increase in longitudinal slope will lead to increase the velocity and consequently caused steep reduction in pressure head which may attained negative values and produce many problems accordingly.

### 4.2.3 Downpull Pressure Coefficient (Kd):

The downpull coefficient (Kd) is considered as major parameter dominated the requirements of lift gate design .The (Kd) is function of (Kt and Kb) which are estimated from previous analysis. The results of current study based upon the experiments were conducted by using hydraulic model of dam tunnel .Seven inclined gate lip shapes were examined for different flow rates and longitudinal slopes. The downpull coefficient (Kd) can be determined by using the following expression:

$$K_d = K_t - K_b \quad (4.7)$$

Where

$K_d$ :downpull coefficient.

The main purpose of studying the hydraulic downpull coefficient (Kd) is to observe the effects of flow conditions, gate geometries and slope will lead to increase or decrease the (Kd) values and whether the results were caused the positive or negative downpull.

(Figures 4.25) to (4-28) are showed the variation of downpull pressure coefficient (Kd) with gate opening ratios (Y/Yo) for various flow rates and slopes of tunnel. It can be seen from (Figure 4.25) that for (QL. And S=0) the positive downpull are created up to (Y/Yo=50%) and then followed to be negative for all gate shapes except gate lip shape with angle ( $\theta = 30^\circ$ ) .Whereas, for (Qmed. and S=0) ,the negative values are appeared beyond (Y/Yo=60%) for just gate lips with angles ( $\theta = 37^\circ, \theta = 40^\circ, \theta = 42^\circ$ ) .Theresults has also been showed ,that for ( $\theta = 30^\circ, \theta = 35^\circ, and \theta = 42^\circ$ ),the increase in flow rate (Qmax.) will caused negative downpull force for (Y/Yo =60% ) and more.

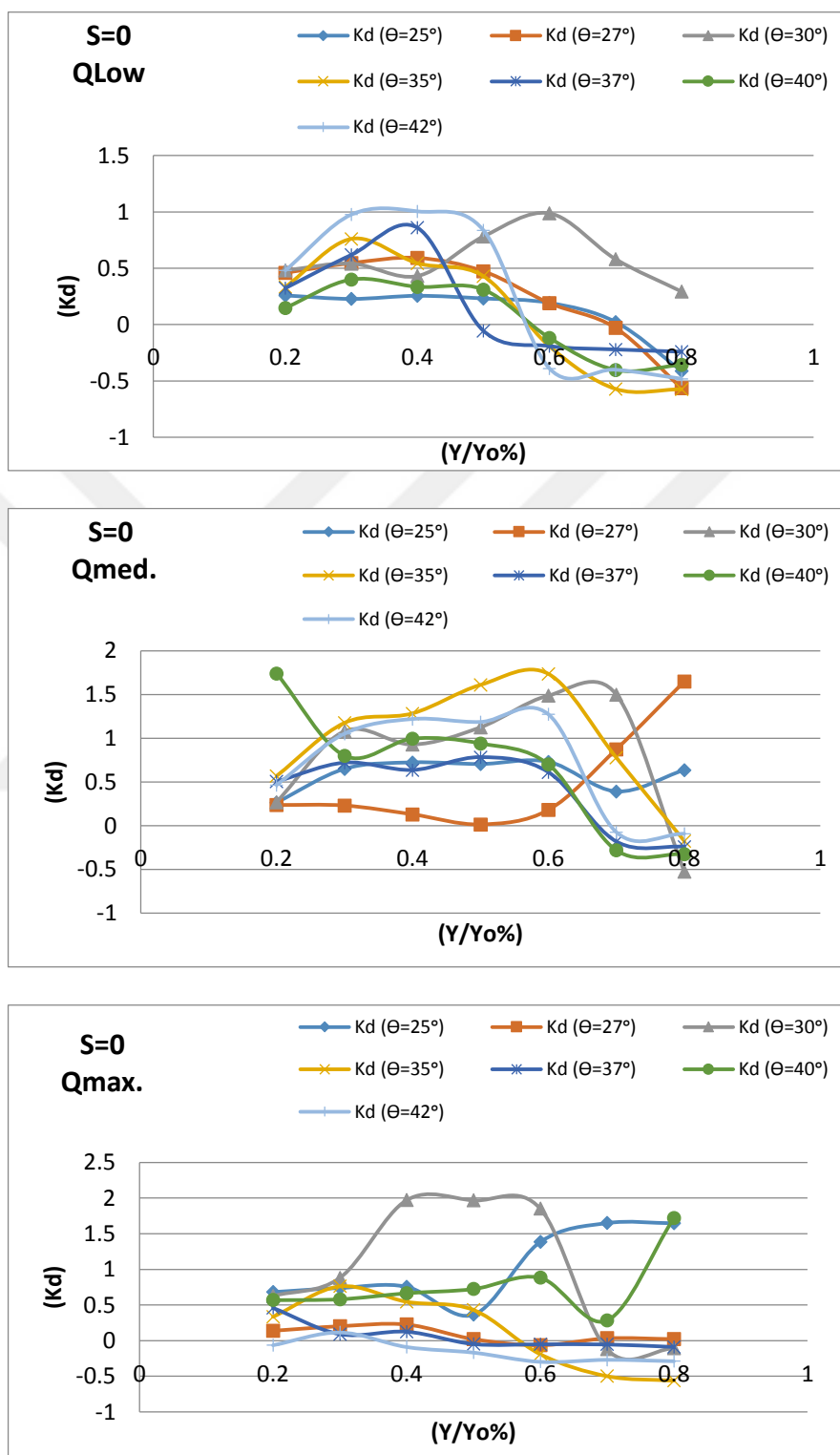


Figure 4.31 Downpull coefficient pressures with gate openings for different shape lips in different discharges when ( $S=0$ ).

Figure (4.26) indicates that for (QL. and  $S=0.25\%$ ) the negative downpull forces are started to establish for ( $\theta = 35^\circ, \theta = 42^\circ, \theta = 25^\circ$ ) from ( $Y/Y_o=50\%$ ) with consecutive values. The values of negative downpull are seemed to be increase as flow rate increased, ( $Q_{med}, Q_{max.}$ ) and also for some gate shapes ( $\theta = 35^\circ, \theta = 42^\circ$ ), the negative values were started from earlier gate opening ratios ( $Y/Y_o=50\%$ ) and for ( $\theta = 40^\circ$ ) just occurred with ( $Y/Y_o=75\%$ ).

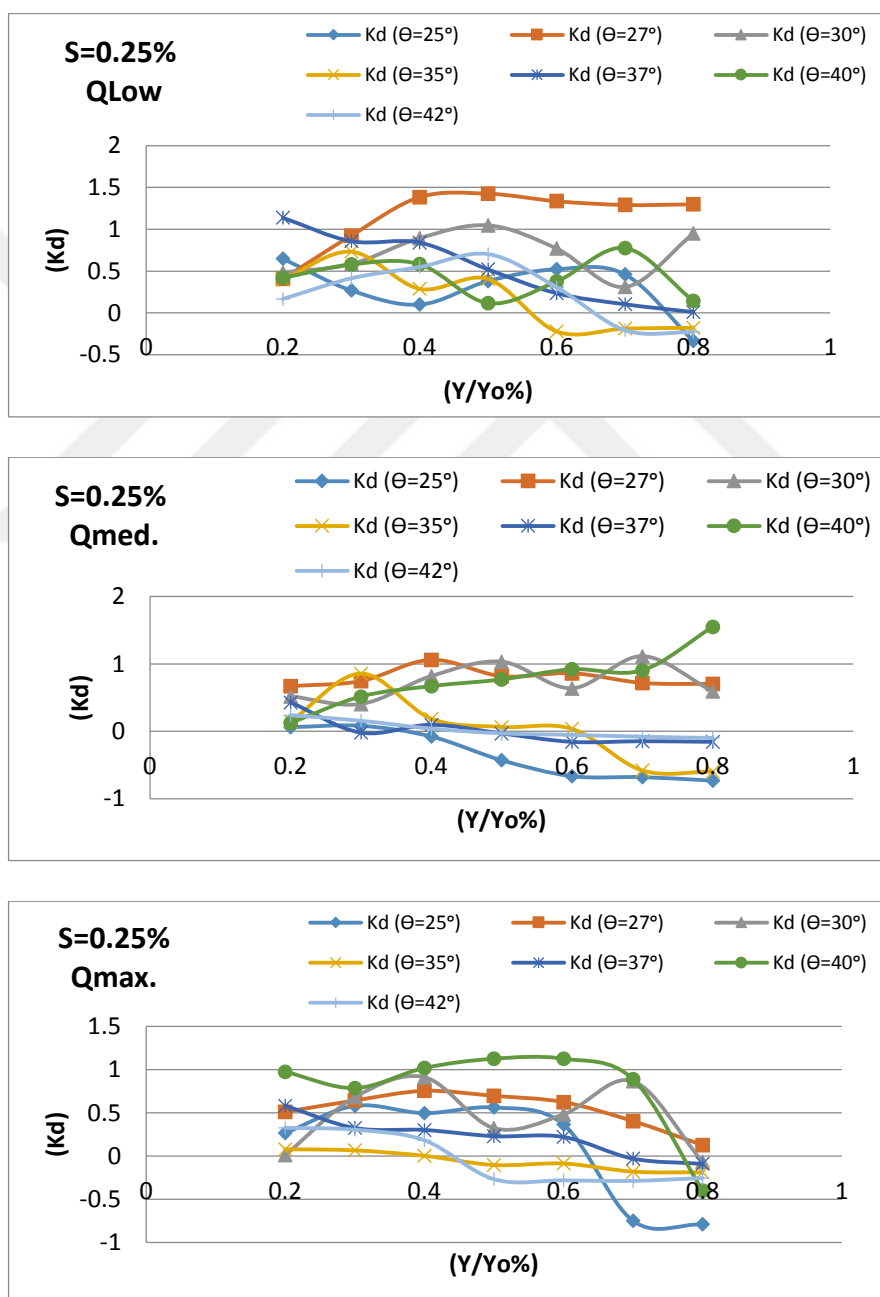


Figure 4.32 Downpull coefficient pressures with gate openings for different shape lips in different discharges when ( $S=0.25\%$ ).

It can be seen from (Figure 4.27) that the increase of slope ( $S=0.5\%$ ) caused much more effects on the incidence of creating the negative values of ( $K_d$ ) with gate openings. The figure shows that occurrence of negative downpull forces for ( $\theta = 25^\circ, \theta = 40^\circ, \theta = 42^\circ$ ) become earlier where started mostly from ( $Y/Y_o$ ) before (50%). Some increase in positive values of ( $K_d$ ) are observed for ( $\theta = 30^\circ$ ) for all values of flow rates and for ( $\theta = 35^\circ$ ) and ( $\theta = 27^\circ$ ) are also observed just for ( $Q_L$ ) ( $Q_{max}$ .) respectively.

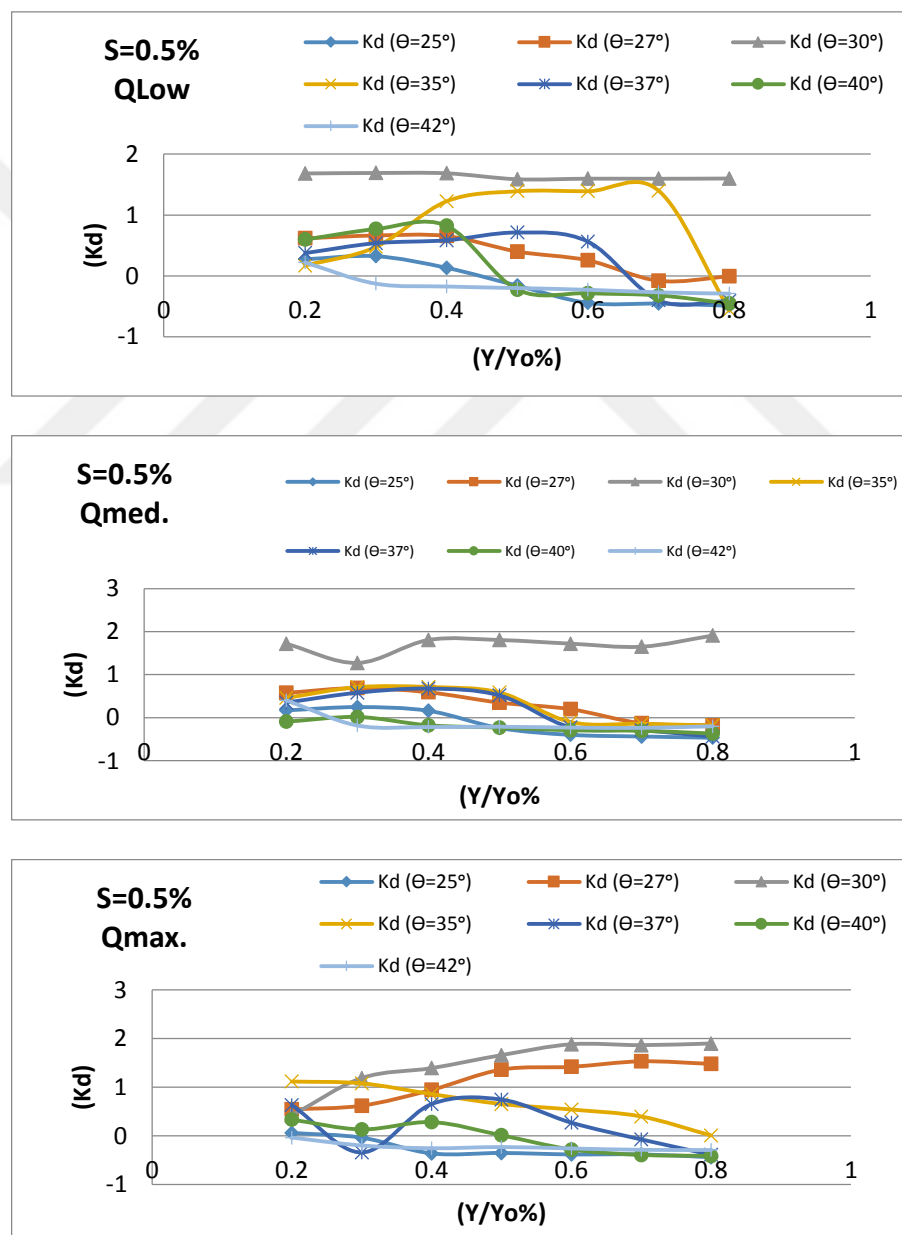


Figure 4.33 Downpull coefficient pressures with gate openings for different shape lips in different discharges when ( $S=0.5\%$ )

The similar of previous effects are appeared in (figure 4-28) which indicates that the increase in slope will lead to bring the occurring negative downpull force in ( $Y/Y_0 \leq 50\%$ ). The importance of negative downpull indication as a values and positions are due its big effects on prevention the vertical lift gate to be closed.

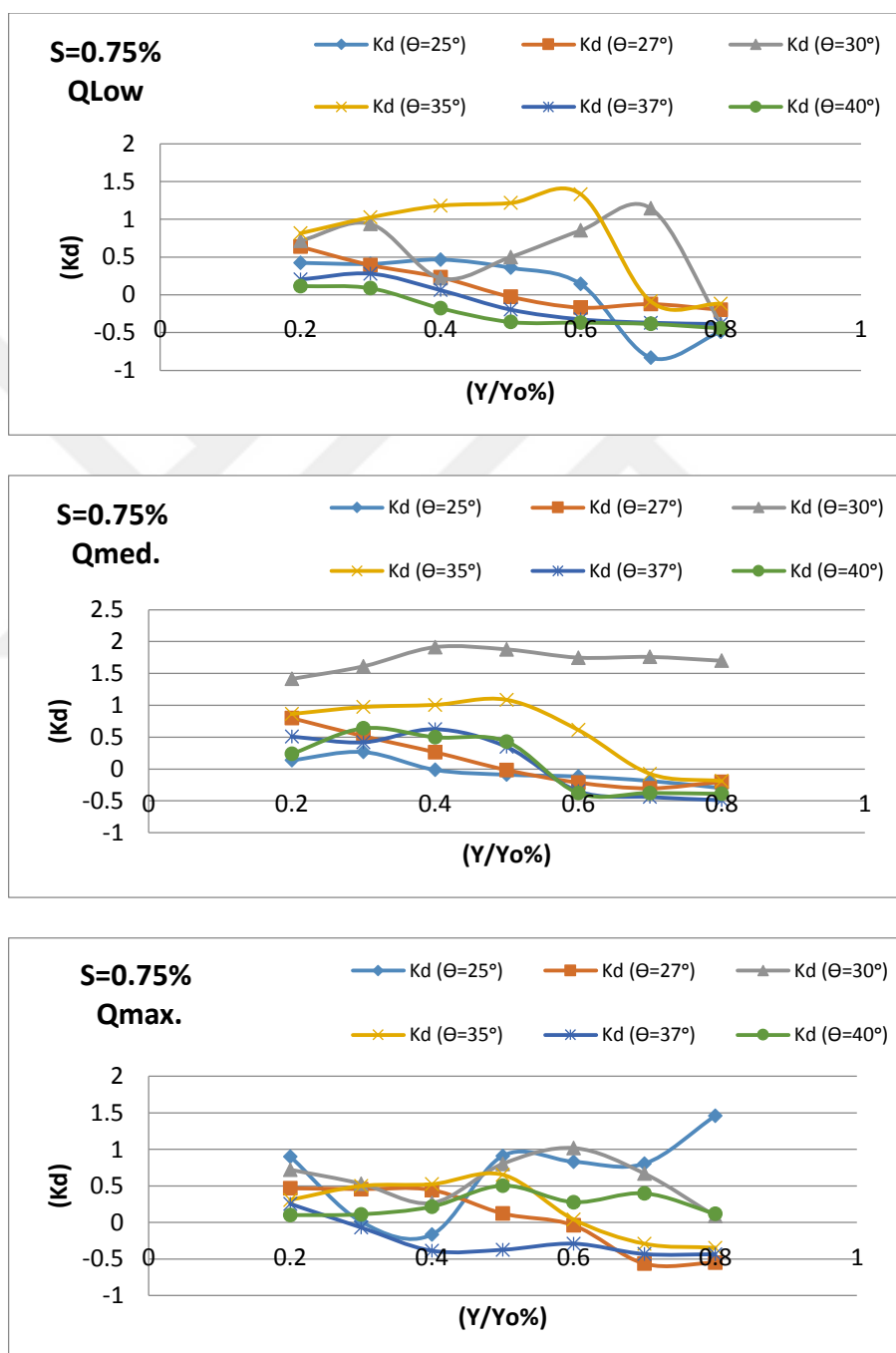


Figure 4.34 Downpull coefficient pressures with gate openings for different shape lips in different discharges when ( $S=0.75\%$ ).

### 4.3 STATISTICAL PACKAGE OF SOCIAL SCIENCES (SPSS) ANALYSIS:

In order to analyse the results of measurements by using the principles of statistics, the Statistical package of social sciences is used to combine many parameters in a suitable predictive function. Many functions are available, but the selection should be controlled by an acceptable value of correlation coefficient which represents one of the best ways to get a good confidence for the applicability of function. In present study the following form of sixth order polynomial function is selected in which the ( $K_b$ ) is considered as dependent variable and has been taken as function of gate lip angle ( $\theta$ ) and gate opening ( $Y$ ):

$$K_b = (A + B.Y + C.Y^2 + D.Y^3 + E.Y^4 + \dots + N.Y^n) \quad (4.8)$$

Where

A, B, .....etc are constants obtained from the results of regression process of software.

Many cases of results were introduced to software to carry out the analysis of nonlinear regression for the data of different opening ratios ( $Y/Y_o$ ) and angles. The following results with often good values of correlations are obtained.

The results of SPSS software analysis are shown in the following tables for selected cases. (Table 4.2) indicates the results of ( $Q_{med}$ ,  $S=0.75\%$ ) for gate lip angles of ( $\theta=35^\circ$ ,  $\theta=37^\circ$  and  $\theta=40^\circ$ ). The form of equation (4.8) is used to determine the predicted values of ( $K_b$ ) for mentioned cases and (Figure 4.28) shows the results of both measured and predicted values of ( $K_b$ ). The same process is repeated for all considered cases and the results are shown in the corresponding tables and figures. It can be obvious from all results that the correlation coefficients have been found with an acceptable limit for such experimental works. However, the functions which were obtained as a result to the regression process can be considered as applicable and useful to form perception with less effort about the ( $K_b$ ) values related to the selected conditions.

Table 4.2 Results of SPSS for [ (Qmed. S=0.75% ) ( $\theta=35^\circ$ ,  $\theta=37^\circ$  and  $\theta=40^\circ$ )]**Parameter Estimates**

Parameter	Estimate	Std. Error	95% Confidence Interval	
			Lower Bound	Upper Bound
A	46.990	40.347	-39.546	133.526
B	-715.241	602.428	-2007.320	576.839
C	4327.956	3550.408	-3286.912	11942.824
D	-13337.565	10633.322	-36143.773	9468.644
E	22093.896	17156.943	-14704.087	58891.879
F	-18676.319	14204.439	-49141.812	11789.173
G	6314.583	4732.714	-3836.079	16465.245

**ANOVA<sup>a</sup>**

Source	Sum of Squares	df	Mean Squares
Regression	7.249	7	1.036
Residual	.528	14	.038
Uncorrected Total	7.777	21	
Corrected Total	4.324	20	

Dependent variable: Kb

a. R squared =  $1 - (\text{Residual Sum of Squares}) / (\text{Corrected Sum of Squares}) = .878$ .

b.

$$K_b = 46.99013 + (-715.241) \times Y + (4327.956) \times Y^2 + (-13337.565) \times Y^3 + (22093.896) \times Y^4 + (-18676.319) \times Y^5 + (6314.583) \times Y^6 \quad (4-9)$$

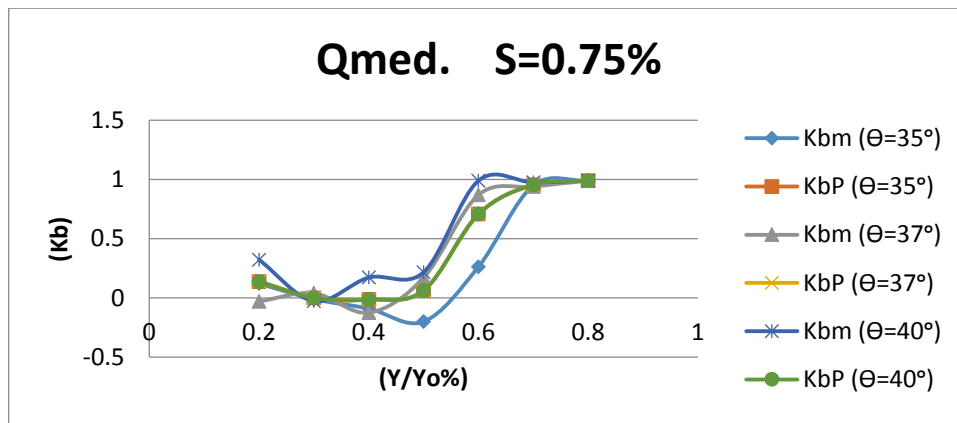


Figure 4.35: Measured and Predicted (Kb) values.

Table 4.3 Results of SPSS for [ (QL. S=0 ) (θ=35°, θ=37°, θ=40° and θ=42°)]

### Parameter Estimates

Parameter	Estimate	Std. Error	95% Confidence Interval	
			Lower Bound	Upper Bound
A	19.691	45.308	-74.533	113.915
B	-290.483	676.497	-1697.335	1116.369
C	1758.041	3986.877	-6533.123	10049.205
D	-5545.453	11940.345	-30376.760	19285.855
E	9508.197	19265.529	-30556.664	49573.057
F	-8328.513	15949.912	-41498.171	24841.145
G	2908.097	5314.201	-8143.388	13959.583

### ANOVA<sup>a</sup>

Source	Sum of Squares	df	Mean Squares
Regression	10.867	7	1.552
Residual	1.331	21	.063
Uncorrected Total	12.198	28	
Corrected Total	6.629	27	

Dependent variable: Kb

a. R squared =  $1 - (\text{Residual Sum of Squares}) / (\text{Corrected Sum of Squares}) = .799$ .

$$K_b = 19.691 + (-290.483) \times Y + (1758.041) \times Y^2 + (-5545.453) \times Y^3 + (9508.197) \times Y^4 + (-8328.513) \times Y^5 + (2908.097) \times Y^6 \quad (4-10)$$

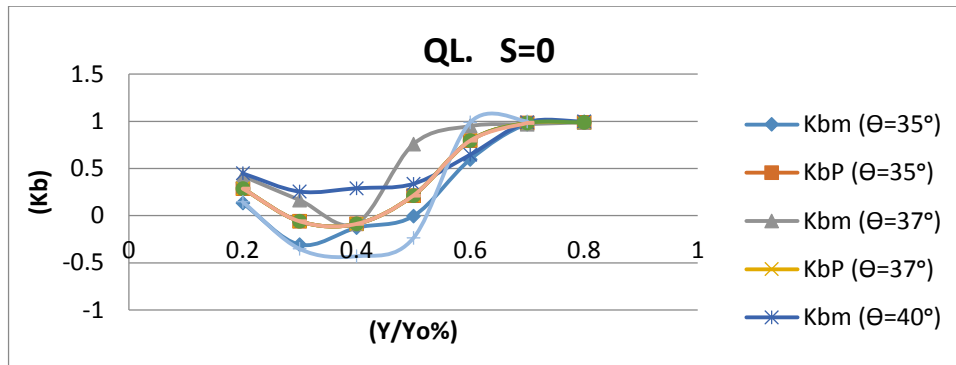


Figure 4.36 Measured and Predicted (Kb) values.

Table 4-4 Results of SPSS for [ (QL. S=0) ( $\theta=35^\circ$ ,  $\theta=37^\circ$ ,  $\theta=40^\circ$  and  $\theta=42^\circ$ ) ]

#### Parameter Estimates

Parameter	Estimate	Std. Error	95% Confidence Interval	
			Lower Bound	Upper Bound
A	-22.369	52.909	-132.398	87.661
B	388.617	789.981	-1254.239	2031.473
di me nsi on0 C	-2586.650	4655.721	-12268.752	7095.453
D	8621.792	13943.581	-20375.472	37619.056
E	-15370.968	22497.882	-62157.876	31415.939
F	13969.088	18626.107	-24766.022	52704.198
G	-5065.467	6205.897	-17971.335	7840.401

#### ANOVA<sup>a</sup>

Source	Sum of Squares	df	Mean Squares
Regression	7.604	7	1.086
Residual	1.815	21	.086
Uncorrected Total	9.420	28	
Corrected Total	8.376	27	

Dependent variable: Kb

ANOVA<sup>a</sup>

Source	Sum of Squares	df	Mean Squares
Regression	7.604	7	1.086
Residual	1.815	21	.086
Uncorrected Total	9.420	28	
Corrected Total	8.376	27	

Dependent variable: Kb

a. R squared = 1 - (Residual Sum of Squares) / (Corrected Sum of Squares) = .783.

$$K_b = -22.369 + 388.617 \times Y + (-2586.650) \times Y^2 + (8621.792) \times Y^3 + (-15370.968) \times Y^4 + (13969.088) \times Y^5 + (-5065.467) \times Y^6 \quad (4.11)$$

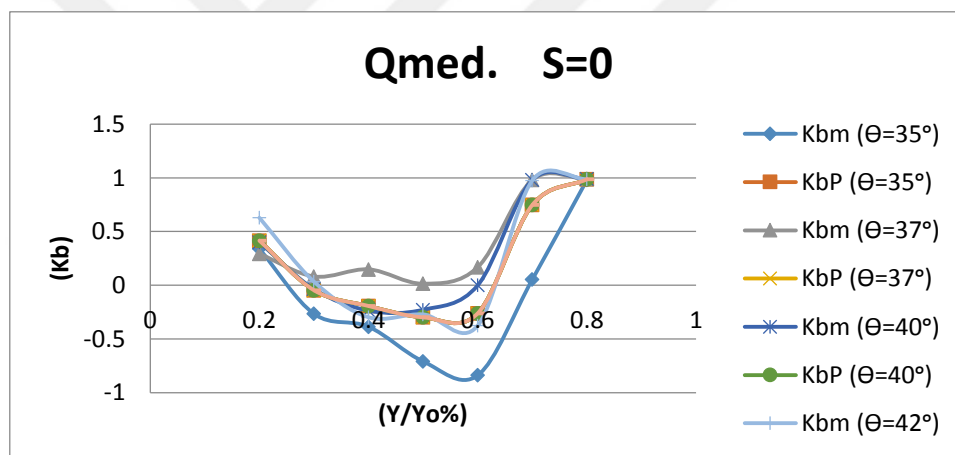


Figure 4.37: Measured and Predicted (Kb) values.

Table 4.5 Results of SPSS for [ (QL. S=0.25% ) (θ=37° , and θ=42°)]

## Parameter Estimates

Parameter	Estimate	Std. Error	95% Confidence Interval	
			Lower Bound	Upper Bound
A	-39.573	30.378	-111.404	32.259
di B	596.955	453.567	-475.561	1669.471
me C	-3522.554	2673.073	-9843.368	2798.259
nsi D	10566.195	8005.656	-8364.175	29496.564
on0 E	-17043.619	12917.034	-47587.551	13500.314
F	14085.757	10694.036	-11201.620	39373.135

### Parameter Estimates

Parameter	Estimate	Std. Error	95% Confidence Interval	
			Lower Bound	Upper Bound
A	-39.573	30.378	-111.404	32.259
di B	596.955	453.567	-475.561	1669.471
me C	-3522.554	2673.073	-9843.368	2798.259
nsi D	10566.195	8005.656	-8364.175	29496.564
on0 E	-17043.619	12917.034	-47587.551	13500.314
F	14085.757	10694.036	-11201.620	39373.135
G	-4680.751	3563.054	-13106.035	3744.533

### ANOVA<sup>a</sup>

Source	Sum of Squares	df	Mean Squares
Regression	8.287	7	1.184
Residual	.100	7	.014
Uncorrected Total	8.387	14	
Corrected Total	.764	13	

Dependent variable: Kb

a. R squared =  $1 - (\text{Residual Sum of Squares}) / (\text{Corrected Sum of Squares}) = .869$ .

$$K_b = -39.573 + 596.955 \times Y + (-3522.554) \times Y^2 + (10566.195) \times Y^3 \\ + (-17043.619) \times Y^4 + (14085.757) \times Y^5 + (-4680.751) \times Y^6$$

(4-12)

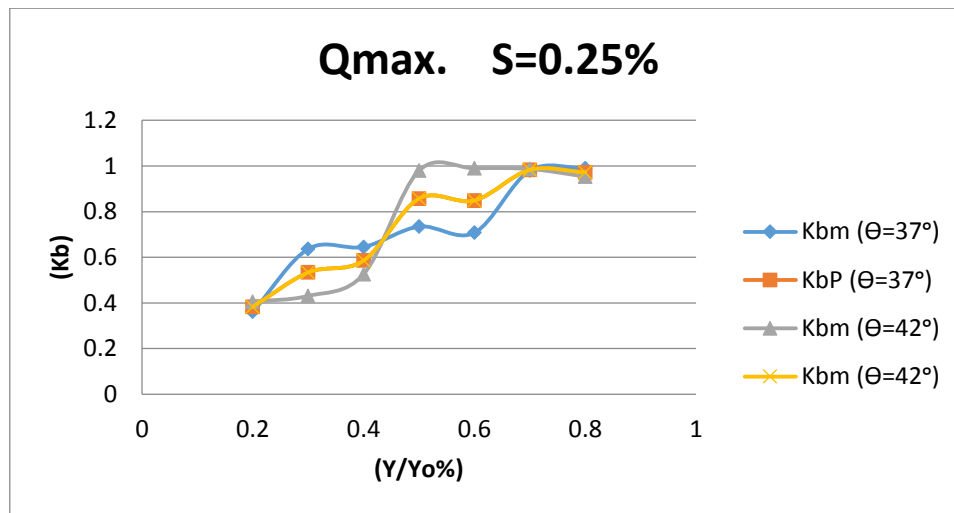


Figure 4.38: Measured and Predicted (Kb) values.

#### 4.4 Upstream Pressure Coefficient (Kf):

The experimental works have also been included the measurements of Piezometric heads through twelve taps inserted in two lines along the upstream face of gate. First line located at a distance (0.25 B) from the gate edge and the second at along the center of gate face, in this study we work on eight taps as shown in (figure 4.33).

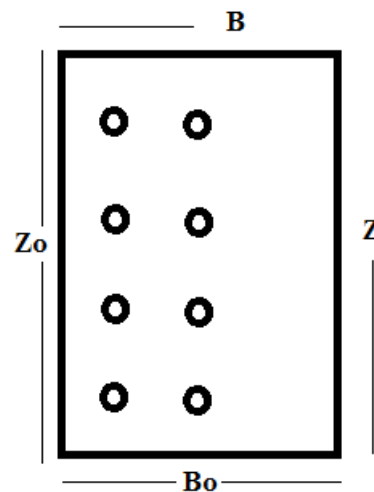


Figure 4-39: Scheme of taps on upstream face of gate

The results of these measurements were used to evaluate the upstream pressure coefficient (Kf) which can be estimated from the following expression:

$$K_f = \frac{H_t - H_d}{v_j^2 / 2g} \quad (4.13)$$

Where

$K_f$ : Upstream pressure coefficient.

The estimation of ( $K_f$ ) is useful to study the impact of dynamic pressure on upstream face of gate and then to provide a suitable design to withstand such forces .In present study, the ( $K_f$ ) values were estimated for various flow rates and gate opening ratios, samples of results are presented in (Figures 4.34 to 4.37) .

It can be seen from (Figures (4.34) and (4.35) that the ( $K_f$ ) values are dropped rapidly up to ( $Z/Z_o=50\%$ ) and then continue to decrease slightly toward the upper edge of gate. The figures are also indicated that the ( $K_f$ ) values along the centre are greater than those applied along the edge of gate and the negative values are seemed to be appeared for ( $Y/Y_o > \%50$ ).

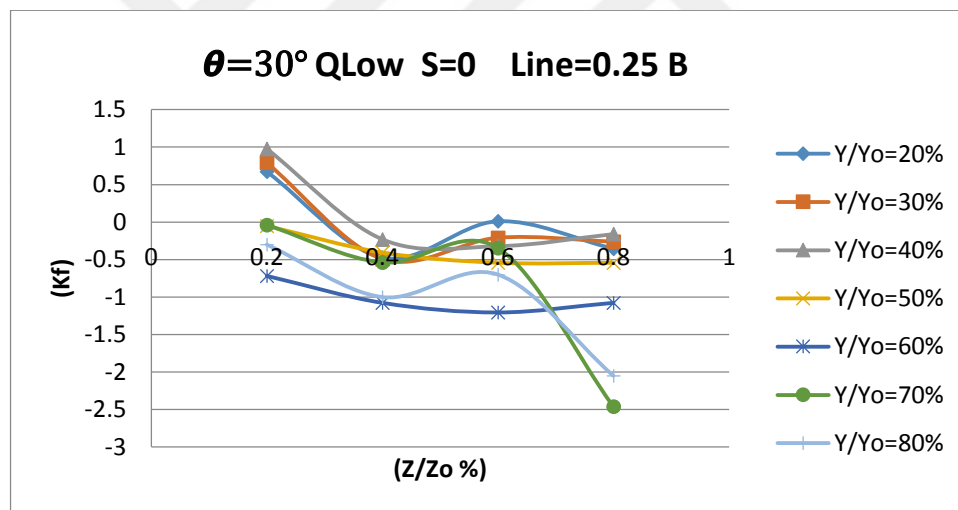


Figure 4.40: Variation of pressure coefficient ( $K_f$ ) along the gate upstream face, for  $X=0.25B$ , and the discharge is low.

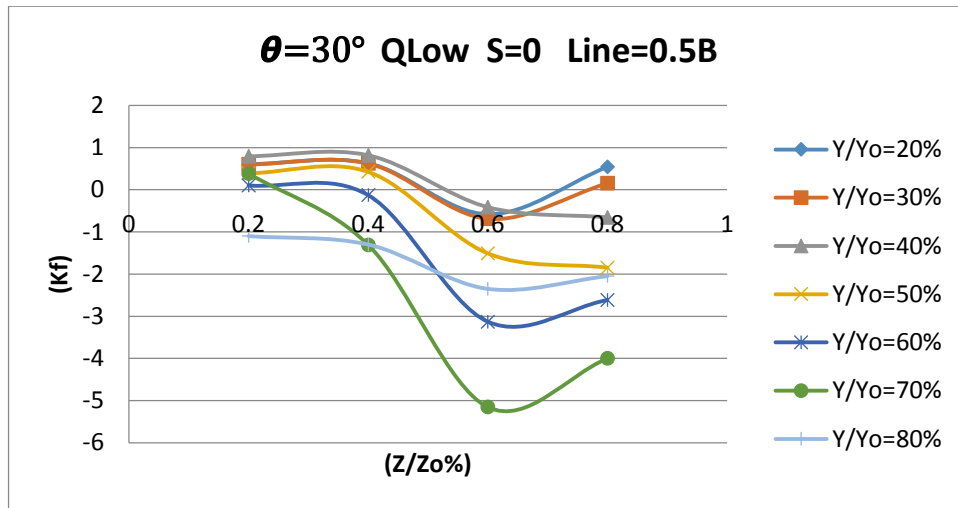


Figure 4.41: Variation of pressure coefficient ( $K_f$ ) along the gate upstream face, for  $X=0.5B$ , and the discharge is low.

(Figures 4.36 and 4.37) are shown that the increase of flow rates are caused some fluctuations in ( $K_f$ ) distribution in addition to a relative increase in values. The figure are shown that the negative values are also start to establish from ( $Y/Y_o=50\%$ ) and more.

The ( $K_f$ ) values may be influenced by many other parameters which are not within the scope of present study.

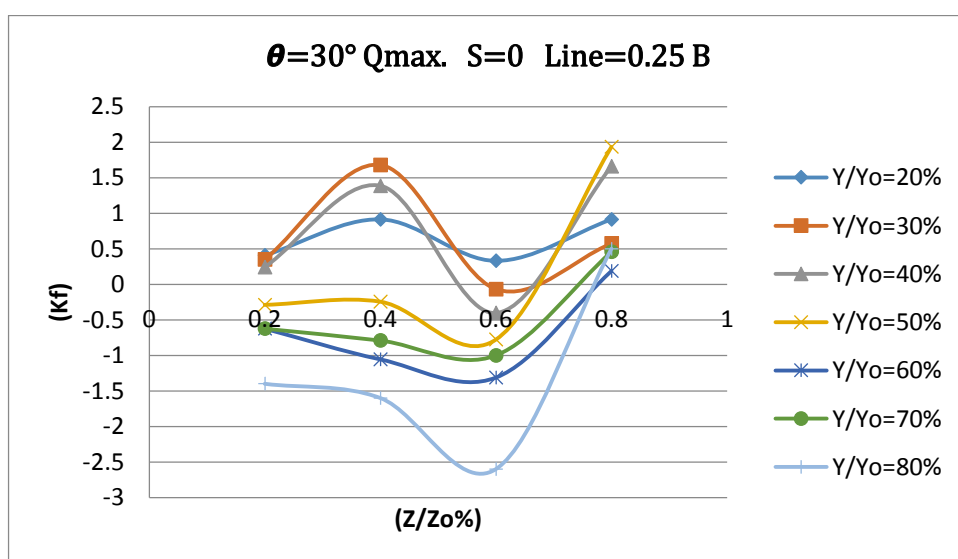


Figure 4.42: Variation of pressure coefficient ( $K_f$ ) along the gate upstream face, for  $X=0.25B$ , and the discharge is maximum.

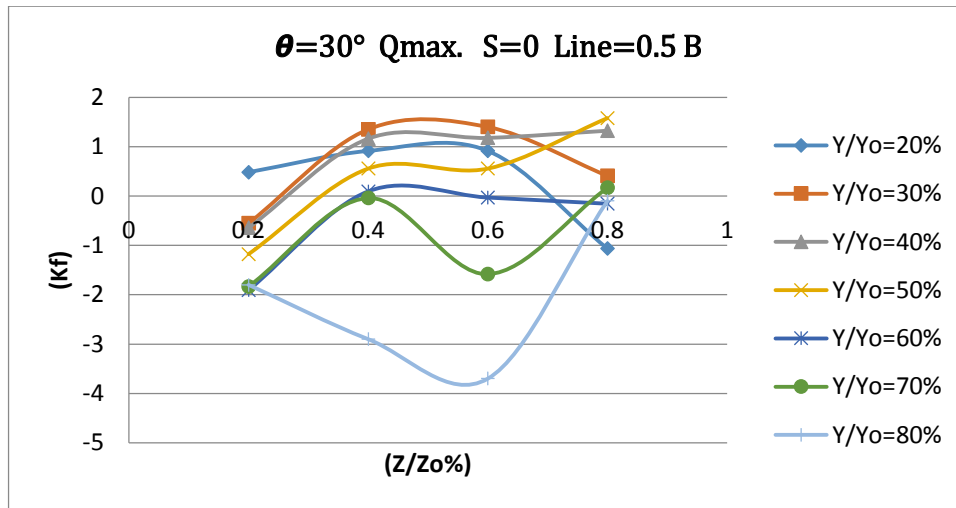


Figure 4.43: Variation of pressure coefficient ( $K_f$ ) along the gate upstream face, for  $X=0.5B$ , and the discharge is maximum .

## CHAPTER 5

### SUMMARY, CONCLUSION AND RECOMMENDATIONS

#### 5.1 SUMMARY:

A physical model is conducted in the laboratory of hydraulic /Ishik University in Arbil, to valuate the impact of hydraulic downpull force on vertical lift gates. The study include a lot of measurements ave been achieved on seven inclined gate lip shapes and cover the effects of different values of flow rates,longitudinal slopes through 84 runs .The upstream and downstram Pressure head ,pressure heads above and below the gates and the upstream and jet velocity measurements have been conducted.

The top and bottom pressure head coefficients and hence downpull coefficient were estimated based upon the results analysis of all sets of measurements .All pressure head coefficients are examined with effects of different gate lip angles , flow rates and longitudinal slopes .

The three dimensions presentation is used to describe the behaviour of bottom pressure coefficients on gate bottom surface which is useful to specify the zones of attachments and reattachment and make indication for possobility for the viabration occurance.

An attemp was used to analyze the results of bottom pressure coefficients ( $K_b$ ) by using the nonlinear regression of Statistical package of social sciences (SPSS).The comparison between the measured and predicted values of ( $K_b$ ) for specific cases were analyzed .

Finally, the study has been included the estimation of upstream pressur coefficient for various gate lip shapes,flow rates and longitudinalal slope.

## 5.2 CONCLUSION:

Some of major conclusions are list as follows:

- 1- The general scheme of  $(Kt)$  profile curves emphasize that only the values have been effectively influenced by gate geometries and consequently an effect it will create on values of downpull force .
- 2-The study indicates that there is no one slope has a definite clearly affects for all cases, and then, each case it may subjected to the influences of its limits. However, the values of slopes ( $S=0.25\%$ ) and to some extent ( $S=0\%$ ) have a greater impact in increasing top pressure coefficient values especially for low discharges of angles ( $\theta = 27^\circ$  and  $\theta = 42^\circ$ ) and medium discharge of angles ( $\theta = 27^\circ$ ,  $\theta = 37^\circ$  and  $\theta = 42^\circ$ ) .
- 3- The maximum flow rate lead to produce some fluctuations for  $(Kb)$  of gate lip shapes with angles of ( $\theta = 25^\circ$ ), ( $\theta = 30^\circ$ ) and ( $\theta = 40^\circ$ ) .
- 4- The  $(Kb)$  values for ( $Q$  max,  $S=0$ ) and all values of flow rates with slope ( $S=0.25\%$ ) are seem to be changed with uniform trend while some fluctuations were noticed for the values of  $(Kb)$  with slope ( $S=0.25\%$ ).
- 5- The general view o the flow rates and slopes effects on the average values of bottom pressure coefficients does not appear to be subjected to specific form.
- 6- The results has also been showed, that the for ( $\theta = 30^\circ$ ,  $\theta = 35^\circ$ , and  $\theta = 42^\circ$ ), the increase in flow rate ( $Q_{max.}$ ) will caused negative downpull force for ( $Y/Y_o = 60\%$ ) and more.
- 7- The results of  $(Kb)$  distribution along and across the gate bottom surface specified that the increase in longitudinal slope will lead to increase the velocity and consequently caused steep reduction in pressure head which may attained negative values and produce many problems accordingly.
- 8- The results of SPSS software analysis are shown that all the correlation coefficients have been found with an acceptable limit for such experimental works. However the functions which were obtained as a result to the regression process can mostly be useful for the estimation of  $(Kb)$  values related to the selected conditions.

9- The studying of upstream pressure coefficient ( $K_f$ ) indicates that its values are dropped rapidly up to ( $Z/Z_0=50\%$ ) and then continue to decrease slightly toward the upper edge of gate. And also are indicated that the ( $K_f$ ) values along the middle part are greater than those applied along the edge of gate and the negative values are seemed to be appeared for ( $Y/Y_0 > 50\%$ ).

10-The increase of flow rates are caused some fluctuations in ( $K_f$ ) distribution accompanied by a relative increase in values.

### 5.3 RECOMMENDATION:

The following recommendations are suggested for further studies:

1. Verify the results the downpull force by using the software of Computational Fluid Dynamics (CFD) .
2. Formulte the main parameters by functional form to create one or more empirical equations for predicting the downpull coefficients and forces with less efforts and acceptable extent of accuracy.
3. Solve the most common problem of pressure fluctuation measurements by using tranceduser device .
4. Study the effect of the upstream and downstream clearances of gate shafts on the downpull force with different ratios of ( $b_1/b_2$ )
5. Increase the rang of flow conditions and try to provide a free flow pattern downstream the gate shaft to evaluate its effects on downpull coefficients.
6. Verify the results by using optimazation program .

## REFERENCES

- Almaini, R. M., Al-Kifae, M. T., and Alhashimi, S. A. M., "Prediction Downpull Force on Tunnel Gate with Different Gate Lip Geometry", *Journal of Kerbala University, Vol. 8, No.4, 2010.*
- AL-Kadi , B. T., "Numerical Evaluation of Downpull Force in Tunnel Gates", Ph.D Thesis submitted to the College of Engineering , University of Baghdad , 1997.
- Ahmed, T. M., "Effect of Gate Lip Shapes on the Downpull Force in Tunnel Gates Experimental Study of Pressure Coefficient along Inclined Bottom Surface of Dam Tunnel Gate", Ph.D Thesis submitted to the College of Engineering , University of Baghdad , 1999.
- Ahmed, T. M., "Experimental Study of Pressure Coefficient along Inclined Bottom Surface of Dam Tunnel Gate", *Eurasian Journal of Science & Engineering, Volume 1, Issue 2, June 2016, Pages 52-53.*
- Ahmed, T. M., and Awat Omer Anwar "Effects of Gate Geometries on Top Pressure Coefficient of Dam Tunnel Gate", IEC 2016 Conference proceeding, Pages 85-90 .
- Amorim, J., and J. de Andrade. "Numerical analysis of the hydraulic downpull on vertical lift gates." *Waterpower. Vol. 99. 1999.*
- Aydin, Ismail, Ilker T. Telci, and Onur Dundar. "Prediction of downpull on closing high head gates." *Journal of Hydraulic Research 44.6 (2006): 822-831.*
- Bhargava, Ved P., and S. Narasimhan. "Pressure fluctuations on gates." *Journal of Hydraulic Research 27.2 (1989): 215-231.*
- Cox Robert G., Ellis B. Pickell and W.P. Simmons, "Hydraulic Downpull on High head Gates", *ASCE Discussion Hy. 5, May, 1960.* Dargahi, Bijan. "Flow characteristics of bottom outlets with moving gates." *Journal of Hydraulic Research 48.4 (2010): 476-482.*
- Drobir H., Volker K. and Johannes S., "Downpull on Tunnel-Type High –Head Leaf Gates".
- Elder, R. A. and Garrison, J. M., "Flow Induced Hydraulic Forces on Three Leaf Intake Gates" *ASCE, Vol. 90, No. 3, pp 215-233, May / Iune.* IAHR/AIRH Hydraulic Report, Balkema, Rotterdam, 2001.
- Khosrojerdi, Amir. "Hydraulic studies of pressure distribution around vertical lift gates." *Indian Journal of Science and Technology 5.3 (2012): 2268-2272.*
- Markovic–Brankovic, Jelena, and Helmut Drobier. "New High Head Leaf Gate Form with Smooth Upstream Face." *Tem Journal: 3, 2013*
- Murray, Robert Ian. "Hydraulic downpull forces on large gates." (1966).

- M. S. Akoz, M. S. Kirkgoz, and A. A. Oner, "Experimental and numerical modeling of a sluice gate flow," *Journal of Hydraulic Research*, vol. 47, no. 2, pp. 167–176, 2009.
- Naudaschers E., Helmut E. Kobus and Ragam R. Rao, "Hydrodynamic Analysis for High head Leaf Gates", ASCE, Vol. 90, Hy. No. 3, 1964.
- Naudascher, E. (1986). "Prediction and Control of Downpull on Tunnel Gates". *J. Hydraul. Engng. ASCE* 112(5),392–416.
- Naudascher, E., Kobus, H. E. and Rao, R.R., "Hydrodynamic Analysis for High- Head Leaf Gates". ASCE, *Journal of the Hydraulic Division*. Vol. 90, No. 3, Pp. 155-192, 1964.
- Naudascher, E. *Hydrodynamic Forces*. A. A. Balkema, Rotterdam, The Netherlands (1991).
- Naderi, Mehdi Nezhad, and Ehsanallah Hadipour. "Numerical Simulation of flow in bottom outlet of Narmashir dam for Calculating of Hydrodynamic forces." *Bull. Env. Pharmacol. Life Sci* 2.11 (2013): 87-93.
- Sagar, B.T.A. and Tullis, J.P. (1979). "Downpull on Vertical Lift Gates". *Water Power Dam Construct.* 12, 35–41.
- Sagar, B.T.A. (1977). "Downpull in High-head Gate Installations, Parts 1, 2, 3". *Water Power Dam Construct.* (3), 38–39; (4), 52–55; (5), 29–35.
- Sagar, B. (1995). "ASCE Hydrogates Task Committee Design Guidelines for High-Head Gates." *J. Hydraul. Eng.*, 10.1061/ (ASCE)0733-9429(1995)121:12(845), 845-852.
- Shamsai, A., and R. Soleymanzadeh. "Numerical simulation of Air-Water flow in bottom outlet." *International Journal of Civil Engineering* 4.1 (2006): 14.
- Taher, Taha M., and Awat O. Anwar. "Effects of Gate Lip Orientation on Bottom Pressure Coefficient of Dam Tunnel Gate." *Arabian Journal for Science and Engineering* (2016): 1-10.
- Thang, Nguyen D., and Eduard Naudascher. "Approach-flow effects on downpull of gates." *Journal of hydraulic engineering* 109.11 (1983): 1521-1539.
- Thang, Nguyen D. "Gate vibrations due to unstable flow separation." *Journal of Hydraulic Engineering* 116.3 (1990): 342-361.
- Uysal, mehmet akiş. Prediction of downpull on high head gates using computational fluid dynamics. Diss. Middle east technical university, 2014.